Durham E-Theses

A Mineralogical and Geochemical Assessment of the Potential Respiratory Health Hazard of Ash from Sakurajima Volcano, Japan.

HILLMAN, SARAH,ELIZABETH

How to cite:

Use policy

A Mineralogical and Geochemical Assessment of the Potential Respiratory Health Hazard of Ash from Sakurajima Volcano, Japan.

Sarah Elizabeth Hillman

Institute of Hazard, Risk and Resilience,

Department of Earth Science,

Durham University.

Thesis submitted for the degree of

MSc by Research

2010

Abstract

Sakurajima Volcano, Kyushu Island is the most active volcano in Japan. Vulcanian eruptions have occurred almost constantly since 1955, and it continues to erupt hundreds of times a year, repeatedly affecting local populations and the environment. Over the past 30 years, multidisciplinary research has been carried out to determine whether volcanic ash is a respiratory health hazard. Some medical work has been carried out at Sakurajima volcano, all of which gave varying results (from toxic to inert) depending on the study design. Here, I use mineralogical and geochemical analyses to address whether the ash from Sakurajima has the potential to be toxic. Ash from the recent eruptions and also historical, plinian eruptions was examined in order to assess the current, and the possible future, potential risk.

The results show that the amount of respirable (< 4 µm) material produced by the volcano is very variable (1.10 - 18.77 vol. %). The finest samples derived from the plinian eruptions but considerable amounts of respirable material were also produced on occasion, from the most recent eruptive phase. The amount of crystalline silica was investigated to determine the potential for the development of chronic respiratory diseases. In general ~7 wt. % cristobalite was found, but no other silica polymorphs were observed. SEM imaging showed no fibrous particles that could cause symptoms similar to asbestos. Surface tests showed that the ash did not produce significant amounts of damaging hydroxyl radicals (0.02-0.1 µmol m^{-2}). The results weakly correlated with the amount of surface iron available to react in the lungs. The findings suggest that the toxicity of the ash is low, but the potential hazard may be increased due to the long timescales for exposure.

Contents

List of Tables

List of Figures

have been excluded.

CHAPTER 5

List of Equations

Declaration

I confirm that no part of the material presented in this thesis has previously been submitted for a degree in this or any other university. In all cases the work of others, where relevant, has been fully acknowledged.

Sarah Hillman

Sarah Hillman

Acknowledgments

This thesis has only been made possible with contributions from a large number of people from several institutions, each of whose help, support and guidance have been vital for the completion of the thesis and deserve special mention.

Most of all, I owe my deepest gratitude to Claire Horwell. Her supervision, advice and guidance throughout my Masters course has formed the backbone of this thesis. Her attitude and expertise have always impressed me and I know that with her I have had the best training and support possible for my work. Her passion and commitment to this field is clear and has always filled me with enthusiasm and developed my fascination with my subject that I hope is reflected in this thesis. I am indebted to her more than she knows. Claire, you have been a real inspiration and role-model for me; it has been a pleasure to work with you and I hope we will do so again in the future. I am extremely gratefully to Alex Densmore for his advice and support throughout my Masters and particularly for his crucial and instructive feedback on all of my work. His input, coming from a different academic specialism, has been invaluable to me to improve the clarity of my work and consider problems from a different perspective. I have been lucky to take advantage of such a great 'science brain'.

I gratefully acknowledge Dr. Yasuhiro Ishmine for his central support in helping me to organise my fieldwork trips and providing me with indispensable contacts in Japan. Without his help the data set would not have existed! His unremitting kindness and hospitality whilst in Japan, and his willingness to help with any questions has been remarkable and incredibly useful. I would like to thank wholeheartedly Tom Bouquet for his help during my first fieldtrip in Japan, taking me to the field sites, providing me with invaluable local knowledge and making my stay a true Japanese experience. This thesis would not have been possible without the support and hospitality of many other Japanese colleagues. Some individuals who need special mention are Dr. Miki, Dr. Fukushima, Mr. Shinichi and Prof. Nakada who have provided me with the samples to analyse. Many thanks go to Prof. Iguchi, Prof. Kinoshita, Prof. Ishihara, Dr. Shimano and Dr. Matsushima who accommodated me in their institutions; gave me vital tours and knowledge of the volcanoes; and provided essential feedback on my results. I am sincerely grateful for all of their input and interest that have helped me to complete this project. I am indebted to the Disaster Prevention Research Institute (DPRI), Kyoto

Chapter 1

Introduction

Volcanoes are one of the most disruptive forces on Earth. Currently, over 500 million people are likely to live in proximity to an active volcano (Tilling, 2005). Concerns about the need for increased knowledge to protect local populations from eruptions have culminated in a large body of scientific work on volcanic risk assessment (Pyle, 1995; Blong, 2000). Recent advances in eruption modelling and prediction techniques and understanding of eruption mechanics have been invaluable in aiding mitigation strategies. However, there is still significant work to be done (Tilling & Lipman, 1993; Small and Naumann, 2001). Hazard managers have to make important decisions about how to best protect local populations. This requires constant volcano monitoring coupled with scientific knowledge of all potential threats and the extent of their consequences. With populations in volcanic areas only predicted to rise, and more than 220,000 deaths attributed to eruptions in 200 years since the end of the 18th Century (Tanguy et al., 1998), the effects of eruptions on human health are a priority for hazard managers (Small and Naumann, 2001; Bernstein and Buist, 1984).

Volcanoes can affect human health in a multitude of ways, depending on the size and type of eruption as well as the vulnerability of populations at risk (Baxter, 2005). In addition to the immediate physical threats of an erupting volcano, considerable health problems may occur over longer timescales and large areas, even from small eruptions, where volcanoes can emit potentially toxic substances (Hansell et al., 2006; Horwell, 2007). A primary example of this is the respiratory hazard posed by fine ash produced during explosive eruptions. Such hazards can sometimes be overlooked or dismissed as insignificant, especially before the eruption of Mt St Helens, USA in 1980. Ash can have far-reaching effects however, as it is easily dispersed over hundreds of kilometres and chronic respiratory problems may not become apparent until many years after exposure.

The potential toxicity of ash erupted from volcanoes has only been recognised within the last half century (Horwell and Baxter, 2006). The first studies followed

the eruption of Mt St. Helens, when it was established that the ash was very fine (containing substantial respirable material, <4 µm aerodynamic diameter) and contained crystalline silica in the form of cristobalite and quartz (Buist, 1982). The amount of crystalline silica contained in the ash was of particular concern as it has the potential to cause severe lung disease. Mineral dusts containing crystalline silica, predominately quartz, have been well-studied in occupational settings and can cause chronic respiratory problems (e.g. Buchanan et al., 2003; Park et al., 2002; Akbar-Khanzadeh and Brillhart, 2002). Cristobalite is a silica polymorph similar to quartz, which is particularly prevalent at dome-forming volcanoes. Cristobalite was thought to be more toxic than quartz, but it is now accepted that the toxicity of both polymorphs are similar (Soutar et al., 2000). Exposure to crystalline silica in either form can cause nodular fibrosis in the lungs, leading to silicosis, a permanent lung-scarring disease, and, in extreme cases, to premature death (NIOSH, 2002). Debate exists over suggestions that crystalline silica can also lead to lung cancer (Wyart-Remy, 2003 and references therein) but despite some scientific controversy it is recognised as a human carcinogen (IARC, 1997).

Knowledge of occupational exposure to mineral dusts cannot however, simply be applied to predict the effects of volcanic ash. Volcanic ash often contains tens of different minerals of which only a small proportion may be crystalline silica (Buist, 1982). Moreover, further research has identified other ash characteristics which may also cause potential toxicity. For example, more recently it has been shown that iron in volcanic ash may also be toxic. Experiments using ash from the andesitic Soufrière Hills volcano (Horwell et al., 2003a) showed that ash could generate substantial quantities of free radicals from surface iron that could potentially damage lung cells and DNA in a mechanism similar to crystalline silica pathogenicity (see Section 2.2). This has raised new concerns about possible health hazards from basaltic volcanoes such as Mt. Etna that are unlikely to form significant amounts of crystalline silica but are iron-rich. Horwell et al. (2007) found that iron-rich ash was much more reactive than andesitic and other low-iron ash types. Additionally, fibrous nanoparticles have been found in volcanic

ash that may cause effects similar to asbestos exposure (Reich et al., 2009). Finally, adsorbed acids and gases present on the surface of freshly-erupted ash may cause airway and lung irritation (Horwell and Baxter, 2006).

Therefore, although theoretical links exist, it has been especially difficult to ascertain whether exposure to volcanic ash could cause lung disease. Several causes of potential toxicity have to be considered and even then, minerals may interact to increase or decrease the potential toxicity of any single characteristic (e.g. Meldrum and Howden, 2002). Furthermore, each ash is unique to its eruption. More than sixty epidemiological and toxicological studies have given inconclusive results regarding the ability of ash to cause chronic (long-term) disease (Horwell and Baxter, 2006). Epidemiological studies are difficult to design well and must take into account exposure and vulnerability, which are very complex and influenced by daily routines at an individual level (Checkoway et al., 2004). Toxicological studies must represent realistic exposures and often lead to difficulties in extrapolating results from animal studies to the human system (Martin et al., 1986). The ambiguity of medical studies has led to mineralogical assessment (e.g. Horwell et al., 2003b) to help clarify the different mineralogical and geochemical characteristics of volcanic ash which could pose health hazards. Mineralogical analyses, which can be carried out more quickly and cheaply than other studies, should be used as a vital first step in determining the risk of volcanic ash to human health. After the eruptions of Mt St. Helens, Buist et al., (1986a) emphasised that there was a need for well-designed, multidisciplinary studies in order to fully understand the chronic threats posed by inhalation of toxic minerals in volcanic ash. However to date, very few other volcanoes for which there is recurrent or prolonged exposure to ash, have been studied in detail with respect to potential respiratory health hazards. Consequently many questions regarding ash toxicity in general, and the role of cristobalite in particular, remain unanswered.

Here, I address this lack of understanding by examining the mineralogical characteristics of Mt Sakurajima volcano, Japan, where numerous health-related

studies have been carried out on the population yet no information is known about the ash from a geochemical perspective. Japan has a population of around 130 million people and has 80 potentially-active volcanoes, many of them sitting close to major population centres. Although the volcanoes are generally well-studied in terms of geology, very little is known about the potential health hazards. Sakurajima volcano in southern Kyushu, southeastern Japan (see Figure 2.3, Section 2.4.1), regularly produces considerable amounts of ash, which falls over large local populations. With Kagoshima city (>600,000 inhabitants) to the west and Tarumizu (~17,800 inhabitants) to the northeast, as well as up to 9,000 people living on the volcano itself, concerns have been expressed about the effect of regular inhalation of ash emitted from Sakurajima (Samukawa et al., 2003). Some toxicological work carried out on samples of Sakurajima ash have yielded varying results (from toxic to inert) depending on study design (see Section 2.4.4) and the numerous epidemiological studies have not established a general scientific consensus about the effect of the ash on local populations, yet no detailed analysis of the characteristics of the volcanic ash itself with respect to respiratory health has been undertaken. This project will address whether ash from Sakurajima volcano has the potential to be toxic, using a comprehensive methodology, with a range of analytical techniques, some of which have only recently been developed for use in this type of study.

1.2   Aims

- To collect and examine a range of samples from around Sakurajima volcano which will reflect the exposure of the population.

- To determine the physical, mineralogical and geochemical characteristics of the ash, based on the most current knowledge about the possible risks to respiratory health from volcanic ash.

- To examine contradictions in the literature about the health effects of Sakurajima volcanic ash and relate these to the results of the current study.

- To inform future risk assessments and help guide the nature of any further research into respiratory health hazards from volcanic ash.

1.3   Rationale

Currently, there is little consensus among different medical studies examining the effects of the ash erupted from Sakurajima on respiratory health. The inconclusive evidence seen in these studies exemplifies the need for detailed characterisation of the physical, mineral and chemical properties of the ash. Local populations, totalling almost 1 million inhabitants within a 10 km radius of the volcano, are frequently exposed to ash from this recurrently-active volcano. With the possibility of even greater exposures in the near future (Ishihara, 2006), mineralogical analyses of the volcanic ash, using representative sampling methods and detailed analyses by scientifically robust methods, are urgently needed in order to provide some conclusive evidence on the potential risk ash that Sakurajima could pose so that appropriate measures can be taken if required.

This project will help to define the potential toxicity of the Sakurajima volcanic ash. The results should be of use to hazard managers and risk assessors, helping them to judge the respiratory health hazard from volcanic ash at the onset of new eruptions of Sakurajima volcano. The study will also contribute to the general understanding of health hazards of all volcanoes, world-wide. With the World Health Organisation's aim to eradicate silicosis globally by 2030 (Fedotov, 2003), there is an increased incentive to establish whether there are links between silicosis and volcanic ash. This cannot be achieved without detailed information from a range of volcanoes, and from different eruption styles. Results of this study will contribute to a needed and growing inventory of volcanic ash and respiratory health studies, examining an eruptive style previously unstudied from a mineralogical perspective.

6

Chapter 2

Literature Review

2.1   Introduction

The field of medical geology, and more specifically the study of volcanic respiratory health is still relatively young. Appropriate methodologies and protocol for assessing the effects of ash on the human respiratory system are still being developed, and studies tend to be specific to a particular volcano. Much uncertainty still exists regarding mechanisms of particle toxicity, the specific hazards posed by volcanic ash and what governs the creation potentially toxic minerals in volcanoes. Therefore in order to gain a good understanding of the current scientific knowledge in this area, both general theories developed in related but non-volcanic settings and very specific findings regarding single volcanic eruptions must be outlined.

This chapter aims to provide a detailed overview of the relevant literature in order to show the development towards, and give a summary of, the most recent scientific knowledge regarding the respiratory health hazards of volcanic ash. Furthermore, the chapter should provide the background knowledge necessary to critically assess the findings of this and other studies. In order to achieve this, I will first review the theories regarding inhaled particle toxicity, to provide some basic biological background before I examine the studies published to date that investigate volcanic ash toxicity for volcanoes other than Sakurajima. I will then give a brief synopsis of the geography, geology, eruption mechanics and eruptive styles of Sakurajima volcano. This should all help to inform detailed examination of medical studies carried out at Sakurajima, and the justification for further study that concludes this chapter.

2.2   The Fate of Inhaled Particles in the Lungs

Acute respiratory effects from volcanic eruptions have been well-documented (e.g. Baxter et al., 1983; Hickling et al., 1999). Heavy ashfall can lead to increased cases of asthma, bronchitis, inflammation of the airways, coughing, breathlessness and general respiratory irritation (Horwell and Baxter, 2006). In

some cases suffocation has also been reported (e.g. Bernstein et al., 1986b). Chronic lung disease is much more difficult to attribute to volcanic eruptions, especially as disease may not become apparent until many years following initial exposure (Miller et al., 1998). When a particle is inhaled, its effect on the body depends on where it is deposited and the associated mechanisms of removal (Schlesinger, 1995). Chronic diseases develop over long timescales (perhaps decades), after prolonged and heavy exposure, and the residence time of a particle in the body will influence the likelihood of disease. Therefore, knowledge of how the pulmonary system interacts and deals with inhaled particles, as well as how defence mechanisms may be compromised by toxic substances is important.

For these purposes, the pulmonary system can be simplified into three main regions: the upper respiratory tract (also referred to as the nasopharynx in the literature), the tracheobronchial tree, and the pulmonary region (Schlesinger, 1995), as shown in Figure 2.1. The upper respiratory tract starts at the nose and mouth and extends down to the voice box. Next the trachea splits into two bronchi one leading to each lung (the tracheobronchial tree). The bronchi continue to split into bronchioles, becoming more numerous and smaller, eventually reaching the pulmonary region which consists of the alveoli and air spaces associated with gas exchange (Dallas, 2000).
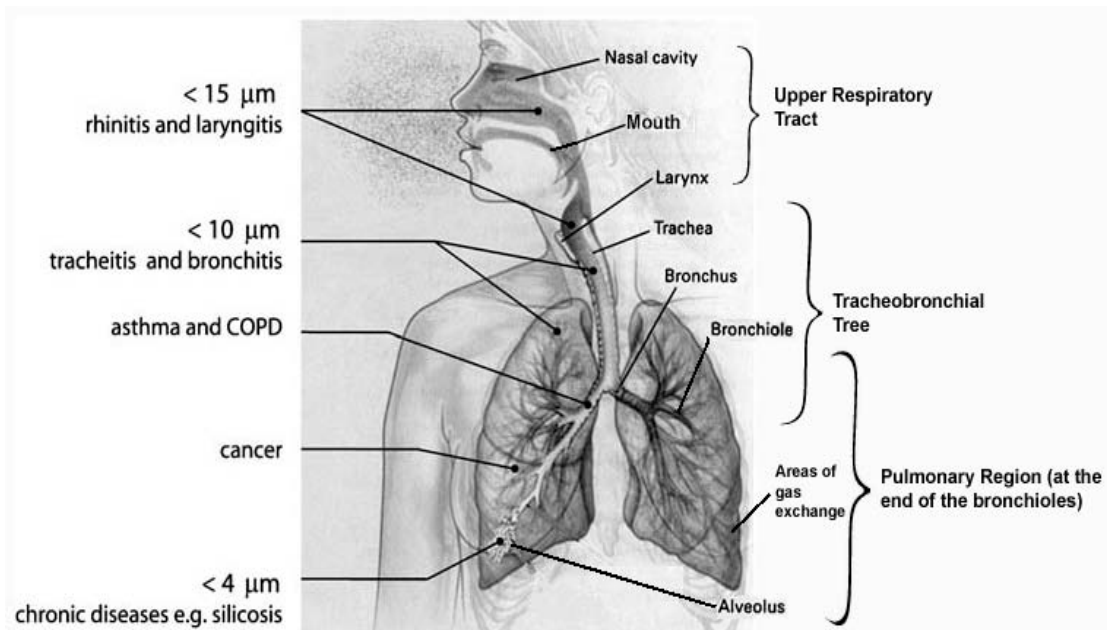
Figure 2.1: The main features of the pulmonary system, including maximum penetration for some particle aerodynamic diameters and possible side-effects of deposition. COPD: Chronic Obstructive Pulmonary Disease. Modified from Horwell and Baxter (2006).

As a particle penetrates further into the body residence times will inevitably increase. The respiratory tract is a complex network of narrow passages, hairs, and branching tubes designed to aid deposition before particles reach the pulmonary region (Buist, 1982). Mechanisms of particle deposition are shown in Figure 2.2. Where a particle is deposited depends primarily on grain size, and to a lesser extent shape, charge and density (Stuart, 1984). Therefore pulmonary toxicologists use the aerodynamic diameter of particles, which takes into account their airborne behaviour, in order to estimate how far they can penetrate into the lungs (Dallas, 2000). The aerodynamic diameter of a particle can be defined as "the diameter of a unit density sphere that would have the identical settling velocity as the particle under consideration" (Lippmann, 1998, pp. 10.6).
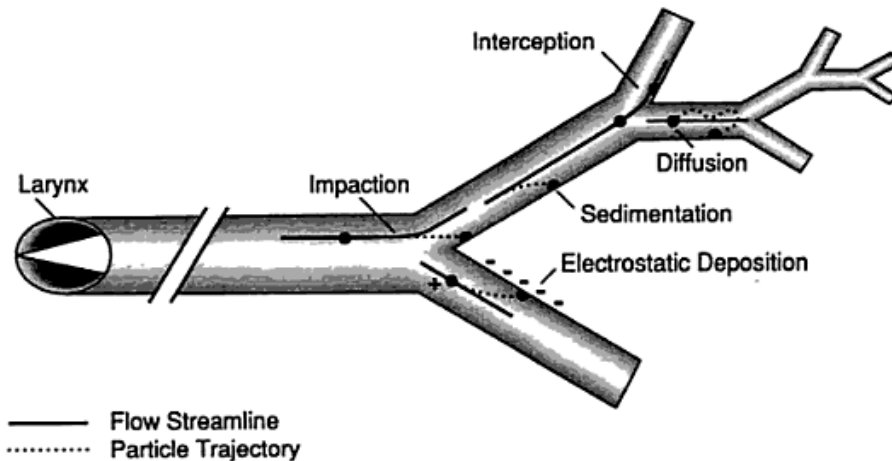
Figure 2.2: Diagram showing the primary mechanisms of deposition. From Schlesinger, 1995. **Impaction:** deposition onto airway surfaces when particles are unable to change course. **Sedimentation**: deposition due to gravity. **Brownian diffusion**: < 1 µm particles coming into contact with airway surfaces through random motion. **Electrostatic precipitation**: deposition of charged particles due to electrostatic interactions. **Interception**: deposition when particles are fibrous.

Only those particles with < 10 µm aerodynamic diameter (referred to as diameter from here on) are able to reach the tracheobronchial tree (Figure 2.1) (Horwell, 2007). These particles are defined as 'thoracic'. Particles with < 4 µm diameter are defined as 'respirable' and may reach areas of gas exchange (Quality of Urban Air Group, 1996). Particles deposited in the upper respiratory tract and tracheobronchial tree can be expelled quickly and with ease by mucociliary transport through sneezing, coughing and nose blowing (Fubini and Otero Areán, 1999). Large quantities of particles reaching the tracheobronchial tree will cause symptoms such as bronchitis or asthma, although chronic disease is very unlikely to develop as clearance is still relatively quick (Schlesinger, 1995).

Respirable particles of less than 4 µm diameter are of particular interest as they can reach the alveoli and are expelled via different mechanisms, which can increase the residence time of a particle in the body, and hence the possibility of cell damage from toxic particles (Schlesinger, 1995). The main removal process in

the alveoli is via alveolar macrophages (Fubini and Hubbard, 2003). Macrophages can locate inhaled particles deposited in the alveoli and ingest (phagocytize) them using enzymes (Dallas, 2000). Phagocytized material is then removed via the mucociliary escalator or lymph nodes (Dallas, 2000). However, some toxic particles cannot be digested and it is these particles that reach areas of the deep lungs that will pose a significant risk with respect to long-term respiratory disease (Horwell and Baxter, 2006). Inability to break down particles causes cell activation, whereby the macrophage produces 'reactive oxygen species' (ROS) to try to break down the particle. This can culminate in the cell becoming overloaded with toxins and dying, discharging phagocytic enzymes and ROS contained in the cell, and re-releasing the particle (Fubini and Hubbard, 2003). Both the re-released particle and macrophage contents can then damage other alveolar cells (Fubini and Hubbard, 2003).

Although there is a well-known relationship between crystalline silica and silicosis, the precise way in which crystalline silica initiates this toxic response in the alveolar macrophages is not well understood (NOISH, 2002). It is thought that one cause of toxicity of silica crystals is when cleavage of Si-O bonds (e.g. through fragmentation of crystals during mining activities) produces free radicals (Si•, SiO•) on particle surfaces (Fubini and Hubbard, 2003; Hamilton et al., 2008). Macrophages ingest silica particles and the free radicals then react inside the cells, damaging them and preventing digestion of the particle (Allison et al., 1966). Free radicals may also be released in the lungs from iron-catalysed reactions (Fubini et al., 1995). For example, surface iron on mineral particles can produce hydroxyl radicals (HO•) through the Fenton reaction:

$$Fe^{2+} + H_2O_2 \rightarrow Fe^{3+} + OH^- + HO\bullet \qquad \text{Equation 2.1}$$

The hydroxyl radical can also be produced through the Haber-Weiss cycle in the lungs or via reactions between surface silica radicals and water or hydrogen peroxide (see Fubini and Hubbard, 2003 for more detail). Again these radicals can react with cells, leading to ROS production and cell damage (Fubini et al.,

1995). Fibrous particles that are thin enough to reach the deep lung but too long to be completely engulfed by macrophages will also lead to macrophage death, producing effects similar to asbestos exposure (Fubini and Otero Areán, 1999).

Continued ingestion and cell activation by macrophages, as well as death of alveolar cells causes persistent inflammation. This can then lead to the formation of nodules or fibrous lesions in the lungs, which may exacerbate into silicosis or other lung diseases (Fubini and Otero Areán, 1999).

2.3   The History of Volcanic Ash and Respiratory Health Studies

Details of thorough risk assessments regarding erupted ash and respiratory health carried out for Mount St Helens and Soufrière Hills volcano are outlined below for comparison with studies of Sakurajima. Investigations on other volcanoes are limited but a brief summary of these is also described. For a more detailed review of the studies see Horwell and Baxter (2006).

2.3.1   Mount St. Helens, Washington State, U.S.A.

The May 1980 eruptions of Mount St Helens produced heavy ashfalls over significant areas of Washington and adjacent states. Concerns were expressed about insufficient knowledge of, and mitigation plans for, risks posed by volcanic ash (Horwell and Baxter, 2006). Confusion over the quantity of crystalline silica contained in the ash quickly led to public anxiety that volcanic ash could pose a significant threat to respiratory health and calls for further investigations into the Mount St Helens ash ensued (Dollberg et al., 1986). Numerous mineralogical, epidemiological and toxicological studies were carried out in a multidisciplinary effort to examine the respiratory effects of the erupted ash. Their collaborative research and approach to the risk assessment of volcanic ash and health was summarised in a special supplement to volume 76 of the American Journal of Public Health in 1986.

Several studies examined the mineralogy of the erupted ash and some quantified the amount of crystalline silica phases (Fruchter et al., 1980; Olsen and Fruchter, 1986; Farwell and Gage, 1981). Problems with interpretation of X-ray diffraction patterns led to disparities between results which were resolved in an inter-laboratory investigation (Dollberg et al., 1986). Eventually, the Mount St Helens ash was quoted to contain 3-7% crystalline silica in the form of quartz and cristobalite (Dollberg et al., 1986). On examination of ash morphology and particle size, Olsen and Fruchter (1986) found no fibrous minerals in the ash, but significant amounts (90% by count) of the particles were less than 10 μm diameter.

Epidemiological studies examined the prevalence of both acute and chronic symptoms after ash exposure. Reports of acute effects included increased emergency room visits for respiratory problems in general (Baxter et al., 1981) and specifically for children with asthma (Kraemer and McCarthy, 1985; Nania and Bruya, 1982), as well as exacerbation of symptoms from pre-existing problems (Baxter et al., 1983), but no effects were visible in healthy children (Buist et al., 1983; Johnson et al., 1982). The National Institute for Occupational Safety and Health (NIOSH) organised studies examining loggers who were more likely to have recurrent exposure to the ash through remobilisation. Acute symptoms such as coughing, chest tightness and eye irritation were higher in loggers than the control groups at first, however by September 1980 symptoms had subsided (Bernstein et al., 1982; Merchant et al., 1982). Buist et al. (1986b) carried out a four year investigation into the lung health of loggers. A decrease in lung function a year after the eruption was observed in both exposed loggers and the control group, although the decrease was much larger in the loggers. By four years after the eruption, no difference between the two groups was observed. Olenchock et al. (1983) found that volcanic ash appeared to affect immune systems in the lungs between six months and a year after exposure. However their results were complex and without a follow up study no long-term implications of their observations can be drawn.

Toxicological studies produced a range of results regarding the impact of ash on pulmonary cells. The use of in vitro vs. in vivo tests, ash concentration, how the ash was administered, the use of different animals, the length of the study and lag times between different exposures could all have been contributing factors affecting the conflicting results (Martin et al., 1986). However, some well-constrained in vitro studies using animal (e.g. Fruchter et al., 1980; Wiester et al., 1985) and human lung cells (e.g. Martin et al., 1984), and in vivo studies using intratracheal instillation (e.g. Beck et al., 1981) or inhalation of ash (e.g. Raub et al., 1985; Grose et al., 1985) all concluded that the ash did not have a high fibrogenic potential (the potential of an inhaled particle to cause fibrous lesions in the lungs) and did not pose any real threat unless prior lung deficiencies existed. Castranova et al. (1982) found that, although function of the lung generally was not affected, volcanic ash from Mt. St. Helens could decrease the ability of macrophages to protect the lung from infection. On the other hand, several investigations using higher exposures of ash did demonstrate reduction in lung function and some fibrogenic potential of volcanic ash, although not to the same extent as quartz (e.g. Green et al., 1982; Martin et al., 1983; Vallyathan et al., 1983; Vallyathan et al., 1984). However even these studies stated that, although the ash could be considered cytotoxic to an extent, it was unlikely that exposures for Mount St Helens were sufficient for the ash to be considered a risk to local populations.

2.3.2   *Soufrière Hills, Montserrat, British West Indies*

The Soufrière Hills volcano on Montserrat began erupting in July 1995. Ash is erupted from Soufrière Hills in two ways: directly emitted by vulcanian, explosive eruptions, and lofted from pyroclastic flows produced by lava dome collapse (Sparks et al., 1998). Dome-formation is associated with the production of cristobalite and collapse can generate large amounts of fine ash. As the predominant wind direction on Montserrat blew ash plumes over the most populated areas of the island, inhabitants were repeatedly exposed to potentially toxic, newly-erupted ash (Wakefield, 2000). When the long-term nature of the

eruption was established it became apparent that investigations into chronic respiratory hazards were needed (Horwell et al., 2003b).

Baxter et al. (1999) studied the mineralogy of the ash and found distinctions between the two types of ash. Dome-collapse ash contained 13-20 weight % of particles < 10 μm, with lower percentages (13-14 wt. %) in ash from vulcanian eruptions. More significantly, the < 10 μm fraction of dome collapse ash contained 10-24 wt. % cristobalite, much higher than the Mount St. Helens ash. Erupted ash had much lower cristobalite content (3-6 wt. %). Examination of airborne particulate matter concentrations also highlighted additional exposures from remobilised ash. In some cases, the airborne concentrations of particles < 10 μm (PM_{10}) were higher during periods of intensive human activity (e.g. during a school lunch break) than during ashfalls (Baxter et al., 1999).

Forbes et al. (2003) examined the respiratory health of children living on Montserrat during the eruptions. They concluded that respiratory health had been affected, with increased reports of wheezing and asthma, and increased incidence of exercise-induced bronchospasm during an exercise test in children from high-exposure areas, compared to children in unaffected areas. An occupational trend in respiratory problems experienced by workers on Montserrat was highlighted by Cowie et al. (2002). Few respiratory problems were apparent in general workers, but people involved with ash clearance experienced some acute symptoms and those with jobs involving higher ash exposures such as gardening or roadside workers had decreased lung function (Cowie et al., 2002).

Horwell et al. (2003b) built on previous studies to give a more comprehensive assessment of exposure and risks to the population. The study confirmed the high amounts of respirable ash and crystalline silica in dome-collapse ash. Further analyses showed that the particles of cristobalite from the dome-collapse ash were in the fine, respirable fraction, which was lofted into the air during pyroclastic flows, whereas the main pyroclastic flow matrix was low in respirable

material and crystalline silica. Particulate concentrations showed that exposure to respirable material was likely to be higher for children than adults for re-worked samples. Surface reactivity was studied by Horwell et al. (2003a) to examine the potential for volcanic ash to produce free radicals in the lungs. Radical production was high, more than twice that of a toxic quartz standard. However the source of free radicals was actually surface iron rather than cristobalite. The crystalline silica was therefore shown to be un-reactive under the conditions of study, but the ash still posed potential risk from surface iron.

Toxicological studies again gave mixed conclusions. Wilson et al. (2000) compared the surface reactivity of ash, quartz and TiO_2 (an inert control). Surface reactivity of ash was lower than quartz but higher than the inert control, although variation between ash from different eruption types was seen. Two papers published on one study concluded that the ash had no effect on the lungs (Berube et al., 2004; Housley et al., 2002). More detailed studies by Lee and Richards (2004) and Cullen et al. (2002) found that the ash caused inflammation but not fibrosis in the lungs. Lee and Richards (2004) used different doses of ash, showing that inflammation only occurred with medium or high exposures, and that there was a delayed effect between exposure and response.

UK governmental officials reviewed the studies on Soufrière Hills volcanic ash and compiled a risk assessment regarding ash exposure and respiratory health. They concluded that the volcanic ash of Montserrat should be considered as a mixed dust, similar to coal, with mild toxicity (Horwell and Baxter, 2006). A recent computer model has predicted quantitative risks of developing silicosis after 20 years of exposure to Soufrière Hills volcanic ash (Hincks et al., 2006). The results expressed that the median risk of contracting silicosis after 20 years of exposure was between 0.5% for an average adult living in the least exposed areas to 2-4% (high risk) in gardeners with the greatest exposures (Hincks et al., 2006). However, after the evacuation of the central and western areas of Montserrat that were most frequently affected by ashfall, exposure to volcanic ash and cristobalite was low, and did not exceed UK or US exposure standards

(Searl et al., 2002). Therefore risks to the population should be much lower than predicted by Hincks et al. (2006). The investigations on Montserrat provide a good collection of scientifically sound results on which a realistic and comprehensive risk assessment could be based.

2.3.3 Studies of other volcanoes

Very few investigations on other volcanoes have been carried out, making conclusions regarding the risk posed by any individual volcano difficult to draw (Horwell and Baxter, 2006). Studies that found correlations between acute respiratory health and exposure to volcanic ash include Gordain et al. (1996) on Mount Spurr, Alaska; Malilay et al. (1996) on Cerro Negro, Nicaragua; Rojas-Ramos et al. (2001) on Popocatepetl, Mexico; and Tobin and Whiteford (2004) on Mount Tungurahua in Ecuador. Tobin and Whiteford (2001) and Naumova et al. (2007), examining Mount Tungurahua and Guagua Pichincha, respectively, both in Ecuador, found strong relationships between volcanic ash exposure and increased acute respiratory symptoms in children. In contrast, other studies, including Bradshaw et al. (1997) and Weinstein and Patelxy (1997) on Mount Ruapehu in New Zealand, Cronin and Sharp (2002) on volcanoes in the Vanuatu Archipelago, and Nania et al. (1994) on El Chichón volcano in Mexico, have found no significant increases in respiratory problems after volcanic eruptions. Vallyathan et al. (1984) examined ash from El Chichón and Galunggung volcanoes as well as Mount St. Helens. All were found to have low (1-2%) cristobalite and were considered slightly cytotoxic in toxicological tests.

Very recently, the ash from Chaitén volcano, Chile has been examined from a respiratory health hazard perspective. Fibrous nanoparticles of beta-cristobalite were identified in the ash by Reich et al. (2009). This was unusual considering that beta-cristobalite was previously thought to only exist at high temperatures. The study also emphasized the gaps in knowledge regarding the toxicity of volcanic ash. For example the toxicity of beta-cristobalite (all previous toxicological work was carried out on alpha-cristobalite) and nano-particles

produced by volcanic ash have not been examined in detail previously. Horwell et al. (2010) also examined Chaitén ash and found that the volcano produced large amounts of respirable material, often with high cristobalite proportions in the bulk (< 1 mm) ash.

2.4   Sakurajima volcano

2.4.1   Background and Geology

Sakurajima is one of the most active volcanoes in Japan, with over 8,000 individual eruptions recorded since 1955 (Okubo et al., 2009). It is located in Kagoshima prefecture, Kyushu Island, southeastern Japan (Figure 2.3). It occupies the northern part of Kagoshima Bay, but lies on the southern rim of the Aira caldera. Kagoshima city is situated ~10 km west of Sakurajima across the bay. A relatively small city by Japanese standards, its population exceeds half a million inhabitants, who regularly deal with disruptions from the numerous explosive eruptions of the volcano (Kinoshita 1996). Sakurajima Volcano Observatory, located on the volcano, is the largest in the world. Much research has been conducted through the observatory to improve the understanding of eruption mechanics and enhance eruption prediction, which has contributed to the production of a hazard map for Sakurajima, although it does not consider the health effects of volcanic ash.
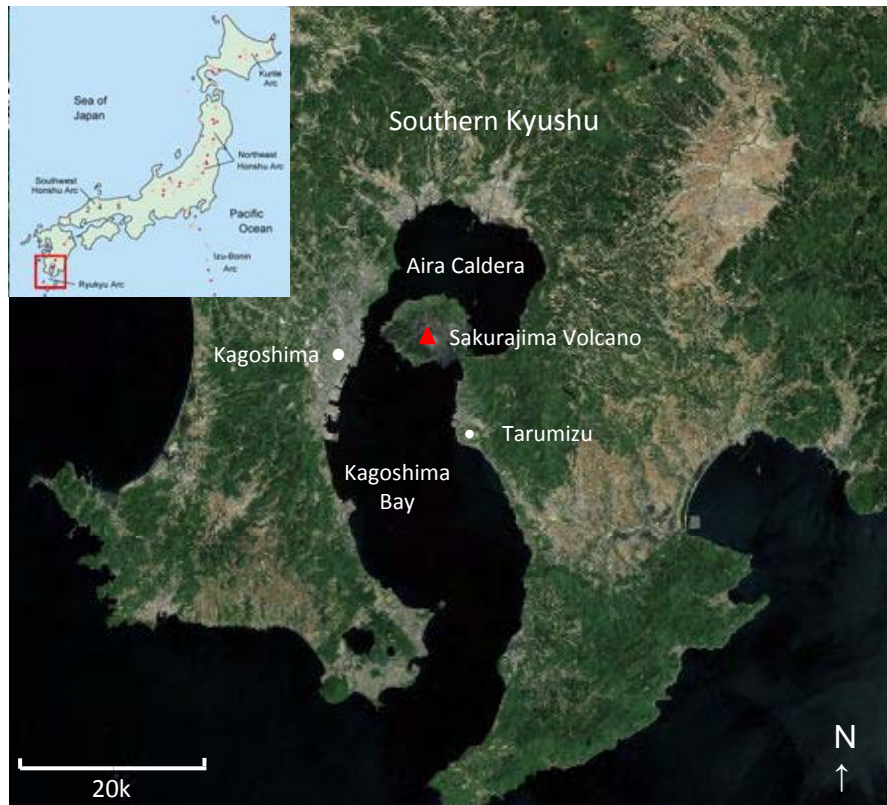
Figure 2.3: Aerial view of southern Kyushu Island showing location of Sakurajima volcano. Inset courtesy of Tom Bouquet.

Sakurajima is an andesitic post-caldera volcano that formed around 13,000 years B.P. (Kobayashi et al., 2007). Sakurajima actually consists of two adjoining stratovolcanoes. The northern crater, Kitadake (1117 m a.s.l.) was the original volcano and stopped erupting ~4.9 ka (Okubo et al., 2009). At roughly the same time (~4 to 3.5 ka) Minamidake, the southern crater (1040 m), began to grow on the slopes of Kitadake (Kobayashi et al., 2007). Now, only Minamidake is active. Several small parasitic cones also exist on Sakurajima along weak zones within the volcano (Durand et al., 2001). The volcano is generally made up of dacitic-andesitic lava flows and pyroclastic deposits, built up from previous plinian eruptions (Kobayashi, 1982). This can be seen clearly in the geological map by Fukuyama and Ono (1981) in Figure 2.4. Rocks are made up of plagioclase, hypersthene, augite and magnetite phenocrysts, with overall SiO_2 ranging from 57-67 wt. % (Fukuyama and Ono, 1981). Decreases in the SiO_2 wt. % of each lava flow with time from the major historical eruptions have been attributed to a coupled magma chamber system and magma mixing (Durand et al., 2001). The

groundmass consists of very fine-grained plagioclase, pyroxene, magnetite, and volcanic glass (Fukuyama and Ono, 1981). The country rocks around Sakurajima consist of shales, granites, sandstones and tuffs (Kobayashi, 1982).

Historical eruptions at the volcano have been recorded since the 8th century, although little is known about early eruptions (Kobayashi et al., 2007). Since 1471 four main eruptive periods have taken place: 1471-1476 (Bunmei era), 1779-1785 (An-ei era), 1914 (Taisho era) and 1946 (Showa era) (Kobayashi et al., 2007; Durand et al., 2001). Each eruptive phase was characterised by a number of explosive eruptions, initially ejecting large amounts of pyroclastic material and ash, followed by effusive lava flows from lateral fissure vents on the flanks of Minamidake summit, still accompanied by pyroclastic flows and ashfall (Fukuyama and Ono, 1981).

Little information is available about the Bunmei eruptions, which lasted for 5 years. Lava flows occurred in 1471, 1475 and 1476, although the majority of the eruption was characterised by pumice falls. The eruption is thought to be the largest pumice eruption of Sakurajima's history, significantly altering the profile of the adjacent Kitadake summit (SABO, 2009) The An-ei eruption was the largest eruption recorded for Sakurajima. In 1779, a large plinian eruption (VEI 4) caused heavy ashfall, followed by extensive lava flows, with widespread damage (Ryusuke, 1998). A total of 1.8 km³ of magma was erupted, including 0.4 km³ of ash during the initial large eruption, and explosive eruptions with heavy ashfall continued for several years including a submarine eruption in the Aira Caldera which triggered a destructive tsunami (Ryusuke, 1998).
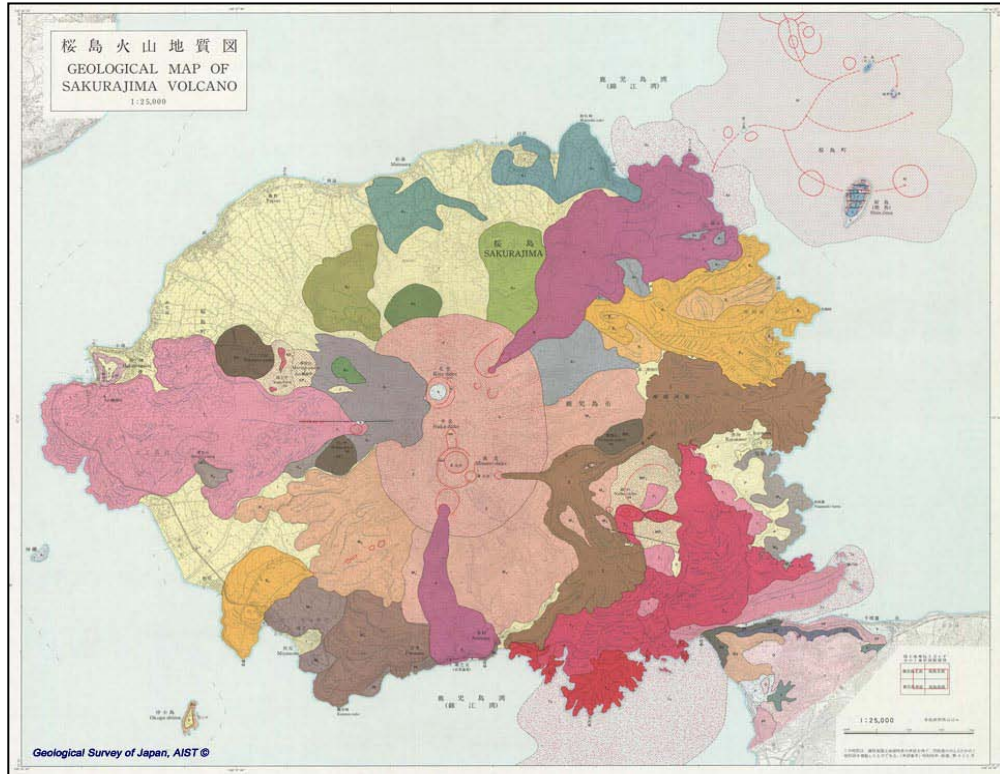
Figure 2.4: Geological map of Sakurajima Volcano, from Fukuyama and Ono, 1981. Image obtained from http://riodb02.ibase.aist.go.jp/db099/volcmap/01/index-e.html National Institute of Advanced Industrial Science and Technology (AIST): Geological Survey Japan.

The largest eruption of the 20th Century in Japan was the Taisho eruption, beginning with a large plinian eruption on 12th January 1914 and ending a period of dormancy of over 100 years (Nakamura, 2006). It erupted 1.6 km³ of magma, including 0.6 km³ of ash and pumice up to 8 km into the atmosphere (Durand et al., 2001). Lava emissions from the eastern vent (see Figure 2.6a overleaf) continued for over a year and by February the lava flow had connected Sakurajima to the Osumi Peninsula (Kobayashi et al., 2007). Ash dispersal was widespread, reaching northern Honshu Island (Figure 2.5).
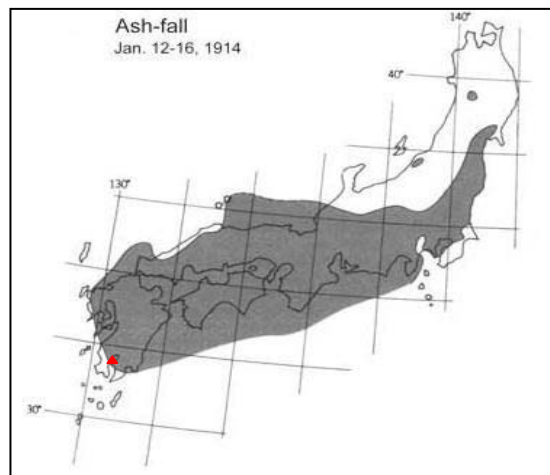
Figure 2.5: Ashfall dispersal from the 1914 eruption of Sakurajima volcano (red triangle). Modified from AIST, GSJ, 2006.

The Showa era eruptive phase was characterised by smaller explosive eruptions of ash, with only one small lava flow (0.08 km²). Sakurajima volcano is predicted to return to the plinian style of eruptions in the future (SABO, 2009). Therefore, the size and style of previous eruptive periods at Sakurajima are important for this study as they will give an indication of potential future health hazard. The lava flow positions and historical eruptive activity of Sakurajima are summarised in Figures 2.6a and b.
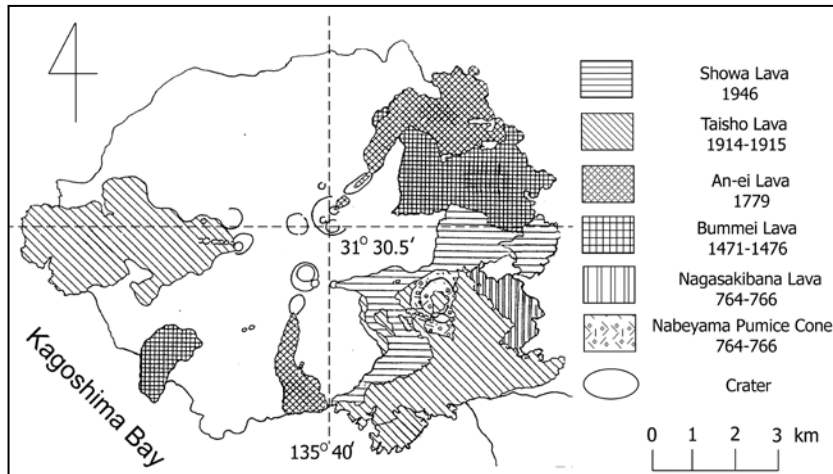
Figure 2.6a: The position of lava flows from the main historical eruptions. Modified from Yu et al. (2001).
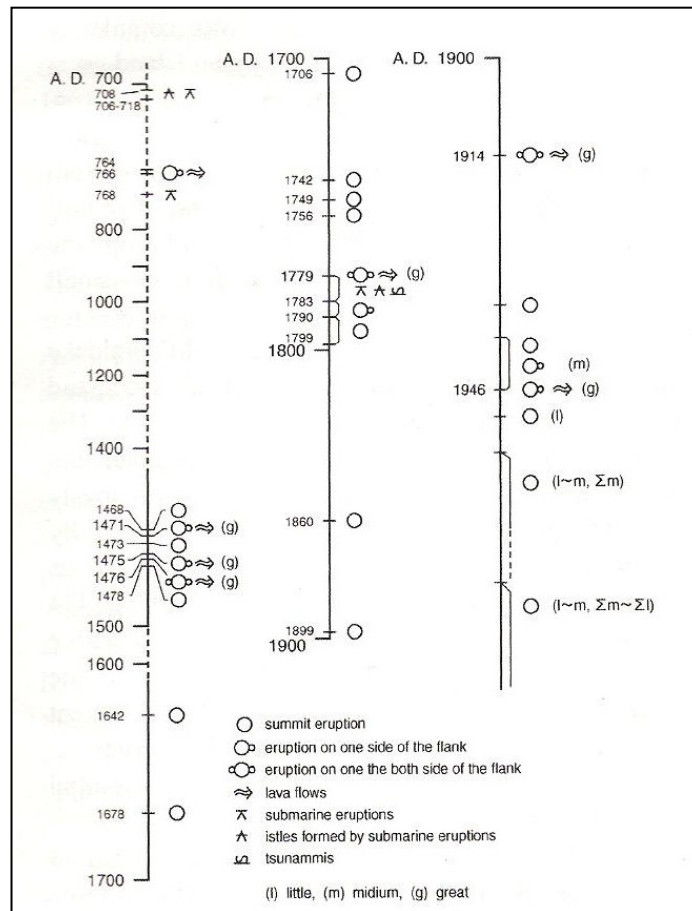
Figure 2.6b: Chronology of the volcanic activity of Sakurajima. From Kobayashi et al. (2007).

The most recent eruptive phase began in 1955. Intermittent eruptions have occurred almost continuously until present, with the most active period being the 1980s and early 1990s (see Figure 2.7). Ground inflation under the Aira Caldera due to magma accumulation actually stopped in 1960-1962 and 1974-1993 when ~10-30 million tons of ash was erupted annually (Ishihara, 2006). From 1993 eruptions became less frequent although there were still usually over 100 explosions per year, erupting several million tons of ash annually until 2001 (Ishihara, 1999).

Since 2001 eruptive activity decreased drastically with fewer than 100 eruptions each year. In 2006 eruptions started to occur at a different vent, the Showa crater near the summit of the south-eastern flank of the volcano (Yokoo and Ishihara, 2007), as seen in Figure 2.8a and 2.8b. This, and the decrease in eruptive activity, especially since 2001 (only 100,000 tons of ash erupted per year), has led to speculation that the conduit to the summit crater has been choked (Ishihara, 2006). However, during 2009 the frequency of explosive eruptions has dramatically increased, and is predicted to continue to do so. 560 ash advisories were issued for 2009, compared to 77 during 2008 (Tokyo VACC, 2009). So far (by February) in 2010 there have been over 100 ash advisories (Tokyo VAAC, 2010). Most eruptions now occur at the Showa crater, with only a very few (2/3 per year) occurring at the summit Minamidake crater (Smithsonian Institute weekly reports, 2009).
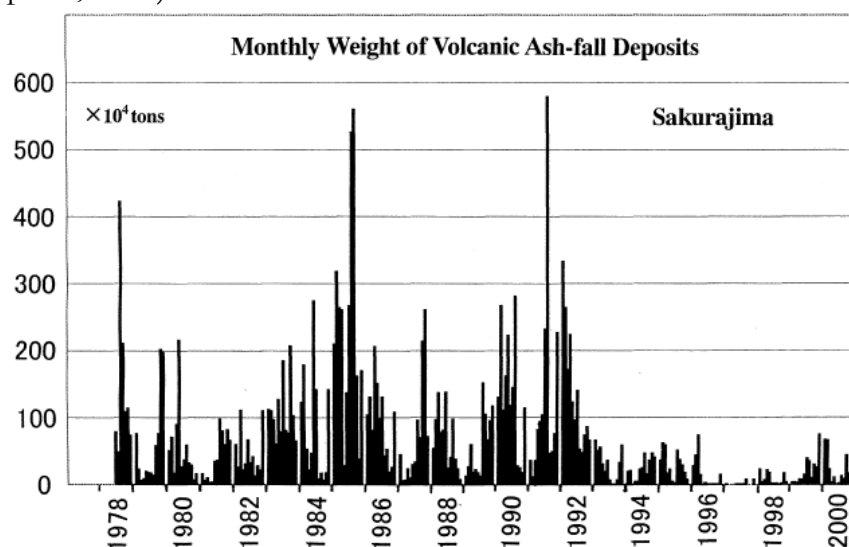
Figure 2.7: Monthly weight of ashfall from 1978-2000. From Eto (2001).

Figure 2.8a: Photograph of the Showa crater from the south-eastern side of Minamidake crater during October 2008.

Figure 2.8b: Photograph of the Showa crater (deeper than 2008) during a small ash explosion, 21st August, 2009.

Future activity at Sakurajima, particularly the possibility of another large eruption, has been examined by Ishihara (2006). Observations of ground deformation indicate that the current volume of magma that has accumulated in the Aira Caldera is ~80% of the volume discharged in 1914, with magma supply rates estimated at 6.9 x 10^6 m^3/year (Iguchi et al., 2008b). This suggests that another large eruption could happen within 20 years or less (Ishihara, 2006). Several scenarios for the next large eruption are possible, including intensification of

vulcanian summit eruptions, opening of new fissure vents, partial collapse of the flank of Minamidake, or submarine eruptions (Ishihara, 2006). Therefore higher exposures to volcanic ash for local populations in the future seem inevitable, and a large eruption would cause heavy ashfall over hundreds of kilometres exposing much larger areas than at present (Kobayashi and Tameike, 2002).

2.4.2 *Eruption Mechanics*

Current vulcanian explosions occur when the solidified lava dome that caps the conduit ruptures, leading to an air shock and emissions of gas and ash (Ishihara, 1985). Intensive geophysical monitoring has helped to produce macroscopic models of explosive vulcanian eruptions at Sakurajima (Iguchi et al., 2008a). A typical vulcanian eruption at Sakurajima can be divided into five main processes as demonstrated in Figure 2.9.
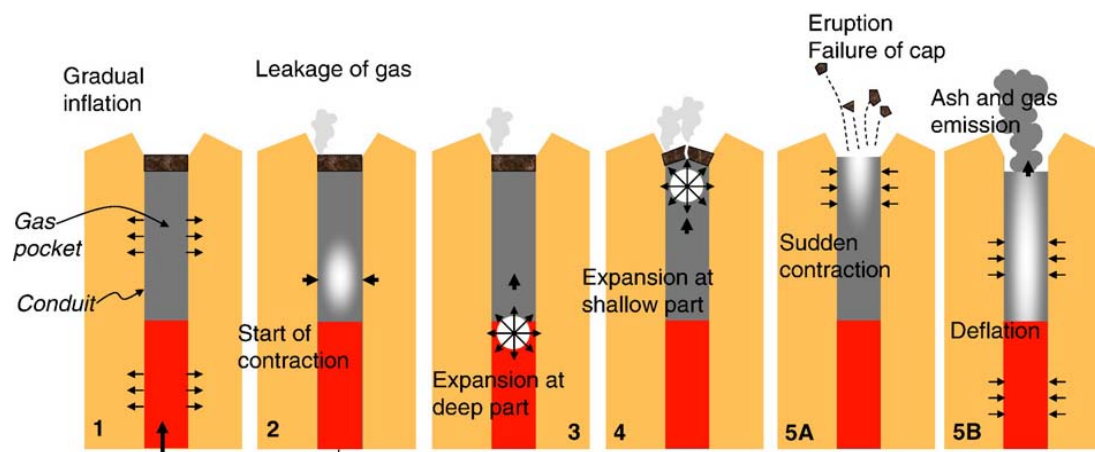
Figure 2.9: Summary of explosive eruption mechanism based on geophysical observations at Sakurajima volcano. From Iguchi et al. (2008)a.

Stage 1: Magma intrusion and accumulation of volcanic gas in the conduit below a confining cap (solidified lava dome), leading to pressure and volume increases.
Stage 2: Leaking of gas as the gas pressure exceeds the strength of the cap, resulting in minor contraction.
Stage 3: Pressure decrease from Stage 2, causes sudden outgassing of water-saturated magma deep in the conduit.
Stage 4: Expansion and increased pressure in the shallower parts of the conduit.
Stage 5: **A**. Increased pressure destroys the cap at the top of the conduit, releasing volcanic products. The gas pocket at upper part of the conduit collapses, inducing contraction and ground deformation in the shallow part of the system. **B**. Ash and gas emission from the conduit, continued pressure and volume decreases progressing down the conduit.

Typical eruption sequences at Sakurajima begin with a phase of strombolian activity, when magma rises to the top of the conduit and a weak, non-explosive eruption from an open vent causes ash and gas to be ejected intermittently (Yamanoi et al., 2008). As activity decreases, lava solidifies at the top of the conduit to form a vent cap (Yamanoi et al., 2008). It is thought that before a vulcanian eruption a gas pocket is created below the lava cap (Ishihara, 1990). It forms because magma rising into the conduit reduces hydrostatic pressure, causing gas bubbles to form via nucleation (Uhira and Takeo, 1994). Separated gas is then trapped beneath the lava plug (Uhira and Takeo, 1994). As more magma intrudes into the conduit, slow expansion exerts pressure on the gas pocket (Iguchi et al., 2008a). As pressure increases, the lava plug swells upwards (Yokoo et al., 2009). This could explain why a small lava dome is often observed before the onset of a vulcanian eruption (Ishihara et al., 1985). The formation of a small lava dome (Figure 2.10) is important for respiratory health hazards as it is an indicator that the ash may contain cristobalite, which is thought to form in lava domes by vapour-phase crystallisation or devitrification of volcanic glass (Baxter et al., 1999).

Figure 2.10: A photograph of a lava dome at the base of Minamidake summit crater, taken on 4th November 1976. The dome is several tens of metres in diameter. From Ishihara (1985).

The initiation of an explosive eruption is due to an initial slight failure of the dome as the upward pressure exceeds the strength of the dome (Iguchi et al., 2008a). The subsequent leakage of gases from the cap leads to a small contraction and decrease of pressure (Ishihara, 1990). This affects deeper (~2 km), water-saturated magmas, and causes rapid outgassing in the deeper magma (Iguchi et al., 2008a). An abrupt increase in volume and pressure at depth leads to expansion in the shallower parts (~0.5 km) of the conduit, destroying the cap and creating an air shock and ejection of volcanic bombs, gas and ash in an explosive eruption (Iguchi et al., 2008a). Finally, as the cap is destroyed there is rapid decrease in pressure and contraction moving down the conduit (Iguchi et al., 2008a). Afterwards, passive emissions of ash and gas are thought to occur from the magma moving up the conduit that has already degassed (Uhira and Takeo, 1994; Kobayashi et al., 2007).

The exact mechanisms that caused the historical plinian style eruptions have not been documented, however they are likely to be related to a coupled magma chamber system that exists below Sakurajima volcano (Uto et al., 2005). The lower, larger chamber is located 10 km under the Aira caldera and the upper chamber is located 4-6 km underneath Sakurajima volcano (Yanagi et al., 1991; Uto et al., 2005). The structure of the chamber system beneath Sakurajima volcano is shown in Figure 2.11.

Examination of the mineralogy of the lava flows revealed a compositional change from dacitic to andesitic over time. SiO_2 percentages have decreased progressively with each large eruption from 67 to 57 wt. % (Yanagi et al., 1991; Uto et al., 2005). A process of magma mixing occurs between volatile-rich basaltic magma and mantle-derived magma, with progressive increases in the amount of basaltic magma over time (Uto et al., 2005). Ash from the recent eruptive phase, however, contains ~62 wt % SiO_2, and no temporal patterns in the composition of the ash have been observed (Ishihara, 1999). Therefore this mechanism may not be relevant to more recent smaller eruptions.
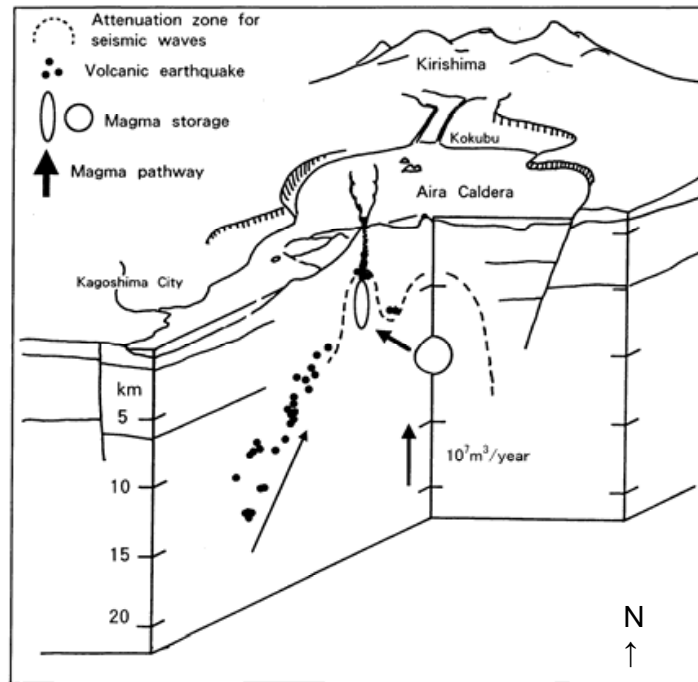
Figure 2.11: A model of the chamber structure supplying magma to Sakurajima volcano. From Ishihara (2006).

2.4.3 Ash dispersal

Volcanic ash erupted from Sakurajima volcano consists mainly of volcanic glass and feldspar as well as small amounts of cristobalite and pyroxene and trace amount of magnetite (Kawano and Tomita, 2001a; Kawano and Tomita, 2001b). Plumes of ash are usually erupted 1 – 3 km a.s.l. with varying ash content depending on the size and type of the eruption (Kinoshita et al., 1993). The plume types and depositional patterns from Sakurajima have been studied extensively using video, satellite and total suspended particulate (TSP) by a series of papers by Kinoshita (1994, 1996) and Kinoshita et al. (1993, 2000). Many scenarios can be seen at Sakurajima but the typical patterns are outlined here.

The dispersal of eruption plumes from Sakurajima is a function of eruption type, magnitude and wind velocity and direction (Kinoshita, 1996). Plumes from Sakurajima vary from single large eruption columns reaching several kilometres

into the atmosphere to several smaller eruption columns from numerous eruptions to easily diffused small plumes, with little or no ash (Durand et al., 2001). Depending on wind strength, plumes may rise straight up to an equilibrium height and turn over (low wind velocity); slant up to an equilibrium height then blowing along the wind direction (medium wind velocity); or have little or no rise under strong winds when the plume is blown almost horizontally away from the crater (Kinoshita, 1994). Occasionally, very strong winds cause the plume to collapse, creating mountain lee waves. These plumes types are shown in Figure 2.12. Kinoshita (1996) found that in general more ash was deposited close to the volcano, with average grain-size decreasing with distance from the volcano.

Vertical wind shear also affects ashfall patterns as it influences the horizontal distribution of the plume. The main horizontal plume distributions and corresponding patterns of ash dispersal are outlined in Table 2.1. Prevailing north-easterly winds during the winter which reverse during the summer (Kiyotaka, 1990), also lead to seasonal changes in the areas affected by ashfall (Imayoshi et al., 1982). Hence, a large variety of ash dispersal and deposition patterns can be observed from Sakurajima. Furthermore, as eruption type and weather conditions vary during a single eruption sequence, so will the spatial deposition of ash (Kinoshita and Togoshi, 2000).

Figure 2.12: Typical plume types erupted from Sakurajima volcano. A: vertical rise, B: slanting rise, C: almost no rise, D: plume collapse. All images obtained from: http://es.educ.kumamoto-u.ac.jp/volc/sakushowa/

Table 2.1: The principle plume types caused by changes in vertical wind shear and associated deposition patterns observed from vulcanian eruptions of Sakurajima volcano. From Durand et al. (2001).

Plume type	Character of ash deposition
Linear advection	Spatially constrained deposition path, giving intense tephra fall in narrow tephra sector
Fan type-dispersion	Spatially extensive but relatively weak ash fall, especially at distal locations since intensity diminishes rapidly downwind as plume spreads
Belt-type diffusion	Acute spatial variations in tephra fall intensity; adjacent regions may experience intense and minimal deposition simultaneously. Tephra may fall in unexpected areas, especially if rapidly changing meteorological conditions cause sudden changes in plume dispersion.
Lee wave formation	Rapid windspeeds may hinder fallout of smaller particles. Linear plume leads to narrow tephra sector. Surface air quality hazard posed on volcano flanks and possibly beyond.

Eto (2001) examined ash deposition and, in agreement with Kinoshita's observations, found that the amount of deposited ash, the airborne ash concentration and the average deposit grain size decreased with distance from the volcano. The results also showed that particular air monitoring stations received a greater number of individual ash-falls, suggesting that most ashfalls were along a narrow belt from a constrained volcanic plume (Eto, 2001). Eto also noted that ash dispersal distance decreases with decreasing wind velocity, and so fine ash is also deposited close to the volcano. However the relationship is not simple, highlighted by Kinoshita et al. (2000) who observed that under very strong wind conditions, the collapse of the plume and subsequent mountain lee wave caused high SO_2 concentration in association with high total suspended particulate measurements within 10km of the volcano. Hirano and Hikida (1988) also observed a decrease in the mean diameter of ash deposits with increasing distance from the volcano.

On the other hand, some of the epidemiological studies on the health effects of Sakurajima ash included some details regarding the ashfall patterns by analysing total suspended particulates (TSP) and suspended particulate matter (SPM; airborne particles < 10 μm), giving conflicting results to Eto (2001). Nishii et al. (1986) found that the concentration of respirable SPM did not correlate with the amount of ashfall and that TSP was highest at a moderate distance from the volcano. In fact, the lowest TSP levels were in Tarumizu, the town closest to Sakurajima in the study (Nishii et al., 1986). They concluded from this that populations at moderate distances would have the highest exposures to volcanic ash (Koizumi et al., 1988). Yano et al. (1986) also found that airborne particulate concentrations under the plume were highest mid-distance from the volcano. However the TSP and SPM data include particulates from sources other than volcanic ash, such as car emissions, and this should be taken into account when analysing results.

With respect to the general grain-size of ash produced by Sakurajima; Yano et al. (1986) observed that 97% of a collected airborne sample was < 10 μm. However, Koizumi et al. (1988) reviewed several studies and concluded that most of the ash was too coarse to be respirable, whilst Toyama et al. (1980) observed respirable spherical particles from 2-5 μm in the ash, and Shirakawa et al. (1984) found that 99% by count of ash particles under 270 mesh size were <10 μm. On the other hand Horwell (2007) analysed one ash sample from Sakurajima. This study found the ash to be very coarse, with 1.95 vol. % < 10 μm and only 0.86 vol. % < 4 μm. Different methods of grain-size analysis means these results are not directly comparable, but they do demonstrate a wide range in the amounts of observed respirable material. Currently no research has tried to reconcile these fundamentally different results, highlighting the need for detailed analysis of the volcanic ash.

2.4.4   Health studies of Sakurajima volcanic ash

A total of 16 studies have been carried out on Sakurajima ash examining the effects on respiratory systems, summarised in Table 2.2. Five toxicological studies have been carried out on the Sakurajima ash. Shirakawa et al. (1984) and Samukawa et al. (2003) both concluded that the ash had some fibrogenic potential. Shirakawa et al. (1984) administered ash via intra-tracheal injection to rats and via inhalation to rats and rabbits. They identified bronchitis, pulmonary emphysema, atelectasis lung, dust nodes and the onset of pneumoconiosis in their studies. During the inhalation experiments, exposure for 4 hours a day to average concentrations of 29 or 18 mg m^{-3} of ash for rabbits and rats continued for 112 days, and animals survived for 200-800 days afterwards. This allowed enough time for any delayed effects of volcanic ash to be seen. Samukawa et al. (2003) conducted a detailed investigation into the pulmonary effects of ash erupted from Sakurajima and ash with SO_2 using an in vitro study on lung macrophages and in vivo investigations on rats. Ash was collected every day for a year, in order to administer representative samples, excluding those collected after rainfall. 85% of the particles were phagocytosed after 24 hours, and no

release of enzymes, which would occur when particles damage the macrophages, was observed in either experiment (Samukawa et al., 2003). The in vivo study exposed rats to 100 mg m^{-3} ash and 1.5 ppm SO_2 for 4 hours a day over 5 days. A control group with no exposure were also studied. This is a very high exposure, but over a short time period. Again particles were easily phagocytosed, suggesting no irreversible damage had been caused (Samukawa et al., 2003). However the process of ingesting the ash particles produced increases in particular proteins, profilins, which are associated with molecular changes that can lead to cell proliferation (Samukawa et al., 2003). In particular, the over-expression of c-jun mRNA in the macrophages of exposed animals may cause carcinogenesis, as has been seen in lungs exposed to asbestos (Samukawa et al., 2003). The authors expressed concerns that carcinogenic responses to volcanic ash exposure have not been studied at Sakurajima, especially as the most common cause of death from cancer in males in Kagoshima has been lung cancer since 1980. They suggested that further epidemiological studies are needed on this issue.

Kariya (1992) and Kariya et al. (1992) examined the lungs of deceased humans and dogs, respectively, who lived within a 10 km radius of Mount Sakurajima. In both cases intrapulmonary particulate deposits and histopathological changes were examined and results were compared with control groups from non-exposed areas. No clear differences in any of the parameters studied were observed between exposed and control groups in either study. In fact, in the study of humans, lung health appeared to be worse in the control group (Kariya, 1992). However annual SPM was higher in the 'control' town than in Kagoshima, suggesting that more pollution in the control area may have affected the results. Finally, Yano et al. (1985) studied the physical characteristics of an ash sample and its in vitro effects on human lungs. Their observations showed ash to be less toxic in the lungs than TiO_2, often used as an inert standard, with no release of macrophage enzymes and no results that could indicate an inflammatory response in the lungs. However the authors did highlight that the time period for their experiments may have been too short for the effects of long-term exposures or slow-developing symptoms to be analysed.

Eleven epidemiological studies have been carried out examining respiratory symptoms and volcanic emissions, nine of which have been carried out by either one of two authors. Wakisaka et al. (1983a) found that the number of deaths due to bronchitis and emphysema were much higher than average in areas of high ashfall. Wakisaka et al. (1984; 1985) also examined mortality statistics from respiratory ailments as a function of distance from Sakurajima and amount of volcanic ash-fall. In all cases correlations were identified between volcanic ash and increased mortality from respiratory illnesses. Wakisaka and Yanagihashi (1986) found that increases in SO_2 concentration led to an increase in mortality the following week throughout the study period. Wakisaka et al. (1989) used data on national health insurance to compare respiratory health in districts in Tarumizu with different exposures to volcanic ash. They found that treatment for acute respiratory complaints was higher in the districts with highest ashfall and a few patients who were diagnosed with pneumoconiosis were inhabitants of high ashfall districts. However, this evidence is largely anecdotal, with no data on occupation and medical history. Finally two studies (Wakisaka et al., 1978; 1983b) examined specifically the effects of volcanic ash on school children. Again, volcanic ash-fall was found to correlate positively with prevalence of respiratory problems.

Yano et al. (1986; 1990) examined the respiratory health of women between 30 and 59 years with no additional occupational exposure to volcanic ash and no history of respiratory problems. These criteria were used to represent a sub-section of the population at lowest risk from respiratory disease. Yano et al. (1986) examined three areas, representing low, medium and high volcanic ash exposures. Only a slight trend in mild respiratory symptoms increasing with increasing ash-fall was identified. Yano et al. (1990) repeated the study, redesigned to eliminate some sources of possible error in the 1986 paper (Yano et al., 1990). Respiratory effects on women were only examined in two towns, Kanoya (25 km from Sakurajima), which experiences heavy ashfalls, and Tashiro, a control town (50 km from Sakurajima). No significant differences in respiratory

symptoms were observed between the two towns (Yano et al., 1990). Yano et al. (1987) examined specifically the respiratory health of loggers who are likely to have increased exposure through remobilised ash. However, once again no relationship between ash exposure and respiratory health was found. Some of the epidemiological studies have been summarised as literature reviews for two conferences (Koizumi et al., 1988; Yano, 1986). However they do not contain the references for the individual papers. Finally, Uda et al. (1999) compared asthma in children living on Sakurajima, in Kagoshima and in Tarumizu, with a control group unaffected by volcanic emissions. Cases of asthma and related respiratory symptoms were not higher in the areas affected by ash-fall from Sakurajima.

As can be seen, there is little consensus between different studies examining the effects of the ash erupted from Sakurajima on respiratory health. Differences in sample locations and methodologies mean that results are generally not comparable. Furthermore, many of the studies do not represent realistic exposure patterns, using general SPM as a proxy for volcanic ash pollution (e.g. Kariya, 1992), disregarding the effects of high concentrations of SO_2 in very local populations (e.g. Wakisaka, 1984), and using unrepresentative ash samples (e.g. Yano et al., 1990) or exposures in toxicological studies (e.g. Samukawa et al., 2003). Moreover, the few published analyses concerning the amount of ash in the respirable fraction have produced a wide range of results. All the studies were carried out before 2003, yet rapid advancements in knowledge and methods over recent years means that assessments can now be made with more confidence. Mineralogical analyses of the volcanic ash, using the most up to date knowledge and analysis techniques will provide new evidence from a previously unconsidered aspect on the potential risk ash from Sakurajima could pose.

Table 2.2: Summary of studies considering respiratory health and eruptions of volcanic ash from Sakurajima Volcano to date.

Reference	Study Type	Study Description	Conclusion	Comments
Samukawa et al., 2003	Toxicological	In vivo experiments on rats and in vitro study of human macrophages.	Ash could be carcinogenic if inhaled.	Very high exposures used.
Yano et al., 1985	Toxicological (some mineralogy)	Studied characteristics of one ash sample and in vitro effects on human lung cells.	The effects of the ash were similar to an inert control.	Experiments may have been too short to observe delayed effects associated with long-term respiratory disease.
Shirakawa et al., 1984	Toxicological	Administered ash to rats and rabbits over long time periods.	Bronchitis, onset of pneumoconiosis, dust nodes observed.	Long time periods allowed time for development of signs of pneumoconiosis.
Kariya, 1992; Kariya et al., 1992	Clinical	Examined lungs of deceased humans and dogs living close to volcano and in a control area.	No differences observed between exposed and control group.	Area used for the control group had higher levels of pollution.
Uda et al., 1998	Epidemiological	Comparison of asthma cases in children living close to Sakurajima and a control group.	No differences observed between exposed and control group.	
Yano et al., 1990	Epidemiological	Respiratory health of women in exposed and control populations examined.	No differences between the areas were observed.	
Wakisaka et al., 1989	Epidemiological	Examined national health insurance claims in different districts of Tarumizu exposed to different amount of ashfall.	Higher number of treatments for acute respiratory problems in high ashfall districts. Only anecdotal evidence of a few cases of long-term disease developing.	
Yano et al.,1987	Epidemiological	Respiratory health of loggers exposed to remobilised ash.	No evidence to show ash exposure adversely affected respiratory health.	
Yano et al., 1986	Epidemiological	Respiratory health of women in 3 towns with low, medium and high ash exposure.	A slight increase in mild respiratory symptoms with increasing ash-fall.	
Wakisaka et al., 1983a, 1984, 1985.	Epidemiological	Examined mortality statistics on deaths from respiratory aliments compared to distance from Sakurajima and amount of ashfall.	Correlation between increased ashfall and death from respiratory illness observed.	Studies did not account for the effects of SO_2 gas in local populations.
Wakisaka et al., 1978, 1983b	Epidemiological	Examined the effects of volcanic ash on the respiratory health of school children.	Found a positive correlation between volcanic ash exposure and decreased respiratory health in school children.	

Chapter 3

Methodology

3.1 Introduction

In this chapter I outline all fieldwork and methods used, as well as providing details regarding all the samples analysed as part of the study. This includes all the samples obtained for Sakurajima volcano, but also some samples from Unzen volcano. The additional samples have been included in this study for comparative purposes only, as analyses were carried out at the same time as the Sakurajima samples and can provide direct comparisons to different eruptive styles using exactly the same analytical methods when discussing the data in Chapter 5. Although comparisons to other volcanoes and studies are also included in Chapter 5, the details of these samples are described here as the data is unpublished and the samples were collected and analysed by the author.

The descriptions of the methodologies in this chapter are written with regards to the Sakurajima samples only, starting with fieldwork and Sakurajima sample descriptions, before moving onto the reasoning for, theories behind and descriptions of all laboratory analyses. The descriptions of the samples from Unzen volcano are given at the end of the chapter as well as the analyses carried out. The methodologies for these samples are exactly the same as described for the Sakurajima samples.

3.2 Fieldwork

3.2.1 Summary

Fieldwork was carried out at Sakurajima, Kyushu Island, Japan, from 5th – 13th November, 2008. The aim of the visit was to collect a range of ash samples from Sakurajima volcano that would represent the types of ash that local populations are exposed to. The volcano was not active during the trip, but samples were obtained from the Furusato Museum of volcanic social impacts on Sakurajima, the Kagoshima branch of the Japanese Meteorological Association (JMA) and Sakurajima Volcano Observatory (SVO), who had all collected fresh samples

after previous eruptions and stored them appropriately to prevent contamination or weathering. Older samples were taken from a stratigraphic sequence at Nagasakibana quarry (shown in Figure and Table 3.1) on Sakurajima which were located in the middle of pumice fall deposits erupted during previous eruptive phases in 1471-1476 and 1914. One sample was collected from a road cutting (Figure and Table 3.1) that was also deposited during the 1914 eruption. Three samples had been sent in advance from a local contact, Dr. Yasuhiro Ishmine. Samples from eruptions in 2009 were collected by Dr. Daisuke Miki (SVO) from clean surfaces and were obtained during a second trip to Japan in August 2009.

3.2.2   Sample Selection

A range of samples was available from each of the archive sources. In general, the samples were not stored categorically, according to date, place etc. Furthermore, only JMA had a systematic sampling scheme in place, so the ash samples available were often inconsistent, making it difficult to use a specific sub-sampling procedure. Therefore samples were chosen that were representative of all the samples available by eye in the absence of immediate information on eruption style, weather conditions and ash characteristics. The chosen samples included, as much as possible, a range of locations and/or dates. All locations for archive samples have been marked in Figure and Table 3.1. All samples were mixed thoroughly before a portion was transferred to labelled plastic bags for return to the U.K. In total, 43 archive samples were collected. The sample collection details and storage conditions for samples from each source are summarised in Table 3.2. They are from the most recent eruptive phase (1954-present), characterised by frequent vulcanian eruptions and ash venting from the summit or the Showa craters (see Section 2.4 for full details).

Figure 3.1: Map showing location of deposit sampling sites (Rd.C and Nag) as well as the locations for the places noted on the archive samples (all others).

Base is ASTER L1A image dated 19/10/2003. For place abbreviations see Table 3.1

Table 3.1: Place name abbreviations and source details for samples at each location.

Abbreviation on Map	Place	Source (sample numbers)
'Site 3'	Residential house in Kagoshima	SVO (SAK19)
Aren	Arena area, Kagoshima	SVO (SAK17)
Tsu	Tsurumaru area, Kagoshima	SVO (SAK18)
Arat	Arata, previously JMA offices	JMA (J32 – J43)
Dol	Dolphin Port, Kagoshima	SVO (SAK51)
SVO	Sakurajima Volcano Observatory	SVO (SAK11, SAK21, SAK48)
SBT	SBT Observation Point	SVO (SAK16)
Sch	East Sakurajima School	JMA (J31)
Furus	Furusato Museum	SVO/Furusato Museum (SAK12, SAK22, FM23–26, FM28, FM30)
Ari	Arimura Lava Observatory	Furusato Museum (FM27, FM29)
Nag	Nagasakibana Quarry	Collected by author (Q1 – Q9)
Kurok	Kurokami Observation station	SVO (SAK13, SAK49, SAK45)
Utok	Utoko Fishing Village	SVO (SAK14)
Kom	Observation Point	SVO (SAK46)
Shir	Shirahama Town	SVO (SAK15)
Rd.C	Road Cutting (1914 deposit)	Collected by author (Q10)
Har	Old SVO – Haratuyama Branch	SVO (SAK20, SAK47)
Har T	Haratuyama Seismic Tunnel	SVO (SAK44, SAK50)

Table 3.2: Summary of the condition of the archive ash samples available from various secondary sources.

Source	Contact	N° Of Samples	I.D code (sample n°s)	Notes on sample characteristics and choice justification	Notes on Collection Procedure
Furusato Museum	Dr. Daisuke Fukushima	7	FM (23-30)	7 samples available, all collected during spring 2008 with similar visible characteristics. Two samples (FM23 & FM30) taken from same eruption at different times to check homogeneity of ash produced through an eruption. Large amount of ash in each sample. 3 samples sent in advance by Dr. Y. Ishimine.	All collected outside Furusato Museum within 24 hours of an eruption. Collected from concrete surface – could be contaminated with dust and other particles already on the surface. Noted that samples were taken from a relatively clean surface. Samples stored in plastic tubs.
JMA	Matsusue Shinichi	13	J (31-43)	Large number of samples available for years; 1958, 1979-1981, 1983-1985, 1987-1990, 1992. All collected from Arena, Kagoshima (except 1958). Range of dates obtained. Representative samples chosen 'by eye' according to colour and visible grain size. Other factors that were considered included the month samples were collected (as there is a seasonal prevailing wind direction) and the amount of ashfall (g m^{-2}).	All samples collected pristine, according to protocol outlined in Appendix A. All stored in plastic vials in a cool, dry storeroom.
SVO	Prof. Masato Iguchi	12	SAK (11-22)	Large number of samples. Three 'sets' collected. 5 samples from different locations for a single discrete eruption. 4 samples from year 2000 – providing different dates and locations to other samples. 3 samples which appeared very fine so were of particular interest.	No systematic sampling scheme in place. Methodology, location and timing of ash collection somewhat random. Most, but not all, samples collected pristine. Samples collected over 24-48hour period.
SVO (2009 samples)	Dr. Daisuke Miki	8	SAK (44-51)	Samples collected during 2009 eruptions by Dr. Miki of Sakurajima Volcano Observatory. All grey ash, from locations on Sakurajima Volcano.	Samples collected off clean surfaces from various points around Sakurajima. Ash samples usually collected over a 24-48 hour period.

Several factors limited the choice of samples. Firstly, some samples did not have a sufficiently large quantity of ash to be analysed. Although this may skew the data set towards heavier ashfalls (either from closer locations or larger eruptions), a minimum amount of ash needed for even basic analyses means it would be impossible to analyse the samples with very small amounts of ash. Depending on the results of this study, further research into exposure to respirable particles over a wider area and greater number of eruptions can be recommended. A few vials were also not considered because they were extremely full. Most samples were not stored in a laboratory and samples had to be transferred in office spaces. Therefore the samples had to be mixed within the vials. Over-packed samples were not chosen as they could not be adequately mixed before transfer. Any samples that had not been kept in sealed plastic containers were not used. As far as possible samples collected in a pristine condition according to the protocol set out by the International Volcanic Health Hazard Network (IVHHN - Appendix A) were chosen, although this was not always possible.

3.2.3   Collection of Deposited Samples

Ten samples from historical eruptions were collected from two ash deposits located on Sakurajima volcano. Historically, large, plinian eruptions have occurred at Sakurajima (see Section 2.4.1). It is important to try to gain some insight into the ash characteristics of these eruptive styles which could reoccur in the future as well as examining samples from the recent eruptive phase. Although weathering will have altered the ash characteristics to some extent, deposited samples from older eruptions can still give a general indication of the potential health hazards should Sakurajima return to its previous eruptive styles.

Samples Q1-Q9 were collected from Nagasakibana quarry on Sakurajima (location shown on Figure 3.1). The deposit consists of three pumice falls (erupted in 1471-1476, 1779-1786 and 1914) that sit on top of the Tenpyohoji lava flow from AD 764 (Figure 3.2). Due to health and safety considerations relating to the height of the deposits only certain sections could be accessed.

Figure 3.2: Photograph of pumice deposits at Nagasakibana Quarry as shown in Kobayashi et al., 2007. Photograph shows the A.D. 764 lava flow, overlain by three pumice fall deposits from the 1471-1479, 1779-1786 and 1914 eruptions. Samples taken from the right hand edge of this photograph.

Samples were collected from ashfall layers that were found between two pumice falls from the 1470s eruptions, located in the lower part of the main deposit. The ash layers were ~45 cm thick and consisted of three sequences, each starting with a dark coarse-grained unit, then a lighter grey unit of mixed grain size, with a thin, light beige, very fine-grained unit at the top of each sequence (Figure 3.3). The more weathered surface of the sequence was scraped away and one sample was carefully taken from each unit and placed into a labelled bag (see Figure 3.3 for sample names and corresponding unit layers). Care was taken not to mix adjacent layers. Each layer was a different colour and so boundaries were clearly delineated. Rain the previous night meant that the sequence was wet, making it easier to collect the samples with minimal contamination.
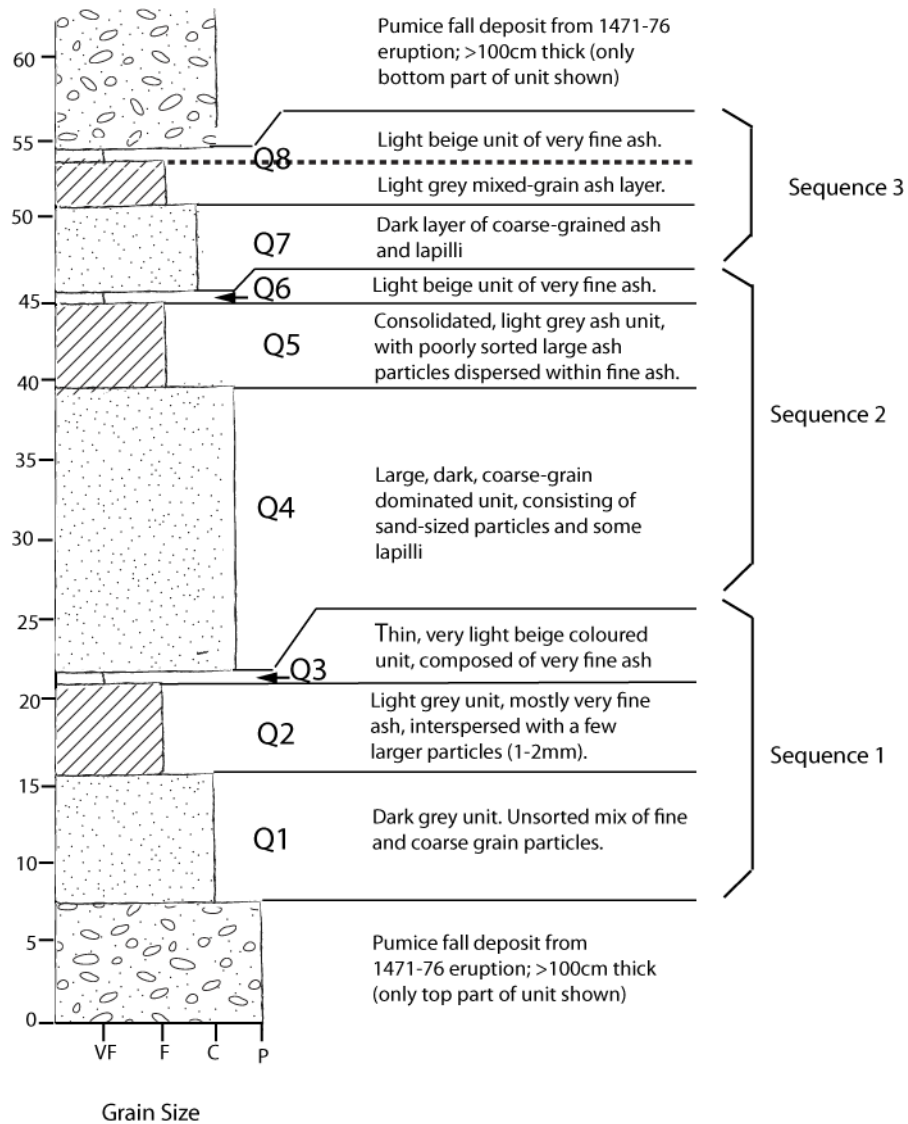
Figure 3.3: Sequence of ash layers located above the 1470 pumice fall at Nagasakibana Quarry. **P**: pumice (dots and ovals), **C**: coarse-grained ash (dots), **F**: fine-grained ash (diagonal lines), **VF**: very fine-grained ash (blank).

Another sample was taken from a second exposure in the quarry where the 1914 pumice had slumped down. This sample was taken from a layer of dark ash in the middle of the pumice fall (Figure 3.4). Finally one sample was taken from an exposed road cutting located on another part of Sakurajima (see Figure 3.1). The entire deposit derived from the 1914 eruption, although it was very contaminated with organic matter.

<u>Figure 3.4:</u> The second exposure at Nagasakibana Quarry, where an ash fall layer sits in the middle of the 1914 pumice fall which has slumped down to an accessible height. Inset shows the dark grey ash layer from which sample Q9 was collected.

3.2.4   Additional Information

The location of each sample had been noted as a name on the archive samples. The location for every sample was found and marked using a GPS whilst in Japan (marked in Figure 3.1). These points could then be used to measure distance and direction from the crater. Some additional information was noted on the sample containers, including date and time of collection and in some cases the amount of ashfall (in g m^{-2}) and eruption time. The missing eruption times and dates were obtained using the archives of the Smithsonian Institute Global Volcanism Program (SGVP) and the ash advisories from Tokyo Volcanic Ash Advisory Centre (TVAAC). Finally, weather conditions on the collection and eruption dates were looked up on www.tutiempo.net. Relevant information can be seen in the summary Table 3.3.

Table 3.3: Summary information for all samples. Abbreviations mean: XRF – X-ray Diffraction; GSA – Grain-size analysis; XRD – X-ray Diffraction; BET – BET surface area analysis; EPR – Electron Paramagnetic Resonance.

Sample I.D.	Eruption Date & (Time)	Collection Date & (Time)	Location	Distance from crater, km	Analyses Completed			Notes
					XRF/GSA	XRD	BET/EPR	
Q1	1471-76	11.11.08	Nagasakibana Quarry (31°33'26.27"N / 130°42'14.90"E)	4.9	X			Samples collected from main quarry sequence, layer A
Q2	1471-76	11.11.08	Nagasakibana Quarry (31°33'26.27"N / 130°42'14.90"E)	4.9	X	X		Samples collected from main quarry sequence, layer B
Q3	1471-76	11.11.08	Nagasakibana Quarry (31°33'26.27"N / 130°42'14.90"E)	4.9	X			Samples collected from main quarry sequence, layer C
Q4	1471-76	11.11.08	Nagasakibana Quarry (31°33'26.27"N / 130°42'14.90"E)	4.9	X			Samples collected from main quarry sequence, layer D
Q5	1471-76	11.11.08	Nagasakibana Quarry (31°33'26.27"N / 130°42'14.90"E)	4.9	X	X		Samples collected from main quarry sequence, layer E

Sample I.D.	Eruption Date & (Time)	Collection Date & (Time)	Location	Distance from crater, km	Analyses Completed			Notes
					XRF/GSA	XRD	BET/EPR	
Q6	1471-76	11.11.08	Nagasakibana Quarry (31°33'26.27"N / 130°42'14.90"E)	4.9	X			Samples collected from main quarry sequence, layer F
Q7	1471-76	11.11.08	Nagasakibana Quarry (31°33'26.27"N / 130°42'14.90"E)	4.9	X			Samples collected from main quarry sequence, layer G
Q8	1471-76	11.11.08	Nagasakibana Quarry (31°33'26.27"N / 130°42'14.90"E)	4.9	X			Samples collected from main quarry sequence, layer H
Q9	1914	11.11.08	Nagasakibana Quarry (31°33'26.27"N / 130°42'14.90"E)	4.9	X	X		Samples collected from second quarry sequence - 1914 sample
Q10	1914-1915	9.11.08	Road Cutting (31°35'53.84"N / 130°37'6.28"E)	4.3	X			Sample collected from road cutting
SAK11	7/8.5.08	9.5.08 (08:00)	SVO (31°35'25.01"N / 130°36'4.97"E)	5.5	X			2 eruptions over 48hours, ash blowing south (7th), then east (8th) collection point located to the west of the crater. Ash remained in atmosphere for 6hours+ on the 7th. Plume height (3.4 – 4 km)
SAK12	7/8.5.08	9.5.08 (09:10)	Furusato (31°33'7.78"N / 130°39'29.06"E)	3	X	X	X	2 eruptions over 48hours, ash blowing south (7th), then east (8th) collection point located to the south of the crater. Ash remained in atmosphere for 6hours+ on the 7th. Plume height (3.4 – 4 km)

Sample I.D.	Eruption Date & (Time)	Collection Date & (Time)	Location	Distance from crater, km	Analyses Completed			Notes
					XRF/GSA	XRD	BET/EPR	
SAK13	7/8.5.08	9.5.08 (10:10)	Kurokami (31°35'0.04"N / 130°42'5.91"E)	4.2	X			2 eruptions over 48hours, ash blowing south (7th), then east (8th) collection point located to the east of the crater. Ash remained in atmosphere for 6hours+ on the 7th. Plume height (3.4 – 4 km)
SAK14	7/8.5.08	9.5.08 (10:30)	Utoko (31°36'3.94"N / 130°42'34.20"E)	5.4	X			2 eruptions over 48hours, ash blowing south (7th), then east (8th) collection point located to the NE of the crater. Ash remained in atmosphere for 6hours+ on the 7th. Plume height (3.4 – 4 km)
SAK15	7/8.5.08	9.5.08 (11:10)	Shirahama (31°37'33.83"N / 130°39'49.19"E)	5.2	X			2 eruptions over 48hours, ash blowing south (7th), then east (8th) collection point located to the north of the crater. Ash remained in atmosphere for 6hours+ on the 7th. Plume height (3.4 – 4 km)
SAK16	6.6.00	6.6.00 (17:00)	SBT (31°34'1.05"N / 130°38'1.08"E)	2.7	X	X	X	One small eruption on the 6th June, no eruptions details noted.
SAK17	7.10.00 (16:42)	7.10.00	Arena (31°36'4.03"N / 130°32'12.69"E)	11.7	X			Collected in Kagoshima city very soon after one large eruption. Plume height - 5km.
SAK18	7.10.00 (16:42)	7.10.00	Tsurumaru (31°35'21.31"N / 130°32'14.66"E)	11.5	X			Collected in Kagoshima city very soon after one large eruption. Plume height - 5km.
SAK19	7.10.00 (16:42)	7.10.00	'Site 3' (31°36'46.16"N / 130°31'43.06"E)	12.8	X	X	X	Collected in Kagoshima city very soon after one large eruption. Plume height - 5km.
SAK20	16/17.12.74	17.12.74	Old SVO (31°35'25.01"N / 130°36'4.97"E)	2.7	X			Collected after two small explosions on the 16th and 17th December, no other eruption details noted.

Sample I.D.	Eruption Date & (Time)	Collection Date & (Time)	Location	Distance from crater, km	Analyses Completed			Notes
					XRF/GSA	XRD	BET/EPR	
SAK21	3.6.84	4.06.84 (09:00)	SVO (31°35'25.01"N / 130°36'4.97"E)	5.5	X	X	X	Collected during a very active period (2-5 eruptions a day) after 3 eruptions on the 3rd June
SAK22	3.12.97 (10:55)	3.12.97 (13:30)	Furusato (31°33'7.78"N / 130°39'29.06"E)	3	X	X	X	Collected after a large explosion, with ~70,000 tons ash fallout over Sakurajima. Ash cloud extended 25km S and 50km E.
FM23	14.4.08 (05:16)	14.4.08 (11:30)	Furusato (31°33'7.78"N / 130°39'29.06"E)	3	X			Collected during a relatively quiet period of volcanic activity (1- 2 eruptions per week). Eruption plume drifted SE, reaching 1.2 km.
FM24	21.4.08 (07:19)	22.4.08 (11:25)	Furusato (31°33'7.78"N / 130°39'29.06"E)	3	X			Collected after the first eruption of a 5 day sequence. Eruption plume drifted SW. The plume height was > 2.4km.
FM25	20.5.08 (12:00)	20.5.08	Furusato (31°33'7.78"N / 130°39'29.06"E)	3	X			Collected just after one explosion, on the 7th day of high volcanic activity including various eruption types. Plume height reached 3.4 km, and drifted S. 10.92mm precipitation fell during the day.
FM26	21.5.08 (07:21)	21.5.08 (13:00)	Furusato (31°33'7.78"N / 130°39'29.06"E)	3	X			Collected just after one explosion, on the 8th day of high volcanic activity. Plume height reached > 2.1 km, and drifted NE.
FM27	3.2.08 (1:18/ 6:54)	3.2.08 (16:10)	Arimura (31°33'15.42"N / 130°40'39.36"E)	3.3	X	X		Collected after 2 explosions, both extending SE. Plume heights were 1.5 – 2.7 km. They were the 1st explosions for over a month.
FM28	5.2.08 (05:36)	5.2.08 (10:00)	Furusato (31°33'7.78"N / 130°39'29.06"E)	3	X	X	X	No explosion noted. Continuous ash venting. Ash was reported but not observed in satellite imagery. Plume height was ~ 2.1km.

Sample I.D.	Eruption Date & (Time)	Collection Date & (Time)	Location	Distance from crater, km	Analyses Completed XRF/GSA	XRD	BET/EPR	Notes
FM29	6.2.08 (1:33/ 2:55)	6.2.08 (17:25)	Arimura (31°33'15.42"N / 130°40'39.36"E)	3.3	X			Very small explosions reported. Ash drifted SE, max. plume height was 2.1 km.
FM30	14.4.08 (05:16)	14.4.08	Furusato (31°33'7.78"N / 130°39'29.06"E)	3	X			Collected during a relatively quiet period of volcanic activity (1- 2 eruptions per week). Eruption plume drifted SE, reaching 1.2 km.
J31	9.6.58 (12:30)	9.6.58 (17:00)	E. Sakurajima High School (31°33'28.92"N / 130°37'47.59"E)	3.6	X			No eruption details found.
J32	14.10.79 (13:21/19 :57/22:47	15.10.79 (09:00)	Arata (31°34'28.88"N / 130°33'12.03"E)	10	X			Few eruption details known. Plume height reach ~ 1.6km. 180 g m^{-2} ash fell in Kagoshima.
J33	8.6.81 (11:28)	9.6.81 (09:00)	Arata (31°34'28.88"N / 130°33'12.03"E)	10	X			Few eruption details known. Plume height reach ~ 2.5 km. 125 g m^{-2} ash fell in Kagoshima.
J34	17/18.9. 83	18.9.83 (09:00)	Arata (31°34'28.88"N / 130°33'12.03"E)	10	X			Continuous ash eruption. 180 g m^{-2} ash fell in Kagoshima. 4.06mm precipitation noted.
J35	Unknown	30.11.83 (09:00)	Arata (31°34'28.88"N / 130°33'12.03"E)	10	X			3 eruptions noted 29th – 30th November. No other eruption details found some 30th eruptions may not be included in the sample. 49 g m^{-2} ash fell in Kagoshima.

Sample I.D.	Eruption Date & (Time)	Collection Date & (Time)	Location	Distance from crater, km	Analyses Completed			Notes
					XRF/GSA	XRD	BET/EPR	
J36	Unknown	6.5.84 (09:00)	Arata (31°34'28.88"N / 130°33'12.03"E)	10	X			Collected on the 4th day of high activity (2 -3 eruptions per day). 5 eruptions noted 5 – 6th May. No other eruption details found – some 6th eruptions may not be included in the sample. 30 g m^{-2} ash fell in Kagoshima. 9.91mm precipitation noted.
J37	Unknown	13.6.84 (09:00)	Arata (31°34'28.88"N / 130°33'12.03"E)	10	X			Collected after 2 eruptions on the 12th. 411 g m^{-2} ash fell in Kagoshima. 27.94mm precipitation
J38	Unknown	25.7.84 (09:00)	Arata (31°34'28.88"N / 130°33'12.03"E)	10	X			Collected after 3 eruptions on the 24th. 76 g m^{-2} ash fell in Kagoshima
J39	Unknown	26.8.85 (09:00)	Arata (31°34'28.88"N / 130°33'12.03"E)	10	X	X	X	Collected after one eruption on the 25th. Drizzle noted. 461 g m^{-2} ash fell in Kagoshima.
J40	Unknown	14.10.87 (09:00)	Arata (31°34'28.88"N / 130°33'12.03"E)	10	X			No eruption details found. Drizzle noted. 58 g m^{-2} ash fell in Kagoshima.
J41	Unknown	16.6.88 (09:00)	Arata (31°34'28.88"N / 130°33'12.03"E)	10	X	X		2 eruptions, plume height ~ 2.7km. Large amount of ash deposited, 2671 g m^{-2} in Kagoshima. Drizzle noted.
J42	Unknown	11.4.90 (09:00)	Arata (31°34'28.88"N / 130°33'12.03"E)	10	X			No eruption details found. 20.57mm precipitation noted. 93 g m^{-2} ash fell in Kagoshima.
J43	Unknown	28.06.92 (09:00)	Arata (31°34'28.88"N / 130°33'12.03"E)	10	X			Ash observed but not accompanied by an explosion. 50.04mm precipitation noted. 86 g m^{-2} ash fell in Kagoshima.

Sample I.D.	Eruption Date & (Time)	Collection Date & (Time)	Location	Distance from crater, km	Analyses Completed			Notes
					XRF/GSA	XRD	BET/EPR	
SAK44	21.8.09 (16:10/ 23:16)	22.8.09 (12:30)	Haratuyama Tunnel (31°35'40.92"N / 130°37'57.43"E)	3.5	X			2 small explosions producing small amounts of ash. No plume drift. Plume reached 2.1 km.
SAK45	20.08.09 (15:18/ 20:34)	21.8.09 (15:30)	Kurokami (31°35'0.04"N / 130°42'5.91"E)	4.2	X			2 small explosions. No plume drift. Plume reached 2.1 km.
SAK46	20.8.09 – 21.8.09	22.8.09 (11:10)	Kom Obs. Point (31°37'3.92"N / 130°41'8.64"E)	4.8				Only extremely small amounts of ashfall. Not enough for any analyses. Collected north of the crater over 48 hours of small explosions and ash venting.
SAK47	20.8.09 – 21.8.09	22.8.09 (10:10)	Old SVO (31°35'25.01"N / 130°36'4.97"E)	2.7	X			Collected over 48 hours of small explosions and ash venting.
SAK48	20.08.09 (15:18/ 20:34)	21.8.09 (10:00)	SVO (31°35'25.01"N / 130°36'4.97"E)	5.5	X			2 small explosions. No plume drift. Plume reached 2.1 km.
SAK49	21.8.09 (16:10/ 23:16)	22.8.09	Kurokami (31°35'0.04"N / 130°42'5.91"E)	4.2	X			2 small explosions producing small amounts of ash. No plume drift. Plume reached 2.1 km.
SAK50	18.8.09 (19:25)	20.8.09 (12:30)	Haratuyama Tunnel (31°35'40.92"N / 130°37'57.43"E)	3.5	X			Collected 48 hours after large eruption. Plume height was 3 km, with little drift.
SAK51	Unknown	20.8.09	Dolphin Port (31°35'32.52"N / 130°33'44.61"E)	9.8	X			Accumulation of small ashfalls in Kagoshima during a period of high eruptive activity (with little or no wind to disperse ash) 10th – 20th August.

3.3   Laboratory Techniques

All samples were analysed for grain size and bulk mineralogy. A subset of the original samples was chosen for more detailed mineralogical and chemical analyses once more information was available. Details regarding sample selection are given in Table 3.3 and are explained in the relevant sections.

3.3.1   Sample Preparation

Before any analyses were carried out all samples were dried and sieved and any organic matter was removed from contaminated samples. Each sample was weighed to 2 d.p., oven dried for a minimum of 12 hours at 80°C and re-weighed. A small amount of bulk dried material was stored in a plastic bag to show the original condition of the ash. Any organic matter was removed from contaminated samples using fine tweezers and aggregates were broken up gently without compromising the structure of any individual particles.

Samples were sieved manually through 2mm and 1mm meshes simultaneously, with decreasing aperture size. Endecotte stainless steel sieves were used. After agitation, the sieve was left still for several minutes with the lid on to allow any fines to settle. A brush was used to ensure all of the fine material was collected in the base layer and transferred into the sample bag. Each layer (>2mm, 1-2mm and <1mm) was removed separately, weighed and placed into an individual plastic bag. Accurate separation and weighing of the fractions are important as the weights are used in calculations of grain-size distributions. The sieve was washed with distilled water and dried between each sample. Particles > 2 mm were not used in any analyses as these particles are not defined as ash. Particles 1-2 mm in size were incorporated into some analyses, such as particle size, but in general only particles < 1 mm were used, as it is the finer fractions of ash that are relevant to respiratory health assessment. The inclusion or exclusion of the 1-2 mm fraction was taken into account when analysing results.

3.3.2   Bulk Compositional Analysis: X-ray Fluorescence

X-ray fluorescence was used to determine the major oxide composition of the ash samples. This information is useful as it can be used to categorise the ash, and also helps to inform the refractive index needed for accurate grain-size analyses. Fusion beads were created to determine the major oxide composition, as melting the ash homogenises the samples and any mineralogical effects (such as preferred orientation) will not interfere with the analyses. All the analyses were carried out in the Department of Geology at the University of Leicester.

3.3.2.1 Sample Preparation and Analysis

Firstly, ~4 g of ash was crushed into a powder using an agate pestle and mortar. The samples were thoroughly mixed prior to sub-sampling by inverting each bag several times and allowing the fines to resettle. This technique is sufficient for a representative sample to be obtained, as described in Horwell (2007). The powder was then dried overnight at 105°C to remove any adsorbed volatiles. The weight of a ceramic crucible (W1) was noted to 4 d.p., the sample added and the new weight taken (W2). Samples were then ignited at 950°C for ~1.5 hours. Samples were removed from the muffle furnace and allowed to cool. Once they had returned to room temperature they were reweighed (W3) in order to determine loss on ignition (LOI) according to the following equation:

$$LOI= 100*(W2-W3)/(W2-W1) \qquad \text{Equation 3.1}$$

Next, a tetraborate flux (sample to flux ratio 1:5, 80% Li metaborate; 20% Li tetraborate flux) was added to each ignited sample. Prior to any analyses on each day, the water loss from the flux had to be determined in order that accurate proportions of flux/sample were used. This was done by weighing out exactly 3 g flux into a Pt/5%Au crucible and melting it using a Spartan gas burner. The flux was allowed to cool, re-weighed to 4 d.p. and the weight loss determined.

For each sample, 3 g of flux plus the correction value accounting for weight loss on heating was weighed into a Pt/Au crucible. 0.6 g of the ignited sample was added to the flux and the two were mixed thoroughly. All weights were accurate to 4 d.p. The sample-flux mix was then heated on a Spartan gas burner to melt and fuse it. The mixture was agitated (by swirling) during fusion to ensure any particles stuck to the sides of the crucible were included and to remove any gas bubbles. The mixture was homogenised by swirling over a Meker gas burner and re-heated on the fusion burner. It was then poured into the centre of a heated Pt/Au casting dish to create a disk of liquid which was cooled under a forced air cooling system until the disk had visibly parted from the casting dish. Finally, each fusion bead was allowed to cool to room temperature, labelled, ensuring that the side for analysis was not touched or contaminated, and the crucible was cleaned in 10% nitric acid solution in an ultrasonic bath for at least 10 minutes. Only titanium-tipped tongs were used when handling the Pt/Au crucibles.

XRF analyses of the beads were carried out by Nick Marsh at the University of Leicester on the PANalytical Axios Advanced XRF spectrometer.

3.3.3   Grain-Size Analysis: Laser Diffraction

Grain-size analysis provides the primary data needed for risk assessment of potential respiratory health hazards from volcanic ash. It can rapidly indicate whether there is a potential risk and whether further analyses are needed, depending on the proportion of the ash that is small enough to be inhaled. There are several methods to determine the grain size of ash particles; however laser diffraction provides accurate, reproducible results very quickly, with little sample preparation, and can measure particles from 0.2 to 2000 µm equivalent spherical diameter, making it particularly applicable for analysis of health-pertinent fractions of ash. Equivalent spherical diameter was measured rather than aerodynamic diameter, as large amounts of ash and very specialist equipment and methodologies are needed to measure the latter, which are outside the scope of this study. Furthermore, most respiratory health studies of volcanic ash have

used laser diffraction methods, meaning these results can be compared to previous studies on volcanic ash and respiratory health that have used the same method (e.g. Horwell, 2007). Laser diffraction should still provide a good approximation of the amount of respirable ash in the samples and studies examining the use of equivalent spherical diameter as opposed to aerodynamic diameter have been examined and discussed in the relevant sections (Section 5.2).

For this study, the Malvern Mastersizer 2000 with Hydro MU attachment in the Department of Geography at the University of Cambridge was used. This employs the Mie light scattering theory to calculate the volume % of different particle sizes. The Mie theory uses the Maxwell equations (which describe the fundamental laws of electromagnetism) to estimate particle size by measuring the scatter and intensity of a laser beam passing through the particles. The theory assumes spherical particle shape, which may lead to non-spherical particles being assigned to different size bins (Eshel et al., 2004). However no theory exists to measure non-spherical particles. All samples were measured. Samples obtained from the 2009 eruptions were analysed at a later point, although samples J43 and S22 were repeated to check the reproducibility of results. Particles larger than 1 mm were not analysed directly to ensure that no particles close to 2 mm that may damage the machine were included. Results were adjusted by subsequent calculations to include the 1-2 mm fraction.

3.3.3.1 Sample Preparation

Samples were mixed by bag inversion and fines allowed to resettle before a sub-sample was removed.

3.3.3.2 Sample Analysis

Each sample was measured in water with ultrasound treatment to prevent particle aggregation. The machine was set-up with the following parameters:

Measurement time:	10 s
Snaps:	10,000
Pump speed:	2,500 rpm
Ultrasonic displacement:	10
Refractive index:	1.63
Adsorption:	0.1

Of these the refractive index is particularly important as it varies among different ash types. The refractive index is needed as it accounts for the absorption of the particle which also influences laser intensity. Detailed information about applying an appropriate refractive index for volcanic ash samples is outlined in Horwell (2007). For Sakurajima ash samples a refractive index of 1.63 was chosen. Although little mineralogical information was available about the ash samples, SiO_2 weight percentages lay predominately in the andesitic range, and this value has been tested and used accurately for andesitic ash from other volcanoes (e.g. Horwell et al., 2003a; Horwell, 2007). Enough sample was added to the water so that the obscuration value was between 5-20% before each measurement was started. Three measurements were taken and the mean calculated.

3.3.3.3 Data Manipulation

Results were expressed in terms of volume % using internally defined bins that are not applicable to health-relevant fractions. Therefore the results were converted to cumulative volume percentages and the percentages for the precise health-pertinent diameters were estimated by interpolation of the bin sizes immediately to either side of the particle size of interest.

In order to incorporate the 1-2 mm fraction of the ash, the data were rescaled, using the fraction weights measured after sieving. However, inaccuracies inherent to sieving and measurement of non-spherical particles meant that first, the fraction weights for some samples had to be adjusted to account for particles that had passed through the 1 mm mesh but were measured as > 1 mm equivalent

spherical diameter by the Malvern Mastersizer. This was done according to the following equations:

$$M1* = M1 - [(M1 \text{ x } v2*)/100] \qquad \text{Equation 3.2a}$$
$$M2* = M2 + [(M1 \text{ x } v2*)/100] \qquad \text{Equation 3.2b}$$

Where,

$M1$ = the original sieved mass of the < 1 mm fraction,

$v2*$ = the vol. % of the sample that was > 1 mm as recognised by the Malvern Mastersizer,

$M1*$ = readjusted fraction weight for the < 1 mm fraction and,

$M2*$ = readjusted fraction weight for the 1-2 mm fraction

This calculates the mass of particles > 1 mm according to the Malvern measurements, that were included in the sieved < 1 mm fraction, and adds or subtracts this to give adjusted sieved weights $M1*$ and $M2*$ for the < 1 mm and 1-2 mm fractions, respectively. The grain-size distributions then also have to be adjusted to account for sieving errors by:

$$P1* = P1 \text{ x } (100/v1*) \qquad \text{Equation 3.3}$$

Where,

$P1$ = the original Malvern vol. % for a particular size bin,

$v1*$ = the vol. % of the sample that was < 1 mm as measured by the Malvern Mastersizer and,

$P1*$ = the adjusted vol. % result, to exclude any particles measured as > 1 mm by the Malvern.

These calculations are necessary as any particles > 1 mm in the Malvern grain-size results need to be removed and added to the sieved weights in order to subsequently rescale the Malvern particle-size distributions to include all particles in the 1-2 mm fraction, as shown in Equations 3.4 and 3.5:

$$P2 = P1* \times (M1*/M1*+M2*) \qquad \text{Equation 3.4}$$

P2 is the final rescaled vol. % for all bins < 1 mm to account for the ash in the 1-2 mm fraction not included in direct measurements. M1* and M2* will be the same as M1 and M2 where no particles > 1 mm have been measured by the Malvern. The 1-2 mm weight is then converted to a vol. % to complete the grain-size distribution:

$$P\ 1\text{-}2mm = (M2* / (M1* + M2*)) \times 100 \qquad \text{Equation 3.5}$$

Detailed worked examples of these calculations for all samples, as well as the bin interpolation and cumulative volume percentage calculations can be examined in the grain-size excel sheet ('GSA') on the Appendix CD (Appendix B).

3.3.4 Determination of Crystalline Silica Content: X-ray Diffraction

X-ray diffraction (XRD) can be used to identify single mineral phases in mixed samples such as crystalline silica in volcanic ash. XRD is preferable to other methods of identifying crystalline silica in ash samples because it can distinguish between the different silica polymorphs and so more exact data can be obtained on the mineralogical properties of the potentially toxic crystalline silica components in the ash. Identifying cristobalite, the most important structure in terms of volcanic ash and respiratory health, has however been problematic (Dollberg et al., 1986) until recently. If plagioclase feldspar is present in the ash sample, the feldspar peaks overlie the cristobalite peaks in the XRD pattern and this inhibits accurate quantification. Previously, the Talvitie method was used, which involves digestion of the sample to remove all non-crystalline silica phases (Talvitie, 1951). However errors can easily be introduced if the digestion time is incorrect. Cressey & Schofield (1996) introduced a new 'peak stripping' method, using an X-ray diffractometer with a static position sensitive detector (XRD-sPSD) which allowed diffraction intensities to be measured across all angles (0-120° 2θ) simultaneously. This also greatly reduces the analysis time, reducing

errors from preferential crystal orientations in the mount, and increasing resolution so that the cristobalite could be distinguished from feldspar. However, knowledge of all other mineral phases is needed in this method. This requires detailed mineralogical studies prior to analysis which can cause problems and errors introduced by the need for appropriate standards for each mineral phase. Both of these methods can be time-consuming, requiring a high level of expertise and experience, and are not appropriate for studies where only a single phase needs to be identified quickly.

Very recently, the 'peak-stripping' method has been modified, using an internal attenuation standard (IAS) to quantify the mineral of interest by treating the IAS and the sample as a pseudobinary phase, thereby avoiding the need for detailed mineralogical analysis of the sample. In this method, reproducible, near-random XRD patterns can be produced quickly, by direct measurement of the sample itself and without prior knowledge of the mineralogy of the sample. A detailed analysis of the new IAS method and comparison to the peak-stripping method is accounted in Le Blond et al. (2009). The relevant parts of the theory are described in the calculations outlined at the end of this section.

Time constraints meant that only 12 samples were used to determine the amount of crystalline silica typically present in Sakurajima ash. Samples were chosen that represented a range of eruption dates and locations, but excluded samples with low quantities of respirable material. Table 3.3 gives the details of the samples used. An Enraf-Nonius sPSD 120° diffractometer at the Natural History Museum, UK was used.

3.3.4.1 Sample Preparation

Firstly ~3 g of each sample (< 1 mm sub-sample) was ground into a powder (~5-20 μm) using an agate pestle and mortar. Ideally, only the respirable fraction of the ash samples would have been used to better represent the exposure of the

local population. However, due to the time constraints on this project, separation of the respirable fraction of the ash was not possible.

Samples were packed into a circular aluminium deep well (15 mm x 1 mm) mount and the surface was slightly roughened using the knife edge of a spatula in a cut-scrape manner (see Batchelder and Cressey, 1998 for detailed description of the preparation methods). This ensured that all samples and standards were well-packed to uniform density, had a flat surface level with the mount rim, but gave a near-random pattern and avoided preferred crystal orientation. The accuracy and reproducibility of XRD patterns using this method of preparation has been demonstrated by Batchelder and Cressy (1998). In addition to the samples, pure standards for cristobalite, quartz, labradorite, andesine and ZnO were also measured.

3.3.4.2 Sample Analysis

A Germanium 111 single crystal was used to produce the X-rays. Before each session the machine was calibrated using NBS silicon powder and silver behenate as external 2θ calibration standards. Enraf-gufi software was then used to carry out the 2θ linearization using a least-squares cubic spline function. The machine was set up with the following parameters:

Radiation:	CuKα1
Slit Size:	0.12 x 5 mm
Geometry*:	33°
Ų:	6.5
EHT:	20 kV
Analysis Time:	10 minutes

*Geometry is the angle of the sample surface to the incident beam.

Each sample and standard was spun in a single horizontal plane whilst measurements were taken for 10 minutes.

Next the samples were mixed with a known amount of the internal attenuation standard (ZnO). Zinc oxide was used for the IAS as it is not present in volcanic ash samples, has a similar attenuation coefficient and its peaks do not overlap any of the crystalline silica peaks. Samples were weighed and ~30-40 wt. % ZnO was mixed into the sample. The exact weight % of ZnO was noted for use in the later analyses. The ash and ZnO were well mixed and re-powdered using the pestle and mortar. The new mix was re-packed into the deep well and re-run for a further 10 minutes. Each sample was only measured once. Ideally, repeat samples would have been carried out, however analyses were limited by the time and resources available for the project. Most measurements were taken in the same session to ensure exactly the same experimental conditions were used throughout the analysis. A few samples were run in a separate session, and for these the standards were also re-run and reproducibility was checked by repeating the analysis of sample SAK21.

3.3.4.3 Data Manipulation

To work out the weight percentage of cristobalite in the sample from the XRD patterns, the cristobalite peaks in the full sample XRD pattern are compared to the pure standard XRD pattern. For this, Enraf-Gufi software was used. The pure phase cristobalite pattern is superimposed onto the mixed pattern data, and the pure cristobalite peaks can then be proportioned down until the counts of the pure phase pattern match the sample pattern as closely as possible (Le Blond et al., 2009). To check the scaling, the software can subtract the proportioned pure standard from the mixed pattern. If the scaling is wrong the residual cristobalite peak in the mixed pattern will sit well above or below the background level. As the feldspar peak still sits over the main cristobalite peak, the peaks for the full pattern data must be used to fit the cristobalite peaks.

However, in order for the two peaks to be comparable in this manner all other influences on peak intensity have to be accounted for as shown in Equation 3.6:

$$X\text{cristobalite} = (t'/t)*(Io'/Io)*[(\mu/\varrho)\text{cristobalite}/(\mu/\varrho)\text{sample}]*W\text{cristobalite}$$

Equation 3.6

Where:

Xcristobalite = the peak intensity of the cristobalite in the mixed sample relative to the peak intensity of the pure cristobalite (the scaled value obtained from Enraf-Gufi),

t'/t = the measurement time for the mixed sample divided by the measurement time for the cristobalite standard,

Io'/Io = the beam flux for the mixed sample divided by the beam flux for the pure standard,

(μ/ϱ) = mass attenuation coefficient and,

Wcristobalite = the wt. % of cristobalite in the mixed sample.

In simpler terms peak intensity is a function of the quantity of cristobalite, measurement time, beam flux, sample volume and sample adsorption. Preparation and measurement conditions ensure that measurement time, beam flux and sample volume are all constant between all samples and standards, so they cancel in Equation 3.6. Therefore in order to ascertain the amount of cristobalite in the sample the mass attenuation coefficient (to account for adsorption) for the sample needs to obtained. The internal attenuation standard can be used to work out the mass attenuation coefficient of the sample only by considering the sample-IAS mix as a pseudobinary phase. This is done by normalising the pattern intensities of the pure ZnO and the ZnO in the mixed sample in LinkFit using a least squares pattern fitting function. Using the known wt. % and mass attenuation coefficient of the IAS, (μ/ϱ)sample can then be worked out:

$$(\mu/\varrho)sample = [(\mu/\varrho)IAS*WIAS*(1/\mathsf{X}IAS\ -1)]/(1-WIAS)]$$

<div align="right">Equation 3.7</div>

Where:

WIAS = the wt. % of ZnO in the sample/ZnO mix,

XIAS = the normalised value for the least squared fit found using the LinkFit program and,

(1-WIAS) = the wt. % of the sample in the ZnO/sample mix.

Once (μ/ϱ)sample has been calculated, Equation 3.6 can be solved to give the wt. % of cristobalite in the sample as shown in Equation 3.8:

$$Wcristobalite = \mathsf{X}cristobalite*(\mu/\varrho)sample \ / \ (\mu/\varrho)cristobalite$$

<div align="right">Equation 3.8</div>

Worked calculations for the sample data can be found in the excel worksheet ('XRD') on the data CD (Appendix B). All equations here were followed according to Le Blond et al. (2009).

3.3.5   *Specific Surface Area: BET Analysis.*

The Branauer Emmet Teller (BET) method was used to determine the surface areas of those samples that were chosen to examine surface reactivity. BET uses the theory of physical gas adsorption to work out the specific surface area of a powder by measuring the amount of nitrogen adsorbed in relationship to pressure, at the boiling point of liquid nitrogen. Surface area was measured in order to standardize the surface reactivity results per unit area of ash. Seven samples were chosen from the twelve used for XRD analysis. The number of samples was reduced because samples were excluded if rain had been noted on the collection or eruption dates, or if collection was known to have been more than 24 hours after the eruption (apart from sample SAK12 which was included as it was the finest archive sample); in this way, only the most pristine samples

were used for surface reactivity analyses (see Table 3.3). The surface area analyses were carried out using nitrogen gas on a Micromeritics TriStar 3000 Surface Area and Porosimetry Analyser in the Department of Chemistry, Durham University.

3.3.5.1 Sample Preparation

Prior to analysis, samples were dried at 150ºC in a vacuum oven to ensure that they were completely dry. Samples were then placed into ½ inch BET tubes, weighed, outgassed using nitrogen gas at 150°C overnight and re-weighed to 4 d.p.

3.3.5.2 Sample Analysis

An isothermal jacket was placed around, and filler rod put into, each tube and the tubes were loaded into the machine. Gloves were worn so that no grease was present on the inside of the tube or on the filler rods. A pressure test was carried out to ensure that the tubes were loaded into ports properly and the weight of each sample to 4 d.p. was given for each corresponding port. The samples could then be measured under vacuum, with the sample tubes immersed in liquid nitrogen. The machine was set up to measure only the first part of the adsorption isotherm ($0 - 0.3$ p/p°) over 10 points, to reduce the analysis time and increase the accuracy of measurements. After each analysis it was ensured that measurements were sufficiently accurate for the parameters of this study (minimum correlation coefficient = 0.999, see Section 4.5.1 for explanation). Analyses for each sample were repeated twice and an average taken.

3.3.6   Surface Reactivity: Electron Paramagnetic Resonance

In the study of mineral dusts, electron paramagnetic resonance has been used as a direct measurement of free radicals produced by fractured surfaces in order to try to estimate the reactivity of particles (Fubini et al., 1995). Recently, this technique has been applied to the study of volcanic ash, focussing on hydroxyl

radical release catalysed by iron on particle surfaces (Horwell et al., 2003a; Horwell et al., 2007). The reproduction of the Fenton reaction (Equation 3.9) that occurs in the lungs is used to give an indication of the potential reactivity of particles in the lungs.

$$Fe^{2+} + H_2O_2 \rightarrow Fe^{3+} + OH^- + HO\bullet \hspace{2cm} \text{Equation 3.9}$$

Electron paramagnetic resonance spectrometry was used to measure the radicals released into solution from the samples. The target free radicals were $OH\bullet$, as according to the Fenton reaction (Equation 3.9). Free radicals have very short half lives and hence cannot be measured directly. A spin-trap is used to stabilise the radicals in the form of adducts which can subsequently be detected and quantified by EPR spectrometry. 5,5'-dimethyl-1-pyroline-N-oxide (DMPO) was employed as a spin trap. Analyses were carried out on a Miniscope 100 ESR spectrometer, Magnettech, at the Dipartimento di Chimica, Università degli Studi di Torino.

3.3.6.1 Sample Preparation

150 mg of ash was added to a darkened bottle (to prevent UV light interfering with the reactions) along with 500 μl phosphate buffer (0.5M) to maintain the solution at pH 7.4 and 250 μl DMPO (0.5M), employed as a spin-trap. 500 μl H_2O_2 (0.2 ml 30wt.% H_2O_2 in 10ml H_2O), was then added immediately, to initiate the Fenton reaction with iron on the ash surfaces. The solution was then placed on a magnetic stirrer. Control experiments, containing no ash, were carried out prior to analysis with ash each day and when a new solution was made up.

3.3.6.2 Sample Analysis

The experiments were carried out for 60 minutes. At 10, 30 and 60 minutes a sub-sample of each solution was analysed. The sub-sample was removed from the bottle into a 50 μl capillary tube using a syringe with a 0.25 μm filter attached

to prevent any ash residue from entering or blocking the capillary tube, also thereby halting the Fenton reaction in the tube. No air bubbles could be present in the capillary tube. The solution was then analysed in the EPR spectrometer, set up with the following parameters:

Receiver Gain:	9×10^2
Microwave power:	10 mW
Microwave attenuation:	10 dB
Modulation amplitude:	1G
Scan (sweep) time:	80 s
No. of Scans:	2
BO Field:	3344.15
Sweep length:	120
Smooth:	0
Steps:	4096

Mn^{2+} in $CaCO_3$ was used as a calibration standard, which was incorporated into the final calculations. Mn^{2+} was used as its peaks do not overlap with those produced by the DMPO adducts. Two repeats were carried out for each sample.

3.3.6.3 Data Manipulation

The twice integrated amplitude of the peaks produced (e.g. Figure 3.5) is proportional to the number of radicals. Peak integration was done using Origin 6.1 software. Integrations were converted to number of radicals by including the peak integrations for the Mn^{2+} calibration standard. Results were expressed per unit area of ash using the results from BET analysis. Calculations can be examined in the 'EPR' excel sheet on the Appendix B CD.

Figure 3.5: A typical example pattern produced by EPR. The Middle four peaks represent OH• radical release and the large outer two peaks are from the Mn^{2+} standard.

3.3.7 Iron Release: Spectrophotometry

Quantifying the amount of iron available at the surfaces of ash particles is important due to the role of surface Fe^{2+} in the Fenton reaction. Spectrophotometry was used to estimate the amount of iron that could be released from the ash surface in the lungs. Ferrozine, a bidentate N donor chelator (pH 4) was used to remove iron species from the particle surface. Ferrozine is a chelator specific to Fe^{2+}, however ascorbic acid can be used in addition to ferrozine to reduce Fe^{3+} to Fe^{2+}. Similarly Fe^{3+} may be reduced in the lungs via the Haber Weiss cycle, making it available for participation in the Fenton reaction. Samples were analysed in the absence and presence of ascorbic acid to estimate the Fe^{2+} and total Fe present. Fe^{3+} can then be calculated by subtracting Fe^{2+} results from those for total iron. Chelated iron reacts with the ferrozine to create a purple coloured complex, the depth of which can be measured by spectrophotometry. Samples were analysed in a Uvikon spectrophotometer at the Dipartimento di Chimica, Università degli Studi di Torino.

3.3.7.1 Sample Preparation

Two lots of 20 mg for each sample were weighed out into labelled centrifuge tubes. 10 ml ferrozine (1 mMol) and 10 ml ascorbate (6 mMol) were added to one tube for each sample, and 10 ml ferrozine and 10 ml bi-distilled water were added to the other. Two control solutions containing no ash were also made up. The solutions were then placed in a shaker set at 37°C.

3.3.7.2 Sample Analysis

Measurements were taken at 4 hours, 24 hours and once every 24 hours thereafter during 7 days, except for the weekend. Therefore measurements were taken on days 0,1,2,3,4 and 7. A sub-sample of 1.5 ml of each solution was removed and placed into a microtube. These were centrifuged for 15 minutes. A maximum of 20 samples can be centrifuged each time. Taking care not to disturb the centrifuged solutions, in order that the ash is not remobilised, 1 ml was extracted and the aliquot placed into a cuvette for measurement. The spectrophotometer set up is as follows:

Wavelength: 562
Delay: 0.55
Average time: 3 seconds
Calc. Mode: OFF

Before analysis, the machine was autozeroed using the corresponding blank sample and an empty cuvette. When the ferrozine blank was used, the empty cuvette was replaced by the aliquots containing only ferrozine and the adsorption was measured. The spectrophotometer was re-zeroed using the ferrozine and ascorbate blank and the procedure was repeated with the corresponding ferrozine and ascorbate solutions. Once the analysis was completed all the removed solution (1.5 ml) was replaced back into the main centrifuge tubes, because the calculations assume constant volume.

However the solutions were not replaced if dilution of the aliquot was required. The spectrophotometer is only accurate up to adsorption values of 2. Therefore if the solution became too dark (deep purple), dilution was required to keep values below 2. The aliquots were diluted with bi-distilled water. Any diluted aliquots could not be replaced into the main centrifuges and so care was taken to note the dilution ratio and the amount of solution removed. For example if an aliquot was diluted 1:1, 0.5 ml of solution was removed from the centrifuged aliquot and mixed with 0.5 ml bi-distilled water. Therefore 0.5 ml was removed from the main centrifuge tubes. Diluting the solution in the cuvette, not the microtube, ensured that any ash present in the centrifuged sub-sample would be replaced into the main centrifuge tube in order that the mass of ash was not reduced. The removed solution and dilution ratio was accounted for in the final calculations.

3.3.7.3 Data Manipulation

In order to calculate the Fe release, spectrophotometer lamp degradation, dilution and surface area had to be taken into account. Adsorption values were converted into units of mMol by the following equations:

$$mM = UA/(\varepsilon *dil) \hspace{4cm} \text{Equation 3.10}$$

Where:

mM = the milli moles of iron released,

UA = the adsorption value (in Arbitrary Units),

ε = the molar extinction coefficient and

dil = the dilution factor of the solution.

mM can then be converted into units of $\mu mol/m^2$ by:

$$\text{ụmol/m}^2 = (mM/V)*(SSA/m) \qquad\qquad \text{Equation 3.11}$$

Where:

V = the volume of solution in the centrifuge tube since the last measurement (to account for removal of diluted solutions),

SSA = the specific surface area and

m = the mass of ash used.

These calculations were done for both sets of solutions to calculate Fe^{2+} and total Fe released for each measurement. Again, worked examples can be found on the Appendix CD ('Fe Release') in Appendix B.

3.3.8 Image Analysis: Scanning Electron Microscope

The Scanning Electron Microscope (Hitachi SU70 SEM) in the Department of Physics, Durham University was used to obtain visual images of the samples for information on particle morphology.

3.3.8.1 Sample Preparation

Aluminium SEM stubs were made up by sprinkling ash from a cotton bud over a polycarbonate disk on top of a carbon sticky pad placed on the SEM stub. At all times during preparation gloves were worn and tweezers were used when handling the stubs as any grease from contact with skin could affect the SEM. The sample stubs were coated with 20 nm Pt using a Cressington 308UHR Ultra High Resolution Coating System in the Department of Biology, Durham University.

3.3.8.2 Sample Analysis

Five samples at a time were mounted into the SEM, taking care not to contaminate the samples, and the chamber vacuum was switched on. Images

were taken at 5.0 kV with the help of Leon Bowen, Department of Physics, Durham University.

3.4   Samples from Mount Unzen

The samples obtained for Unzen volcano were erupted during 1990-1995. For good summaries of the eruption see Takahashi et al. (2007) and Shimizu et al. (2007). Three samples (UNZ.01-UNZ.03) were from the Volcano Research Centre, Earthquake Research Institute, University of Tokyo and given by Professor S. Nakada of Shimabara Earthquake and Volcano Observatory. The samples are derived from lofted ash from pyroclastic flows and were collected soon after dome collapses, all within 24 hours and before rainfall. A further three ash samples (UNZ.05, UNZ.06, UNZ.08) were collected from ash deposits at Kita-Kamikoba, Shimabara city and Minami-Senbongi. The ash layers sit between pyroclastic flows in a stratigraphic sequence. One of these samples was collected by Prof Nakada, and the other two were collected by the author during August 2009. Samples UNZ.04 and UNZ.07 were collected from the main pyroclastic matrix so are not included in the analyses. The relevant information is summarised in Table 3.4.
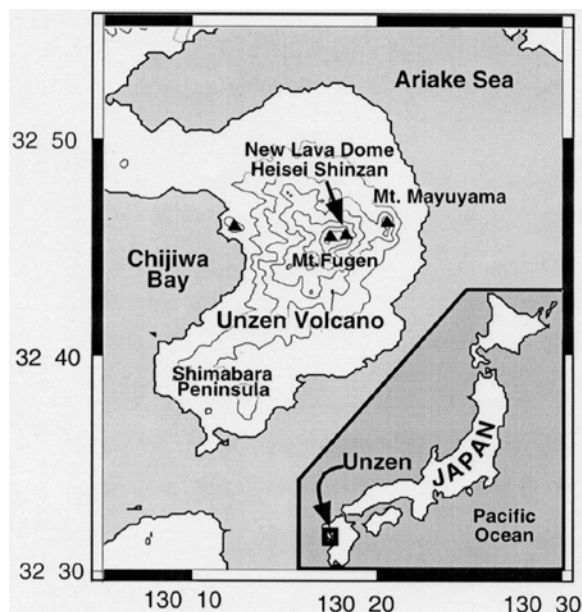
Figure 3.6: Location map of Unzen Volcano and Mt Fugen, the main, active peak of the volcano. From Matsushima and Takagi (2000).

Table 3.4: Sample information for samples collected from Unzen volcano. SEVO stands for Shimabara Earthquake and Volcano Observatory.

Sample I.D	Eruption Date	Collection Date	Location	Analyses Completed	Notes
UNZ.01	22.04.92	23.04.92	Yama-no-tera	GSA	Collected from tree leaves ~2km SE of the dome.
UNZ.02	14.08.92	14.08.92	SEVO	GSA, XRD	Collected from non-contaminated surface ~5km E of the dome.
UNZ.03	03.04.93	03.04.93	SEVO	GSA, XRD	Collected from non-contaminated surface ~5km E of the dome.
UNZ.05	1991-1992	unknown	Kita-Kamikoba	GSA	Collected from an ashfall deposit above a pyroclastic flow surge.
UNZ.06	23.06.93	28.08.09	Minami-Senborgi	GSA	Collected from the upper fine ash layer of Unit 1 in Figure 3.6
UNZ.08	23.06.93	28.08.09	Minami-Senborgi	GSA	Collected from the coarse ash layers of Unit 2 in Figure 3.6
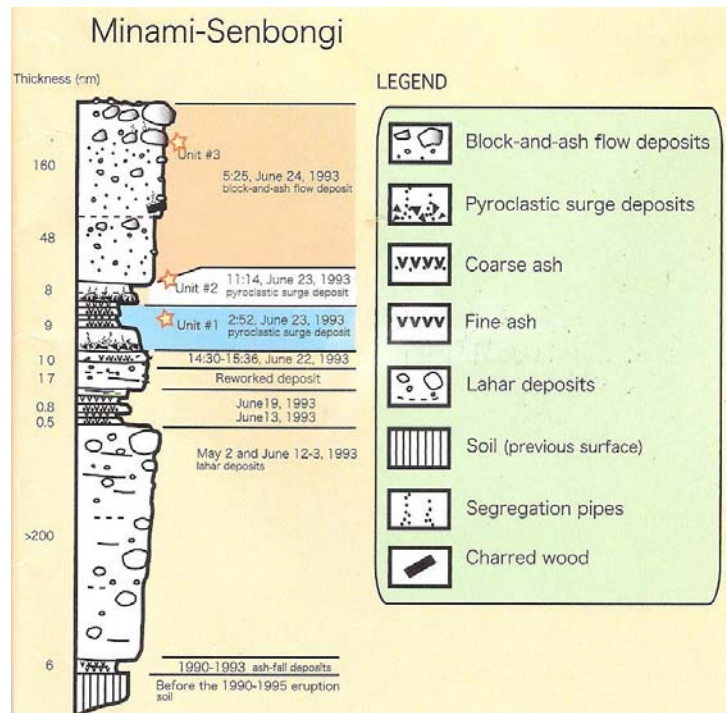
Figure 3.7: Stratigraphic sequence at Minami-Senbongi, from Shimizu et al. (2007).

Chapter 4

Results and Analysis

4.1   Introduction

In this chapter, the results obtained from all the laboratory analyses are described in detail. Some basic interpretation of the data is carried out where appropriate in order to address the research aims. Results here are presented for Sakurajima volcano only and do not include the data obtained for other volcanoes so that interpretation of the Sakurajima data can be made separately and with greater clarity, before considering a wider context. The chapter should provide a thorough overview of the findings and their relevance to the study for each section to provide the basis for more subjective and broad-based interpretations in Chapter 5.

4.2   Ash characterisation

A general overview of the type of ash produced by Sakurajima volcano is summarised using the results of the bulk chemistry analyses by XRF.

4.2.1   Total Alkali-silica results

Samples are categorised on a Total Alkali-Silica (TAS) plot (Figure 4.1). Almost all the samples from Sakurajima are andesitic apart from a group of 9 samples (Q1 – Q8) which are dacitic and 2 samples (FM27 and SAK12) that sit just inside the basaltic andesite category. Samples Q1 – Q8 (black circles) were all collected from a stratigraphic sequence of ash layers that sit between pumice falls dated to the 1470s eruptions and are all dacitic. The two other deposited samples (Q9 and Q10, black circles) from the 1914 eruption, are andesitic (61.4 and 60.4 wt. % respectively). A wide range of SiO_2 weight percentages can be seen, including the older deposit samples, but also within the archive samples (56 – 62 wt. %) which are all from the most recent eruptive phase (all symbols other than black circles). The total alkali results lie in a relatively narrower band, but showing a positive trend between total alkali values and increasing silica weight percent.
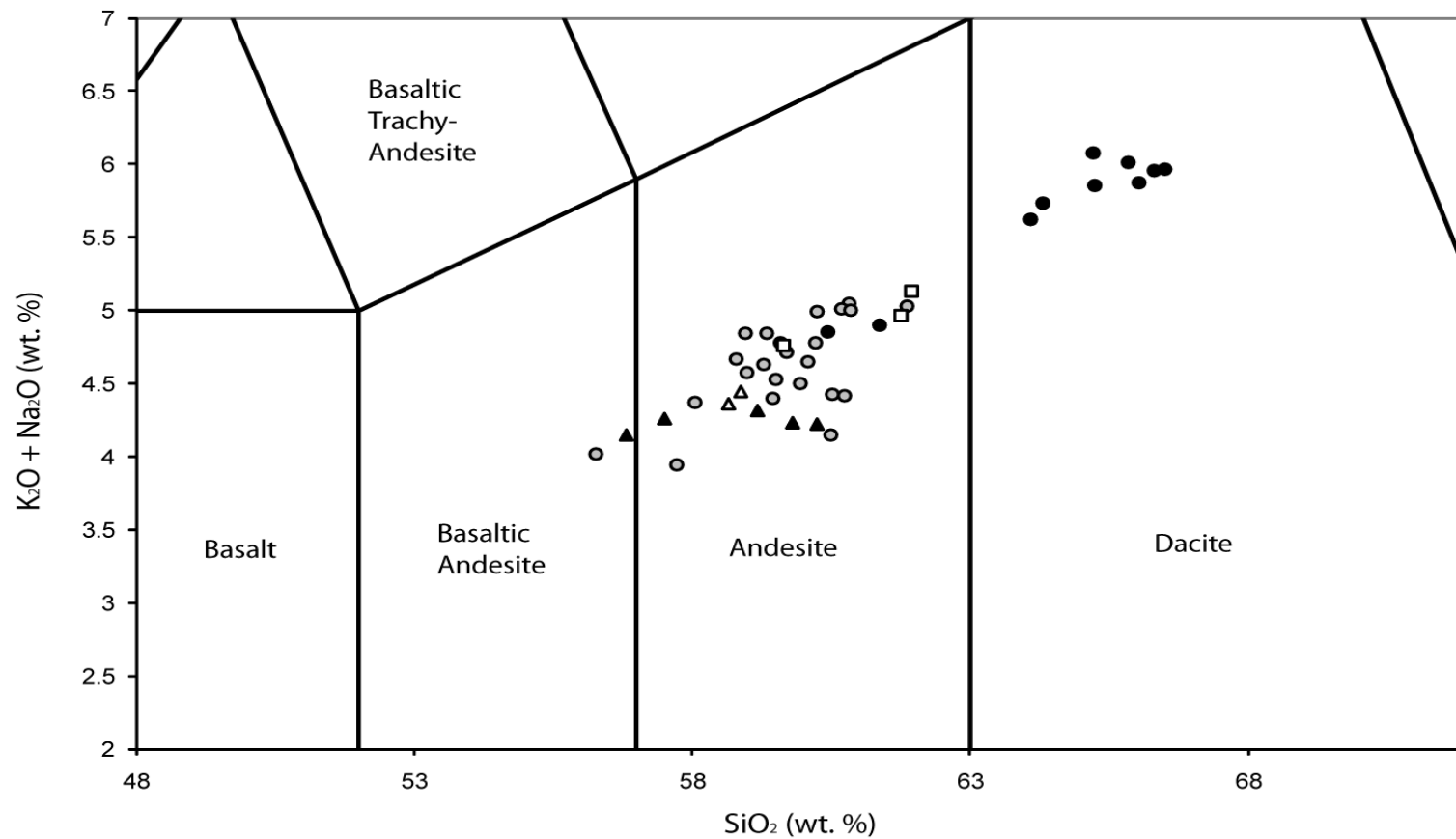
Figure 4.1: Total alkali-silica (TAS) plot for all samples, cropped to show only the relevant categories. **Black circles:** deposited samples from the 1470s and from 1914. **Black triangles:** samples SAK11-SAK15, from 7th-8th May 2008. **White squares:** samples SAK17-SAK19, from 7th October 2000 eruption. **Grey triangles:** samples FM23 and FM30, from 14th April, 2008. All other archive samples are indicated by grey circles.

The results for the archive samples spread across the whole andesite category and just within the basaltic andesite category. Results vary even for samples from the same eruption sequence. For example, samples SAK 11-SAK 15 (marked as black triangles) were all collected on the same morning (9th May), but from separate locations after a series of eruptions on the 7th – 8th May. During this time the wind changed direction blowing south and then east. There is a clear distinction in SiO_2 values between those samples located to the south of the vent (SAK11 and SAK12, 56.8 and 57.5 wt. % SiO_2 respectively) and those located to the east and northeast (SAK13-SAK15, with higher SiO_2 weight percentages). Similarly, samples SAK 17 – SAK 19 (white squares) were collected on the same day, but SAK18 has ~3 wt. % less SiO_2 (59.6 wt. %) than SAK17 and SAK19 (62.0 and 61.8 wt. %), despite only a single eruption being recorded before sample collection. On the other hand, samples FM 23 and FM 30 (grey triangles) are also from the same eruption sequence and closely match on the TAS plot.

These results demonstrate the range of ash produced from Sakurajima, even within short time periods. The dacitic samples support the magma mixing theory outlined in Section 2.4.2 and are derived from a different magma type than the archive samples as could be expected from deposits of older eruptions. The large differences in total alkali and silica contents among samples collected during the last eruptive phase are probably representative of the varied eruption styles at Sakurajima. Even when examining eruptions only several days or hours apart, the range in values can be large. The distinct wind change during the eruptions before the collection of SAK11 – SAK15 and corresponding separation between the samples on the TAS plot is a good example of this. It is likely that the ash located to the south was derived primarily from the 7th May eruptions whilst the samples located in the E and NE were mostly made up of ash from the 8th May eruptions, which are much more silica rich, and could be derived from a different, perhaps more evolved magma.

The data highlight the rapidly changing nature of the ash erupted over very short timescales. The samples from secondary sources, who collected them over set periods of time rather than from discrete eruptions, may contain ash from several

eruptions that produced ash with very different characteristics. Therefore generalisations cannot be drawn from the analysis of single samples and only a broad indication of the overall potential health hazards should be interpreted from the results.

4.3   Physical Characteristics

In this section, particle-size distributions and ash morphology results are summarized before more detailed analysis focussing on the health-relevant data is given.

4.3.1   Particle-size Distributions

Figures 4.2 a-f show six grain-size distribution patterns, representing typical examples of the range found in the data set. The results are plotted with Hi μm (the upper limit of each bin category) on a logarithmic scale. The results are expressed using Hi μm as it is more relevant for health assessments, and a logarithmic scale is used to show the spread and distribution of the data more clearly as it tends to cluster between 0.5 μm and 500 μm. Most of the samples have a negatively skewed log-normal shaped distribution (e.g. Figures 4.2a-c). However, ten samples less closely represent the shape of log-normal distribution, with deviations occurring especially for values between 1000 μm and 2000 μm or in the skew tail (Figure 4.2d shows an extreme example). Deviations between 1000 μm and 2000 μm are particularly common. This could be due to sample contamination from other sources but may be because the results were calculated using the sieved mass data, resulting in only one data point for this size bin. In the coarse bins, data are also easily skewed by a few large particles. A number of samples (5 in total) have grain-size distributions which show a bi- or tri- modal shape (as in Figure 4.2e) and 3 samples have very complex distribution shapes (e.g. Figure 4.2f). Although many samples conform to a general pattern, a large amount of variability regarding spread, position of the main peak and tail characteristics is still present.
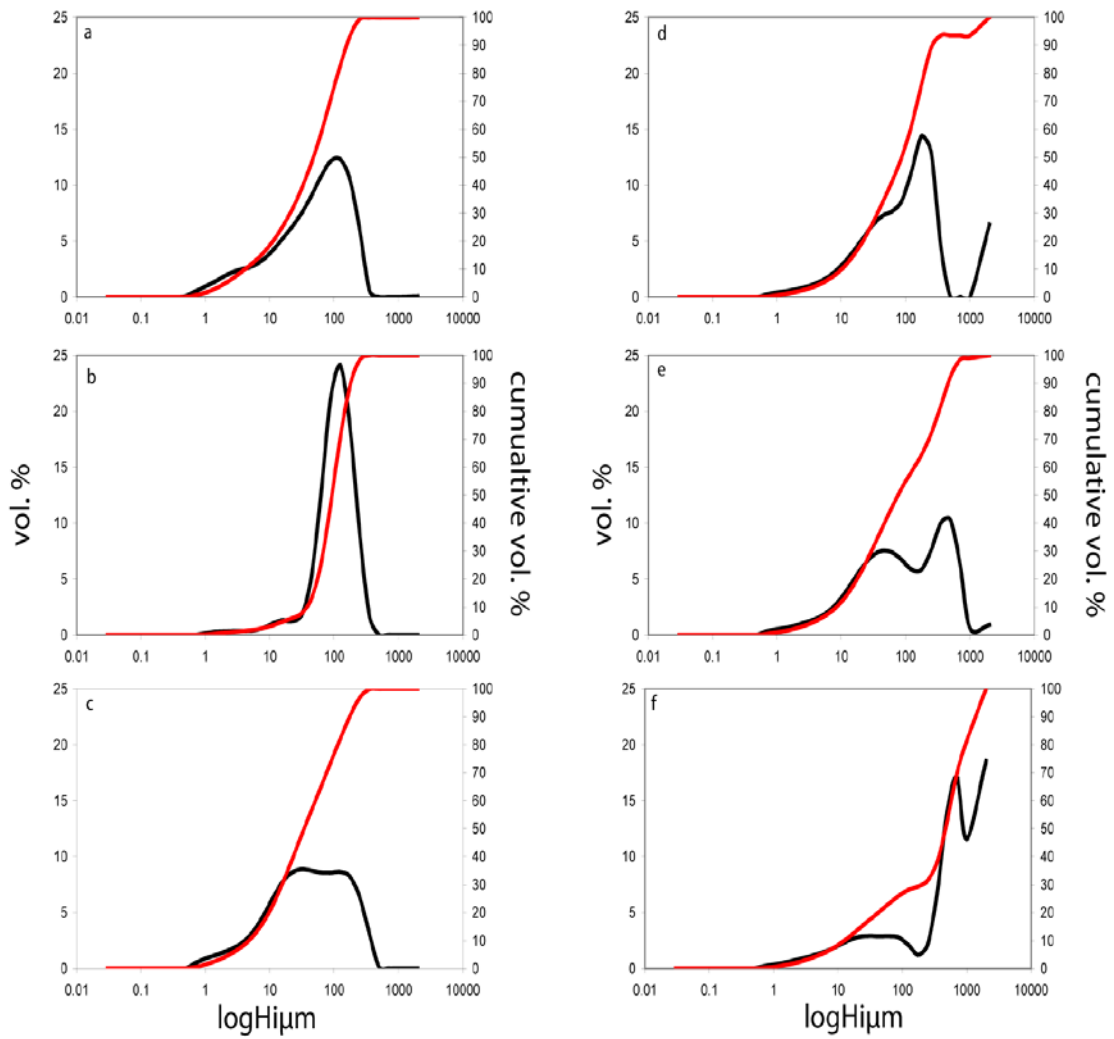
Figure 4.2: Examples of grain-size distributions that represent the range seen in all the Sakurajima samples. **a)** SAK12 **b)** SAK44 **c)** J42 **d)** Q9 **e)** SAK21 **f)** SAK17. The black line represents the actual grain-size distribution and the red line shows the cumulative distribution.

4.3.2 *Examination of health-relevant fractions*

The health-relevant particulate examined here focuses on the 'respirable' (< 4 µm) and 'thoracic' (< 10 µm) fractions of the samples. The amount of ultra-fine material (< 2.5 µm) and near nano-scale particulate (< 0.5 µm) are also considered. The cumulative volume percentages for health-pertinent bins are summarised in Table 4.1.

Table 4.1: Quantity of ash in fractions relevant to respiratory health. The < 0.5 μm fraction is quoted to 3 d.p in order to distinguish between those samples with a very small vol. % < 0.5 μm and those with none.

Sample I.D	Cumulative volume %				
	< 0.5 μm	< 2.5 μm	< 4 μm	< 10 μm	< 15 μm
Q1	0.008	3.00	4.92	11.42	15.84
Q2	0.046	9.61	15.12	39.62	59.09
Q3	0.041	10.85	18.77	46.16	58.61
Q4	0.001	1.63	2.75	6.52	9.05
Q5	0.024	3.54	5.44	12.87	19.37
Q6	0.042	9.07	15.13	39.93	55.48
Q7	0.000	0.89	1.53	3.88	5.56
Q8	0.040	7.32	11.26	32.42	51.09
Q9	0.013	2.43	3.99	9.81	14.38
Q10	0.001	1.05	1.70	4.10	6.26
SAK11	0.029	5.99	9.29	17.46	22.89
SAK12	0.104	6.26	9.66	18.43	24.26
SAK13	0.018	3.88	6.31	13.37	17.98
SAK14	0.019	3.46	5.32	10.73	15.15
SAK15	0.026	4.85	7.52	15.02	20.45
SAK16	0.018	3.52	5.73	12.88	17.91
SAK17	0.012	2.35	3.87	8.39	11.34
SAK18	0.018	2.82	4.59	10.42	14.92
SAK19	0.006	2.59	4.33	8.71	10.96
SAK20	0.000	1.18	2.04	4.29	5.90
SAK21	0.021	3.08	4.98	11.81	17.27
SAK22	0.021	4.05	6.71	14.79	20.17
FM23	0.014	2.36	3.72	8.16	11.42
FM24	0.024	3.72	5.58	10.97	15.56
FM25	0.028	5.22	8.39	18.07	24.78
FM26	0.074	5.57	8.90	19.12	26.12
FM27	0.094	3.51	5.47	13.03	19.62
FM28	0.026	4.59	7.46	17.04	23.77
FM29	0.113	4.89	7.81	18.47	27.09
FM30	0.014	2.47	3.90	8.57	11.97
J31	0.000	1.04	1.89	5.04	7.07
J32	0.017	2.30	3.70	9.09	13.43
J33	0.000	0.54	1.10	3.04	4.15
J34	0.003	1.46	2.34	5.12	7.49
J35	0.000	0.95	1.61	3.95	6.13
J36	0.095	3.63	5.38	13.24	20.71
J37	0.005	1.90	3.14	7.41	10.49
J38	0.016	2.59	4.26	10.94	15.96
J39	0.011	2.69	4.35	9.52	13.39
J40	0.005	2.00	3.36	8.20	11.59
J41	0.005	1.59	2.62	6.67	10.29
J42	0.031	5.28	8.47	20.50	29.18
J43	0.007	2.38	3.85	9.50	14.34
SAK44	0.000	0.94	1.43	3.10	4.55
SAK45	0.001	1.89	3.13	7.54	11.15
SAK47	0.001	2.23	3.67	8.75	12.84
SAK48	0.001	2.39	3.94	9.37	13.82
SAK49	0.001	2.56	4.24	10.17	14.71
SAK50	0.001	2.86	4.64	10.36	14.73
SAK51	0.000	0.75	1.27	2.63	3.67

The amounts of thoracic and respirable material in the ash samples from Sakurajima vary greatly and generalisations are difficult to make regarding the ash produced by the volcano as a whole. Figure 4.3 shows the grain-size distributions up to 15 μm, with 10 μm and 4 μm marked to show the cut-off for thoracic and respirable particles. The graph clearly demonstrates the range in amounts of respirable material in the samples. However, there is a large separation between four samples (samples Q2, Q3, Q6 and Q8), with extremely high proportions of respirable material and the rest of the samples. These values are all from the samples that were collected at the main deposit at Nagasakibana Quarry. The trends are also reflected when examining grain-size distributions up to 10 μm, with the fine-grained units of the main quarry deposit having even greater proportions of fine ash fractions.
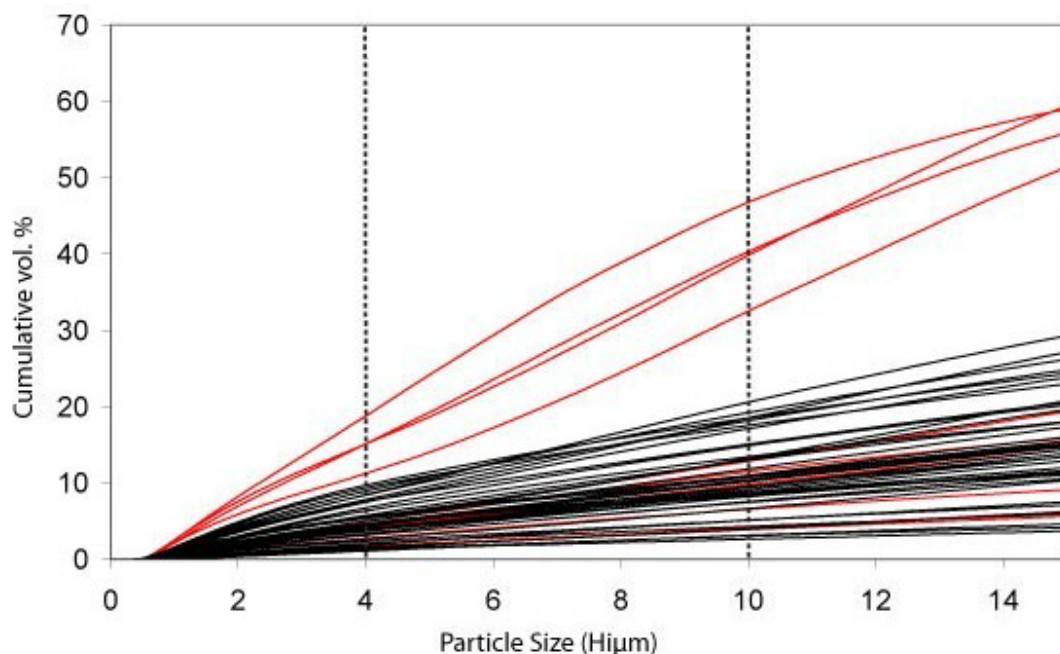
Figure 4.3: Grain-size distributions up to 15μm for all samples, with 10μm and 4μm, below which particles are defined as 'thoracic' and 'respirable' respectively, marked by the dotted lines. The red lines represent deposit samples and the black lines show the archive samples.

Table 4.2 shows the range of thoracic and respirable material for the deposit and the archive samples. In the deposit samples the range is larger. The 1470s ash layers were separated into three sequences, with each layer becoming progressively fine-grained within each sequence (see Section 3.2.3). This could be

because the eruptions during the 1470s tended to deposit progressively finer material over several hours, resulting in the creation of some very fine-grained samples. The two samples derived from the 1914 eruption (Q9 and Q10), which were not sorted, are more similar with respect to the quantity of thoracic and respirable material but quite coarse-grained (see Table 4.1 for specific volume percentages). When examining the archive samples only, the range is much smaller and the volume percentages are lower overall. The majority of the samples contain 3-6 vol. % < 4 μm and 8-12 vol. % < 10 μm. However, some samples (e.g. SAK11, SAK12, FM25 and FM26) contain substantial quantities (~9 vol. %) of respirable material, whilst others are extremely coarse-grained (e.g. J33, J35, SAK44 and SAK51, ~1 vol. % respirable material; see Table 4.1 for specific percentages). Therefore, although the range is smaller compared to the deposit samples, the differences in grain-size characteristics between the archive samples can still be large.

Table 4.2: Summary statistics for the volume percentage of particles below 4 μm and 10 μm for deposit samples and archive samples.

	Vol. % <4 μm (deposit)	Vol. % <4 μm (archive)	Vol. % < 10 μm (deposit)	Vol. % < 10 μm (archive)
Mean	8.06	4.75	20.67	10.60
Maximum	18.77	9.66	46.16	20.50
Minimum	1.53	1.10	3.88	2.63
Range	17.24	8.56	42.29	17.86
Standard Deviation	6.41	2.32	16.80	4.79

For samples from the more recent vulcanian eruptions, no trends relating the amount of respirable material to eruption characteristics, weather conditions, location or SiO_2 weight percent (from the XRF results) could be interpreted from the grain-size results (e.g. Figures 4.4 and 4.5). This is likely to be due to the limited range of variables represented within the data set (e.g. distance from volcano) and inadequately detailed information about the eruptions at the time of

sample collection, meaning that not all variables can be quantified or controlled. Therefore, general trends are unlikely to become apparent.
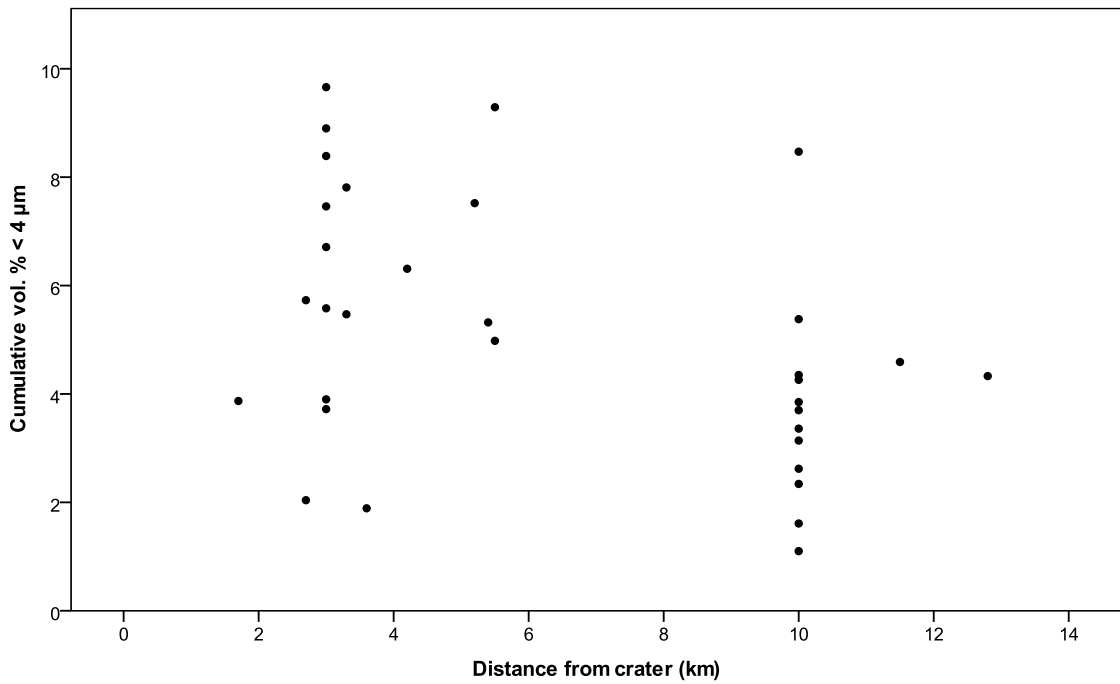

Figure 4.4: The amount of respirable material in various samples against distance of deposit from the crater.
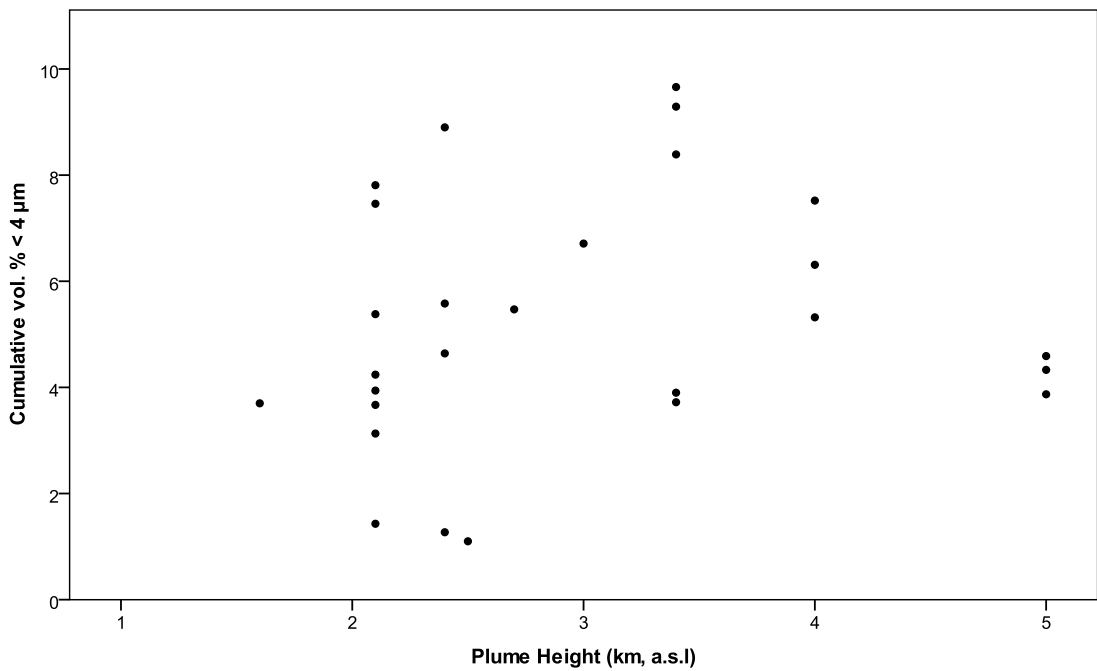
Figure 4.5: The amount of respirable material in various samples against the maximum plume height of the eruption.

Despite the lack of overall trends, interpretations of single results or small groups of results can be made where sufficiently detailed eruption information has been noted, in a similar manner to the analysis of the TAS plot. For example, the separation seen between samples SAK11 - SAK12 and samples SAK13 - SAK15 on the TAS plot (Section 4.2), can also be identified in the grain-size results, with samples SAK11 - SAK12 containing much larger amounts of respirable material. This could be because the ash from the earlier eruptions was not dispersed quickly and could still be observed from a satellite 6 hours after the eruption, allowing more time for fine-grained particles to fall out from the plume. However, unlike the XRF results, in all other cases where samples were collected during the same eruption sequence (samples SAK17-SAK19; FM23 and FM30; FM25-FM26; FM28-FM29; SAK45 and SAK49) the grain-size results are similar.

4.3.4   *Relationships between health relevant fractions*

In general there are very strong linear correlations between the various health pertinent fractions, as demonstrated in Figure 4.6. Therefore if a large amount of thoracic material is observed, it can be expected that there will also be high amounts of respirable and ultra-fine material. However, the quantity of particulates close to the nano-scale appears to vary independently of the other fractions, with samples containing similar quantities of respirable material having almost none of these extremely fine particles, whilst others include comparatively large proportions of particles < 0.5 μm (Figure 4.7). In particular, samples SAK15, FM29, FM30, J32 and J39 stand out with large amounts of sub 0.5 micron particles compared to the amount of respirable material (circled on Figure 4.7). It must be taken into account, however, that the accuracy of the Malvern Mastersizer is questionable for particles with diameters < 0.2 μm, which may affect these results.
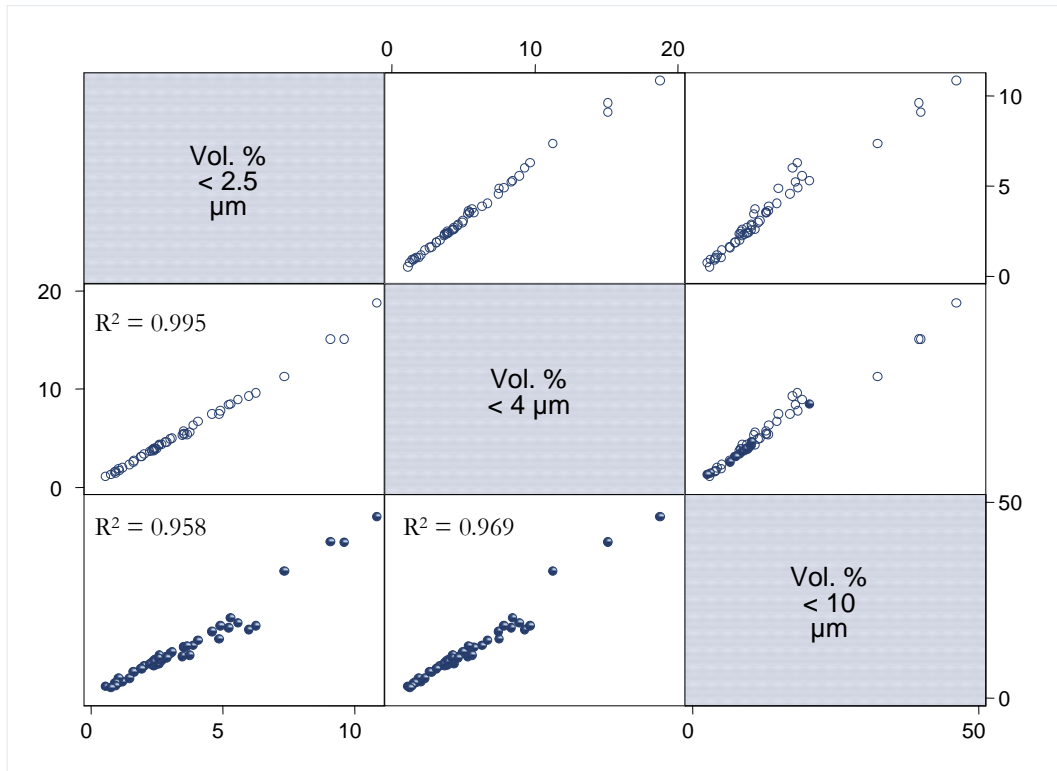
Figure 4.6: Correlation matrix showing the relationships between the amount of material in the health-pertinent fractions of the samples. R^2 values are shown in the bottom graphs.
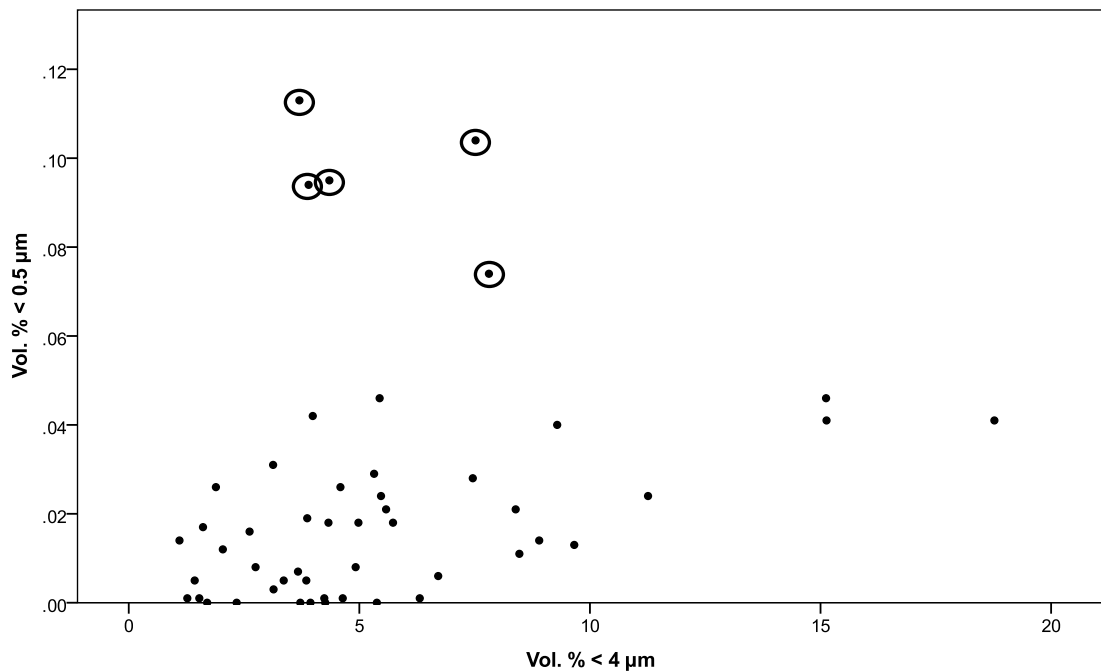
Figure 4.7: Scatter graph showing the amount of respirable material relative to the amount of sub 0.5 micron material. Circled samples are samples SAK15, FM29, FM30,

J32 and J39 that have very large vol. % < 0.5 μm compared to the amount of respirable material.

4.3.5   Particle Morphology

Particle morphology can provide insights into ash formation, but more importantly, is examined here as it will influence the behaviour of the particles after entering the respiratory system. The particle morphology of the Sakurajima ash samples is generally blocky and angular (Figures 4.8a and 4.8b). Smooth planar faces can be observed (Figure 4.8c), although stepped and conchoidal fractures (Figures 4.8c and 4.8d); chips and cracks (Figures 4.8b and 4.8d) are also common. Many particles are elongate or wedge-shaped (Figure 4.8c). Some particles are flat, with broad, dominant surfaces and chipped edges (Figure 4.8g). Most, but not all (e.g. Figure 4.8e), particles appear to be poorly or non-vesicular.

Finer particles are also angular and include all of the characteristics outlined above, although particles tend to be less elongate and a greater proportion of wedge-shaped and circular particles (Figures 4.8f and 4.8j) are present. Many fine particles are adhered to the surfaces of larger particles (Figures 4.8a-i) or have formed agglomerates (Figure 4.8k), and are rarely found separated from other particles. Both circular and fibre-like ultra-fine particles can also be observed on the surface of larger particles (Figures 4.8h and Figure 4.8i).
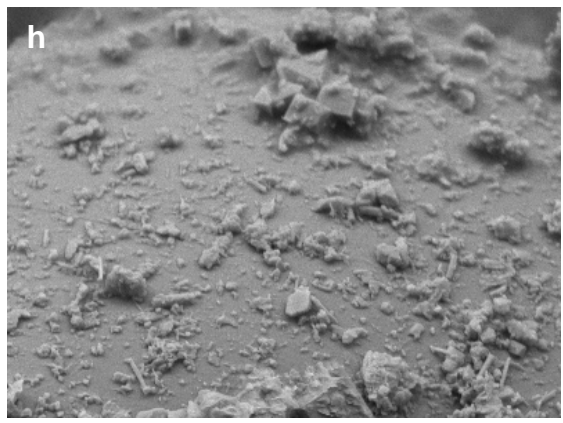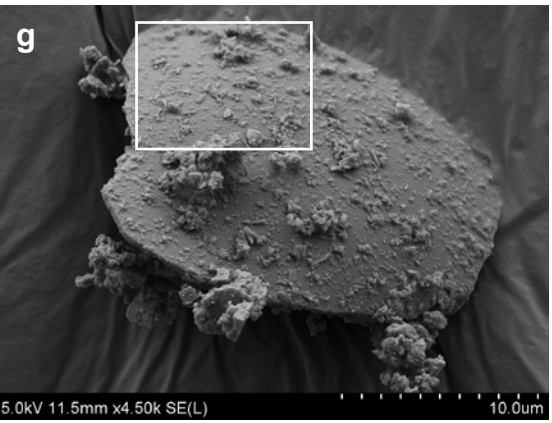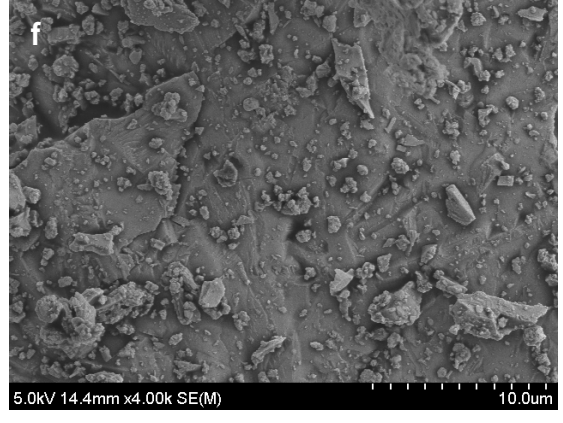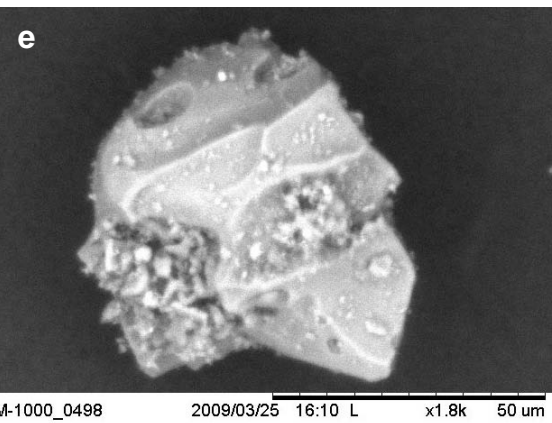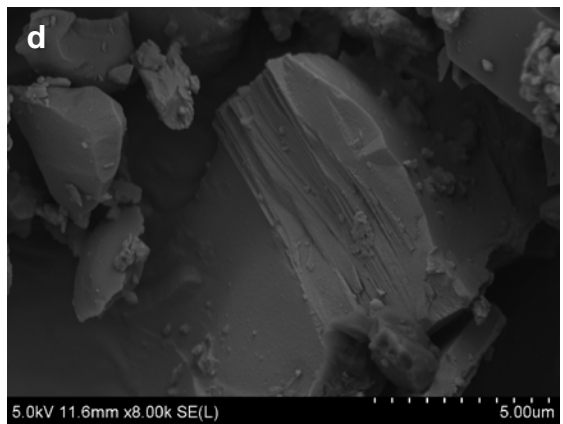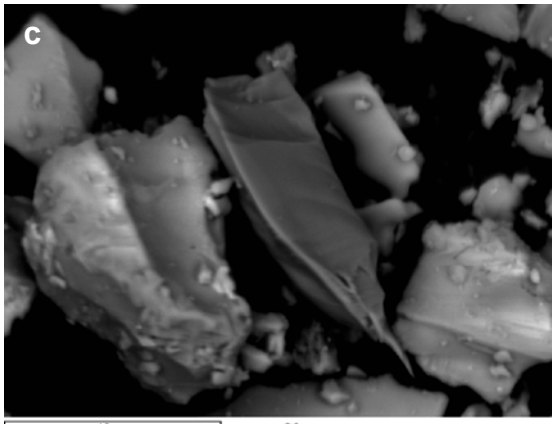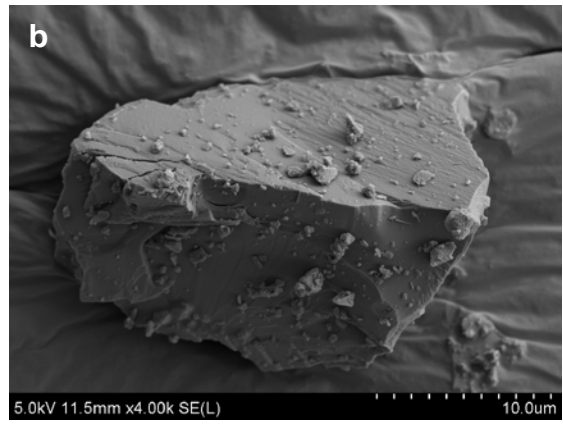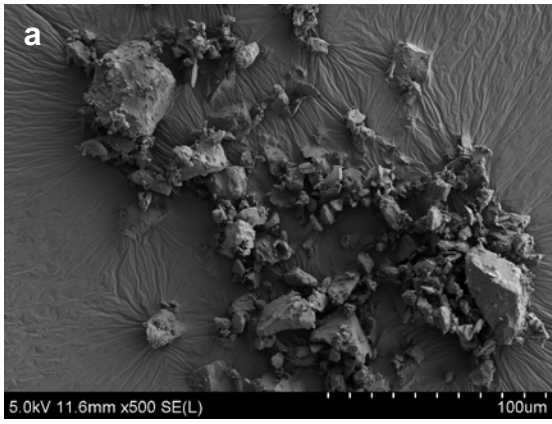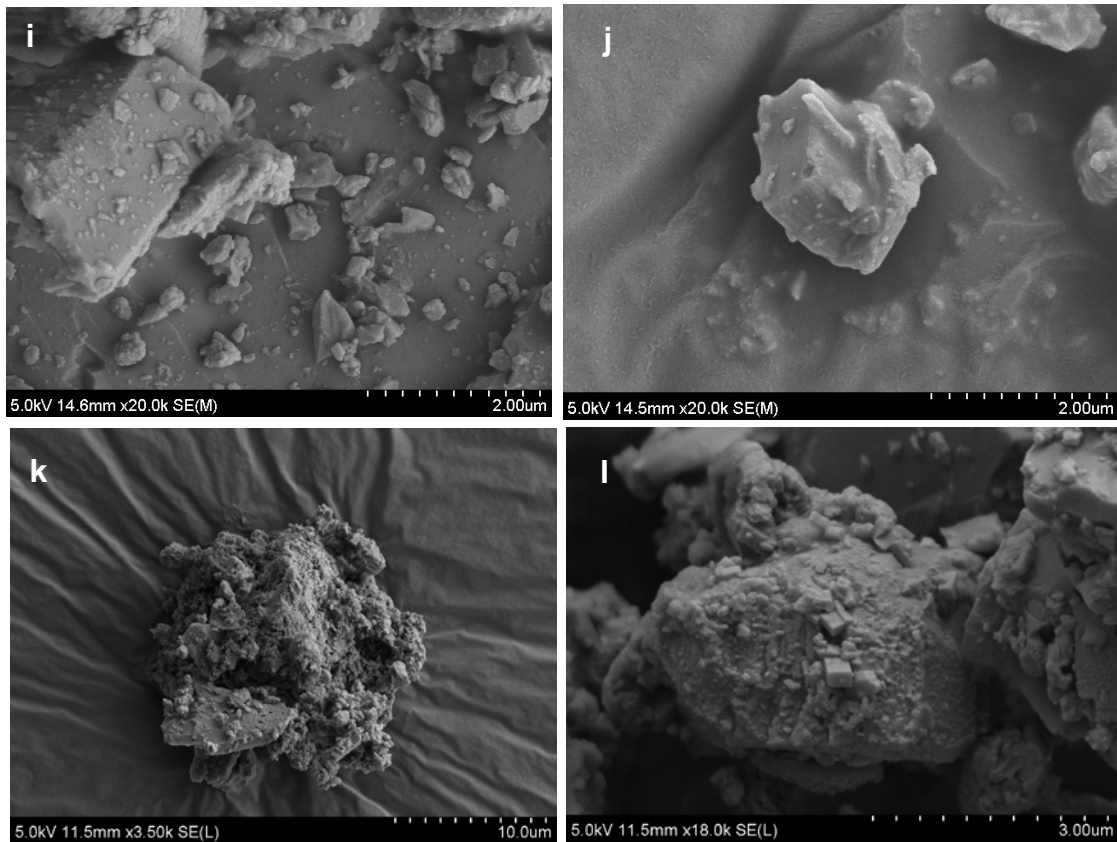
Figure 4.8: SEM images of ash particles from Sakurajima volcano. **a)** Sample Q2, group of typical ash particles of various sizes. **b)** Sample J39, typical blocky particle with chips and cracks. **c**) Sample Q2, uncoated, wedge-shaped particles with conchoidal fractures. **d)** Sample Q2, close image of stepped fractures and a v-shaped chip. **e)** Sample SAK12, uncoated, unusually vesicular particle with vesicles filled with fine particles. **f)** Sample J39, group of fine particles < 10 μm. **g)** Sample SAK12, flat particle with a smooth circular face with many nanoparticles adhered to the surface. **h)** Sample SAK12, zoom of the white square in photograph g, showing many circular, but also some fibre-like fine particles. **i)** Sample SAK19, ultra fine particles. **j)** Sample FM28, typical particle in finer ash fractions. **k)** Sample SAK12, typical circular agglomerate of small particles. **l)** Sample J39, fine particle with moss-like texture and evidence of crystal formation.

4.4 Identification of potentially toxic minerals

Mineralogical assessment by X-ray diffraction was used to identify crystalline silica in 12 samples. Detailed examination of complete ash mineralogy was not carried out as analysis focussed on identification and quantification of crystalline silica phases that are relevant to respiratory health. However, some general, subjective mineralogical assessments can be made based on matching archive peak positions (see Appendix C for stick-fit diagram) and are stated here to provide an indication of the array of minerals present in the Sakurajima samples.

All the diffraction patterns are complex, demonstrating that a number of different minerals are present (as seen in Figures 2.9 and 2.10). There is a large amount of fluorescence background intensity, caused by the presence of amorphous iron oxide, likely to be from magnetite (Figures 2.9 and 2.10). The patterns are not uniform, suggesting that the samples are made up of different mineral compositions. For example, all patterns contain strong plagioclase feldspar peaks, but the peak positions indicate that within the sample set the plagioclase compositions probably range from labradorite to andesine. Samples SAK12, SAK22 and FM27 also contain anhydrite, and augite is only present in sample SAK22.

Figure 4.9 shows the XRD pattern for sample FM 28 with the positions for cristobalite, quartz, tridymite and andesine peaks marked. Part of the plagioclase feldspar pattern sits at the same position as the major cristobalite peak and will obscure it. However, in the XRD pattern shown, over-amplification of the feldspar peak is evident at the position of the cristobalite peak (marked by 'C'), indicating the presence of cristobalite in the sample. No tridymite or quartz is observed.
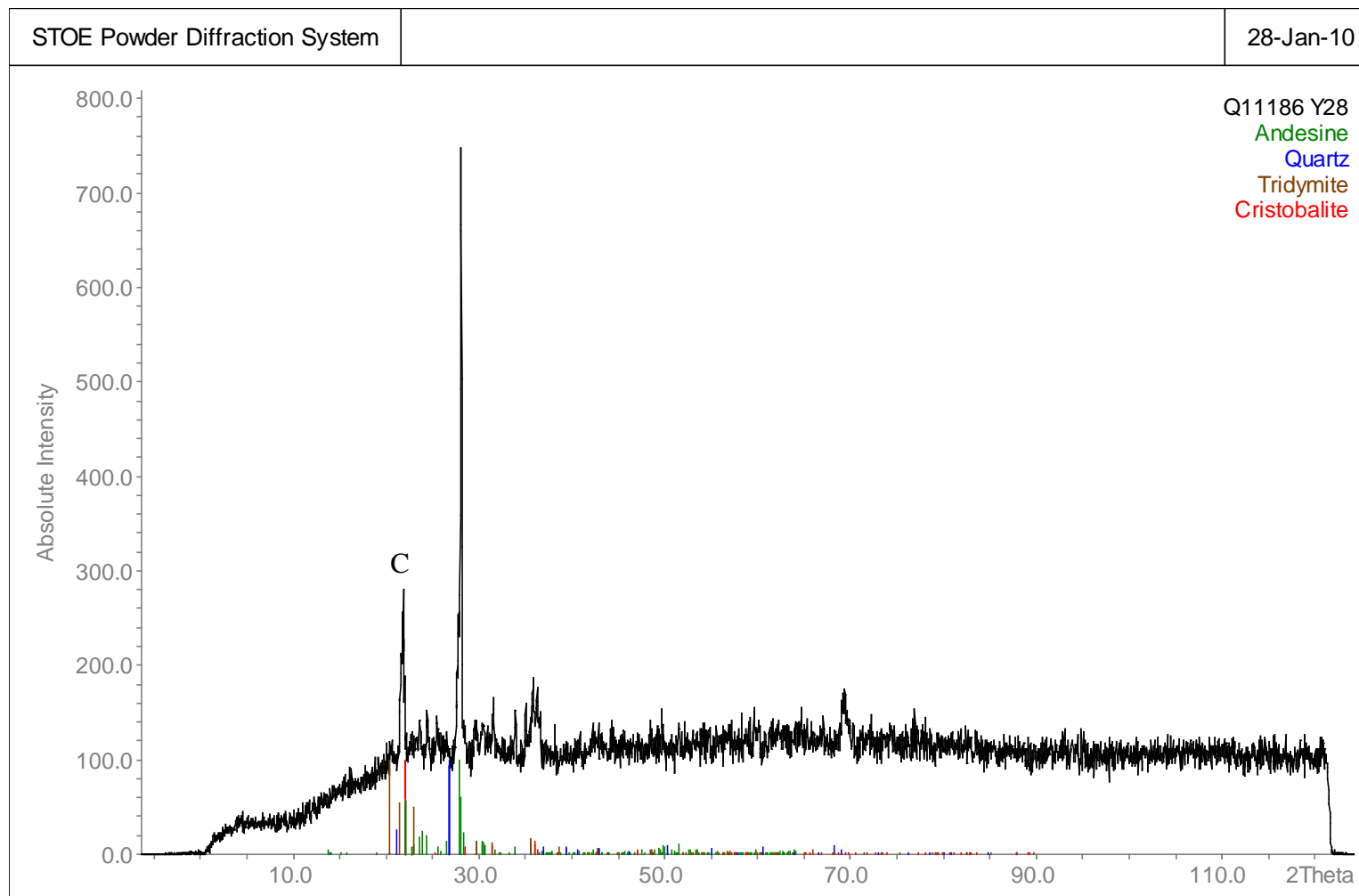
Figure 4.9: XRD pattern for sample FM 28, with 'sticks' showing the peak positions for andesine, quartz, tridymite and cristobalite.
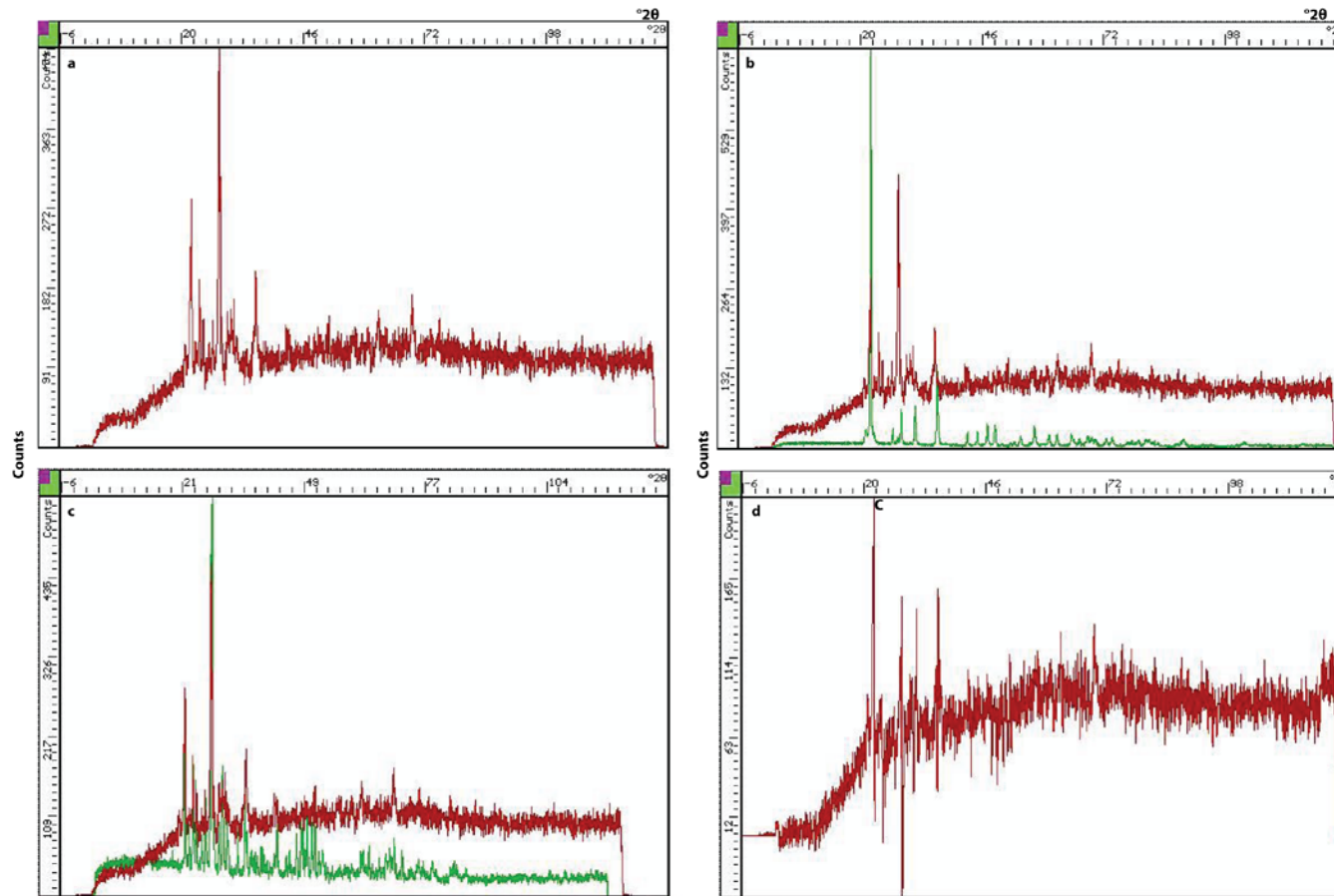
Figure 4.10: GUFI software images of sample SAK19 (red pattern); **a**-full sample XRD pattern; **b**-full sample XRD pattern and overlying pure cristobalite standard XRD pattern (green pattern), scaled to 25%; **c**- full sample XRD pattern and overlying pure andesine standard XRD pattern (green pattern), scaled to 50%; **d**-sample XRD pattern, with andesine signal removed. Some negative peaks occur due to non-perfect plagioclase match, residual cristobalite peak at ~22° 2θ is, however, clearly visible.

Figure 4.10 demonstrates how, by overlying pure standard XRD patterns and using peak-stripping, the presence of cristobalite can be confirmed. The background fluorescence, 'noisy' data and strong feldspar peaks are all plainly evident in this pattern (Figure 4.10a). Yet the atypical intensity of a minor feldspar peak (Figure 4.10c), and the presence of a peak after the feldspar signal has been removed (Figure 4.10d), at ~22° 2θ, where the major cristobalite peak sits (Figure 4.10b), are clearly visible.

All the samples appear to contain beta cristobalite, visible as a shoulder on the low angle side of the peak near 22° (Figure 4.11) although, as the peak is hidden, it is difficult to conclude this with absolute certainty. Regardless, the difficulty in distinguishing cristobalite in the full sample patterns, as well as the small residual peaks after removing any feldspar signal, suggest that the amount of cristobalite in the samples is small.
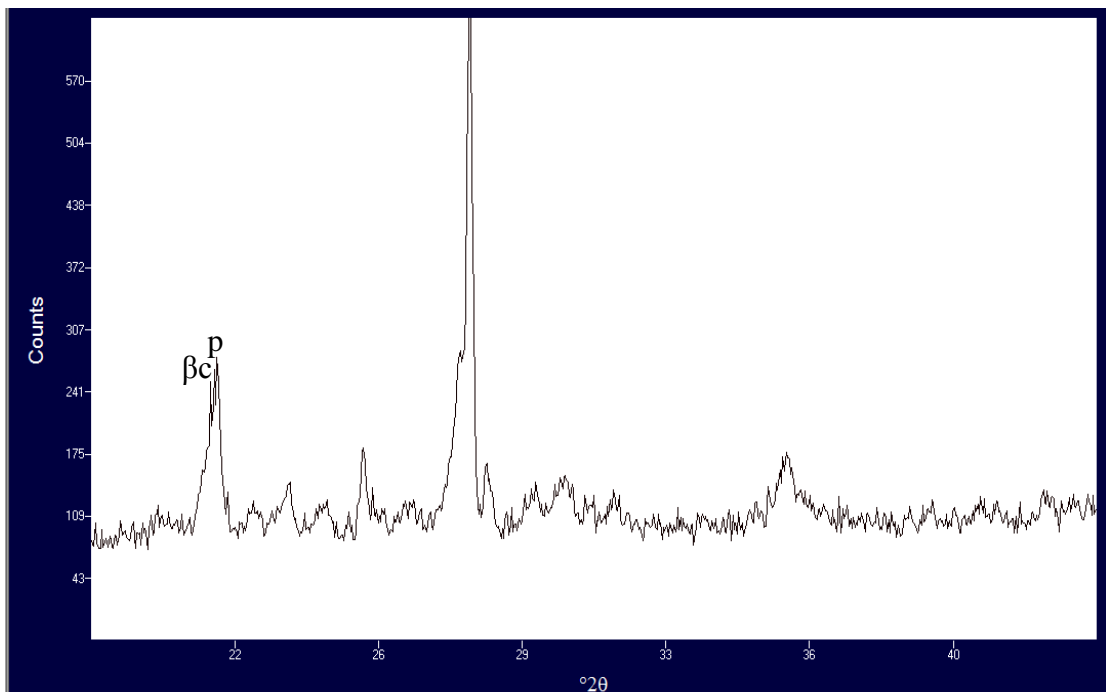
Figure 4.11: XRD pattern for sample SAK22 zoomed into 18 – 44 °2θ. Marked are the beta-cristobalite shoulder (βc) on the low angle side of the plagioclase peak (p) at 22 °2θ.

The quantified results derived from the XRD patterns can be seen in Table 4.3. As suggested by the XRD patterns the weight percentages of cristobalite in the samples are low, ranging between 2-8 wt. %, with ± 1-3 wt. % error. The quarry

samples of the 1470s ashfall layers have low cristobalite contents (~2-3 wt. %), in contrast to the sample from the 1914 ash layer which contains ~6 wt. %. For the samples collected in the most recent eruptive phase the amount of cristobalite ranges between 4-8 wt. %, with most samples containing ~6-7 wt. %. Interestingly, samples FM27 and FM28, which had the lowest and highest cristobalite contents respectively out of the archive samples were erupted within a few days of each other, although by contrasting eruptive styles.

Table 4.3: Weight percentage of cristobalite in each sample, +/- 1-3 wt. %

Sample I.D.	wt. % Cristobalite	Notes
Q2	2	Quarry deposit, 1470 eruption, fine-grained unit
Q5	3	Quarry deposit, 1470 eruption, coarse-grained unit
FM27	4	3-2-08, collected after an eruption on the same morning – 1st eruption for a month
SAK12	5	9-05-08, collected after a series of eruptions over 2 days
Q9	6	Quarry deposit, 1914 eruption.
SAK22	6	3-12-97, collected several hours after a large eruption, 70,000 tons of ash erupted on Sakurajima.
J39	6	26-8-85, collected during several days of eruptions and ash emission
J41	6	16-6-88 collected after two large eruptions, depositing record amounts of ash in Kagoshima city.
SAK21a	6	4-6-84, collected during a very active period after three eruptions the previous day, 1st analysis carried out 11-05-2009
SAK21b	7	2nd analysis of sample carried out 23-11-09
SAK16	7	Collected 6-6-00, eruption details not found.
SAK19	7	7-10-00, collected ~1 hour after a large eruption, but from a contaminated surface.
FM28	8	5-2-08, collected during continuous ash emission

Each quantification was checked by several users, who all came to good agreement, within 1 wt. %, to ensure that bias was not being introduced in the pattern interpretation. Sample SAK21 was run twice, on separate days and on different XRD-sPSD instruments, to check reproducibility of results. Figure 4.12

shows the two XRD patterns, which match closely apart from an additional peak in the pattern for SAK21a (marked by an asterisk) which is due to a defect in one of the XRD machines. Table 4.3 shows that the two analyses on sample SAK21 are within 1 wt. %.
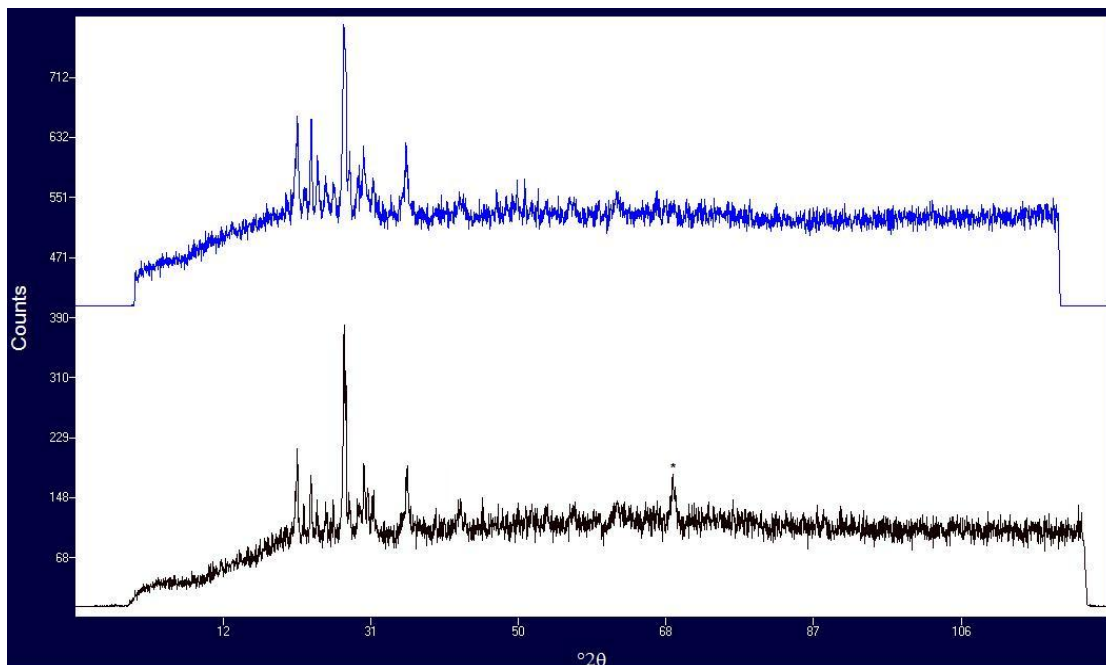
Figure 4.12: XRD patterns for sample SAK21 measured on different days and on two different instruments. * shows a peak present due to a machine defect. Blue pattern was analysed on 23-11-09 (SAK21b); black pattern was analysed on 11-05-09 (SAK21a).

4.5   Surface reactivity

The number of free radicals (specifically hydroxyl radicals) and the amount of iron (total, Fe^{2+} and Fe^{3+}) released from particle surfaces and their relationship to each other are examined to estimate the surface reactivity. Differences in surface area are accounted for by expressing the measurements as m^2 g^{-1}. The absolute amount of radicals and iron released over the course of the experiments is also assessed. Only pristine samples (collected within hours of eruption and stored in a dry environment) with a cumulative volume percentage of respirable material above 4 % were used in these analyses.

4.5.1 *Surface area*

The BET specific surface areas for the Sakurajima samples range between 0.5-3.8 m^2 g^{-1}, as shown in Table 4.4. The isotherm graphs and correlation coefficients for the results can be found in Appendix D. All results produced by the instrument were accurate to a correlation coefficient of at least 0.999. For BET specific surface area the instrument correlation coefficient should ideally reach 0.9999, however, this is only possible when the instrument has at least 40 m^2 of surface area to measure. This is not possible when analysing volcanic ash samples, where the surface areas are low and the tubes will not hold sufficient masses of ash. Therefore a coefficient of 0.999 was accepted for these samples and repeats were used in order to try to ensure better accuracy of the results. The errors quoted here have therefore been worked out using the differences between the repeat results and are not the lower values quoted in the machine calculations.

Table 4.4: Specific surface area BET results, average taken from 2 measurements.

Sample ID	Average BET specific surface area (m^2/g)
SAK12	3.86 (+/- 0.10)
SAK16	1.48 (+/- 0.15)
SAK19	0.50 (+/- 0.04)
SAK21	1.34 (+/- 0.08)
SAK22	3.12 (+/- 0.17)
SAK28	2.61 (+/- 0.16)
J39	0.47 (+/- 0.11)

4.5.2 *Hydroxyl Radical Release*

The number of hydroxyls released per unit surface area for the samples is very low (Figure 4.13). Only two samples released more than 0.21 μmol m^{-2} of hydroxyl radicals, samples SAK19 and J39. All of the other samples produced values between 0.05 and 0.21 μmol m^{-2}. Distinctions between these samples are difficult to make as such low results means that the differences between the samples are extremely small and often the results lie within each others' errors

(Figure 4.14). Experiment kinetics further complicate comparison between the lower 5 samples, as samples SAK12 and SAK16 have a marked increase in hydroxyl release at 30 minutes compared to at 10 and 60 minutes, whilst hydroxyl release in the 3 other samples remains almost constant throughout the experiment. Still, it can generally be said that samples SAK12 and FM28 have the lowest values, with less that 0.1 μmol m^{-2} over the whole course of the experiment, and the other three samples cluster slightly higher, between 0.1 and 0.2 μmol m^{-2}.
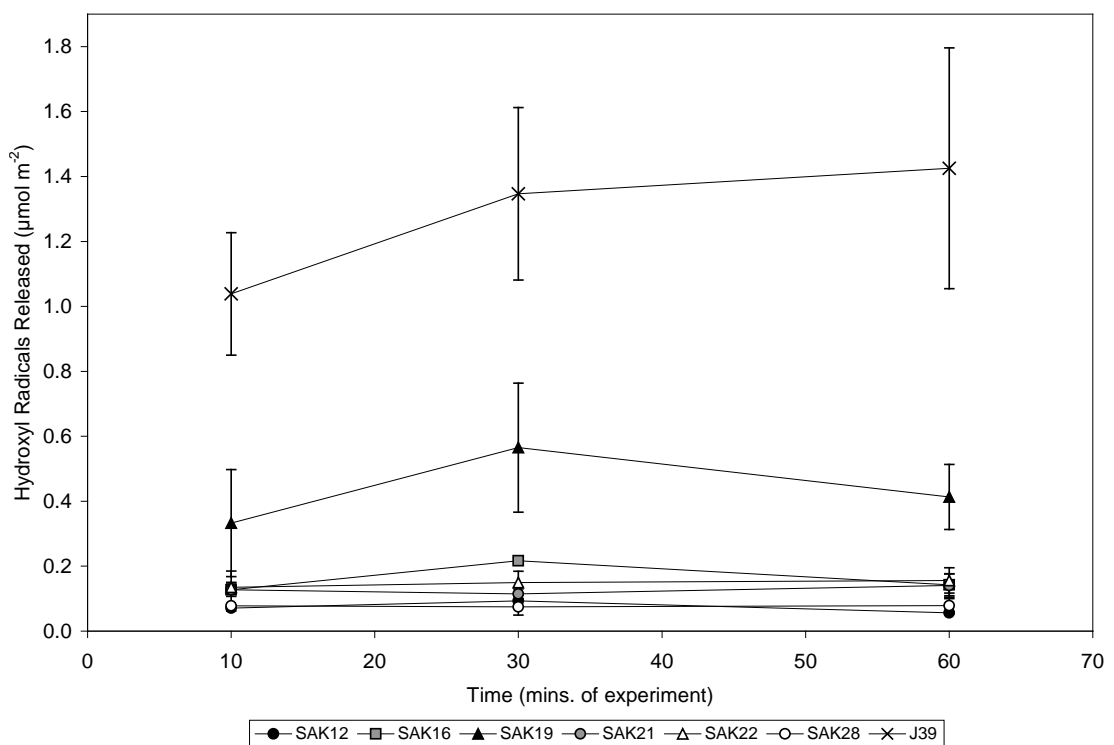
Figure 4.13: Hydroxyl radical release per unit surface area at 10, 30 and 60 minutes after the start of the experiment.
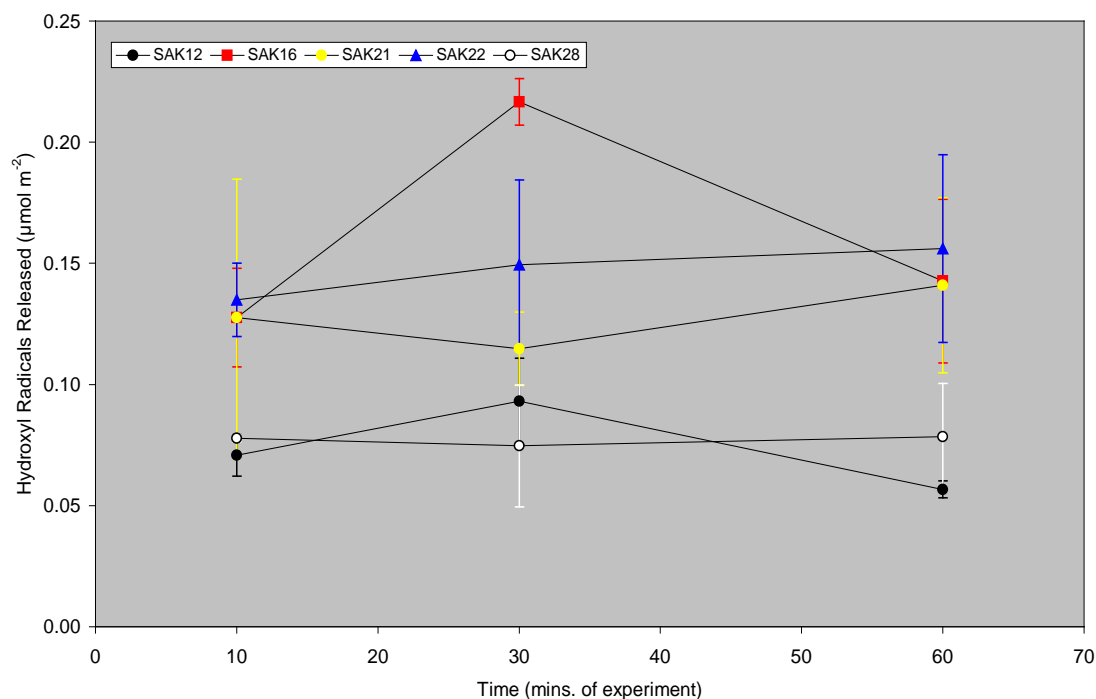
Figure 4.14: Hydroxyl radical release per unit surface area at 10, 30 and 60 minutes after the start of the experiment. Samples SAK19 and J39 have been excluded and the sample error bars and symbols are represented in different colours in order that the errors for each sample can be better identified.

The samples that produced the highest number of radicals per unit area were also the samples with the lowest specific surface areas (<1 m^2 g^{-1}). Although this does not explain the higher surface reactivity, it may mean that other samples may have released a higher number of radicals despite a lower surface reactivity. Figure 4.15 shows the total hydroxyl radical release over the experiment, without taking into account the surface area of the samples. Sample J39 still has a higher result than the rest of the samples, although sample SAK19 released similar quantities of free radicals to the other samples, whilst sample SAK22 released more. Once again, detailed comparisons between the samples are hindered as samples sit within the errors of other samples. Despite this, the results demonstrate that surface area available is not a major influence on hydroxyl release, which must be controlled primarily by other factors.
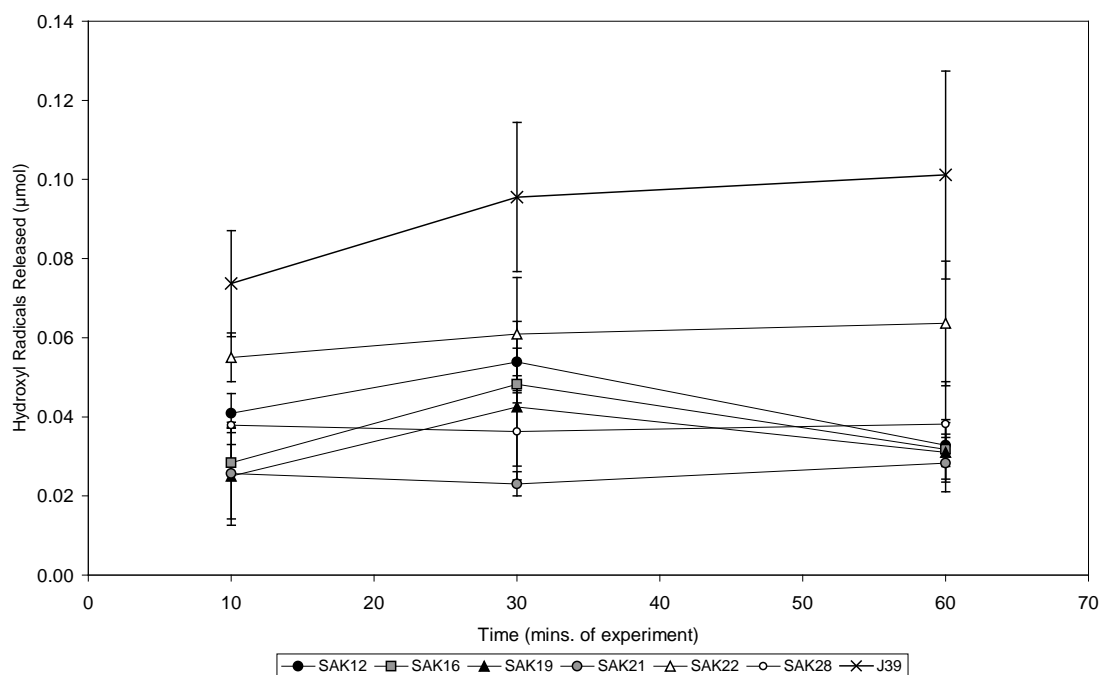
Figure 4.15: Total number of hydroxyl radicals released by each sample at 10, 30 and 60 minutes after the start of the experiment.

4.5.3 Iron Release

The results for total iron and Fe^{2+} for each sample over the 7 day experiment are shown in Figures 4.16a and b. Samples J39, SAK22 and SAK19 had the highest amounts of total iron released per unit surface area. This is not reflected when examining Fe^{2+} release, where samples SAK22, SAK19 and SAK12 have much higher results and J39 produces comparatively smaller amounts per unit area than the other samples.
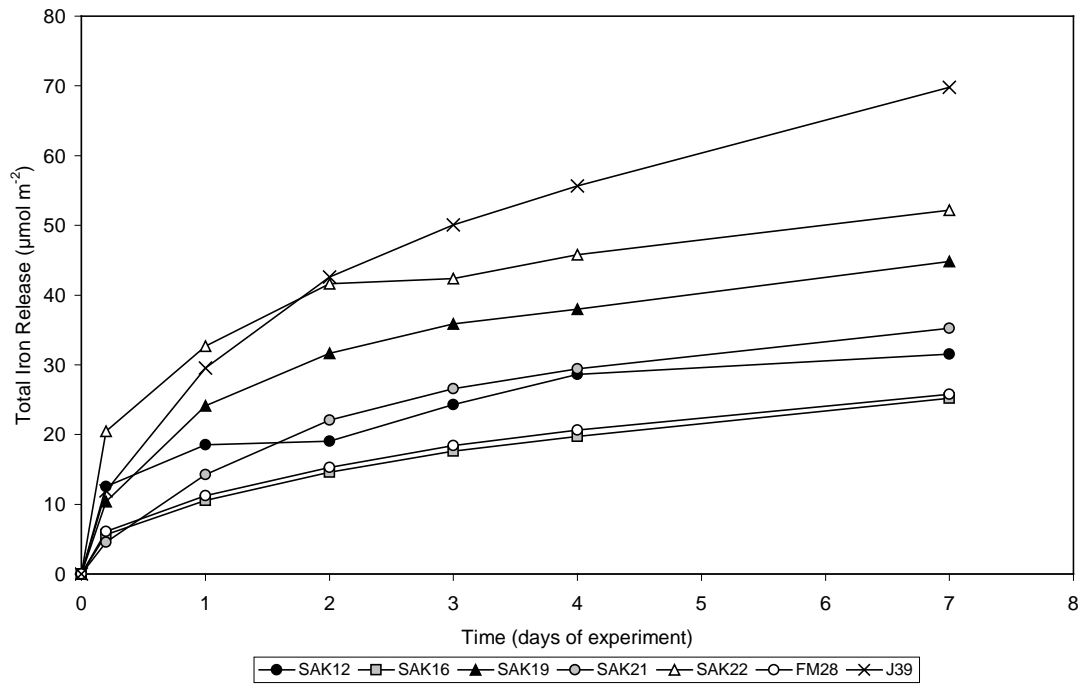
<u>Figure 4.16a</u>: Amount of total iron released over the course of the experiment.
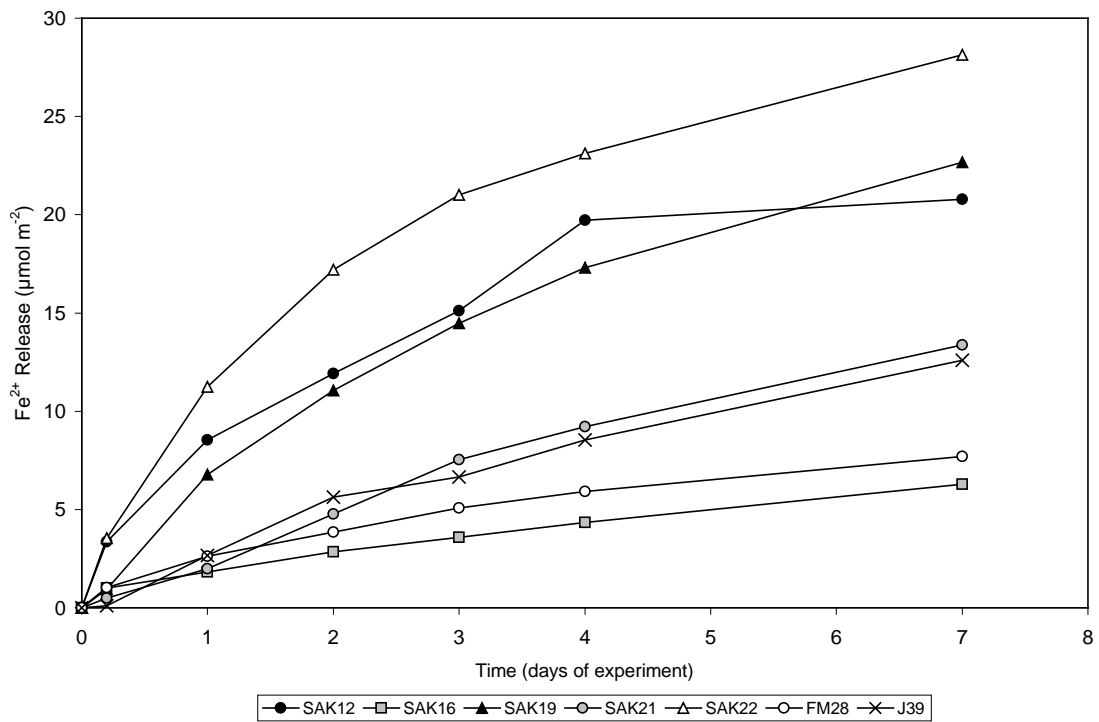
<u>Figure 4.16b:</u> Amount of Fe^{2+} released over the course of the experiment.

Once again, care should be taken not to assume that high iron values per unit area mean that large absolute amounts of iron are released. For example at 7 days the absolute amounts of total iron released for sample J39 (with highest release per m^2) is less than a quarter of samples SAK22 and SAK12 (Table 4.5). For the total iron results, it appears that the surface area is a larger (although not the only) influence on the absolute amount of iron released than the number of hydroxyl radicals released (Figure 4.17).

Table 4.5: Comparisons between the Specific Surface Area, Total Fe per unit area and absolute Total Fe released.

Sample I.D.	Specific Surface Area (m^2 g^{-1})	Total Fe Release per unit area at 7d (µmol m^{-2})	Absolute Total Fe Released at 7d (µmol)
SAK12	3.86	27.14	104.71
SAK16	1.48	25.19	37.39
SAK19	0.50	44.81	22.45
SAK21	1.34	35.23	47.24
SAK22	3.12	45.42	141.93
FM28	2.61	32.08	83.60
J39	0.47	69.80	33.02
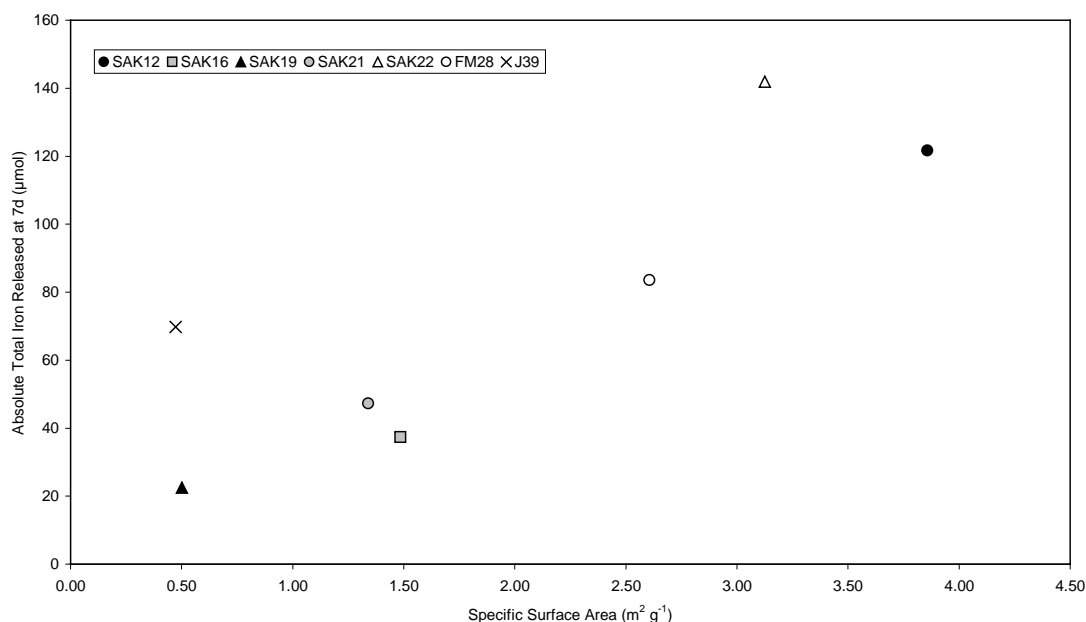
Figure 4.17: Relationship between specific surface area and the amount of total iron released.

Figure 4.18 shows the results for total iron, Fe^{2+} and Fe^{3+} with each sample on a separate graph so the kinetics of the experiments can be seen more clearly. It should however be noted that as Fe^{3+} was not measured directly, but was worked out by subtracting the Fe^{2+} results from the total iron results, these results will not reflect the true kinetics of Fe^{3+} production, but the kinetic differences between the other two results. Fe^{3+} has been included here as the final results should still give a good estimate of the amount of Fe^{3+} released after 7 days, and the results for previous days help to exemplify kinetic differences between total iron and Fe^{2+} release for the samples.

The kinetics through the experiment are similar for all samples, regardless of surface area or amount of iron released. Generally, a very rapid initial increase in total iron in the first four hours can be seen. A high rate of increase continues during the first and second days, apart from sample SAK12 where the amount of iron remains constant between 24 and 48 hours. From days 4-7 the amount of total iron released continues to increase steadily although the rate is much slower for all samples. However the kinetics of Fe^{2+} release are somewhat different. Initial Fe^{2+} release is low (except in samples SAK12 and SAK22), and in some cases no Fe^{2+} is released at all during the first 4 hours. Throughout the experiment Fe^{2+} is then released at a relatively constant rate.

Despite similar kinetic patterns for most samples, the proportions of Fe^{2+} and Fe^{3+} vary greatly. Samples SAK12 and SAK22 are the only samples where at 7 days the amount of Fe^{3+} release is less than that of Fe^{2+}. For sample SAK19 the amount of both species is almost the same and all other samples contain more Fe^{3+} than Fe^{2+}, although the proportions of each still differ.
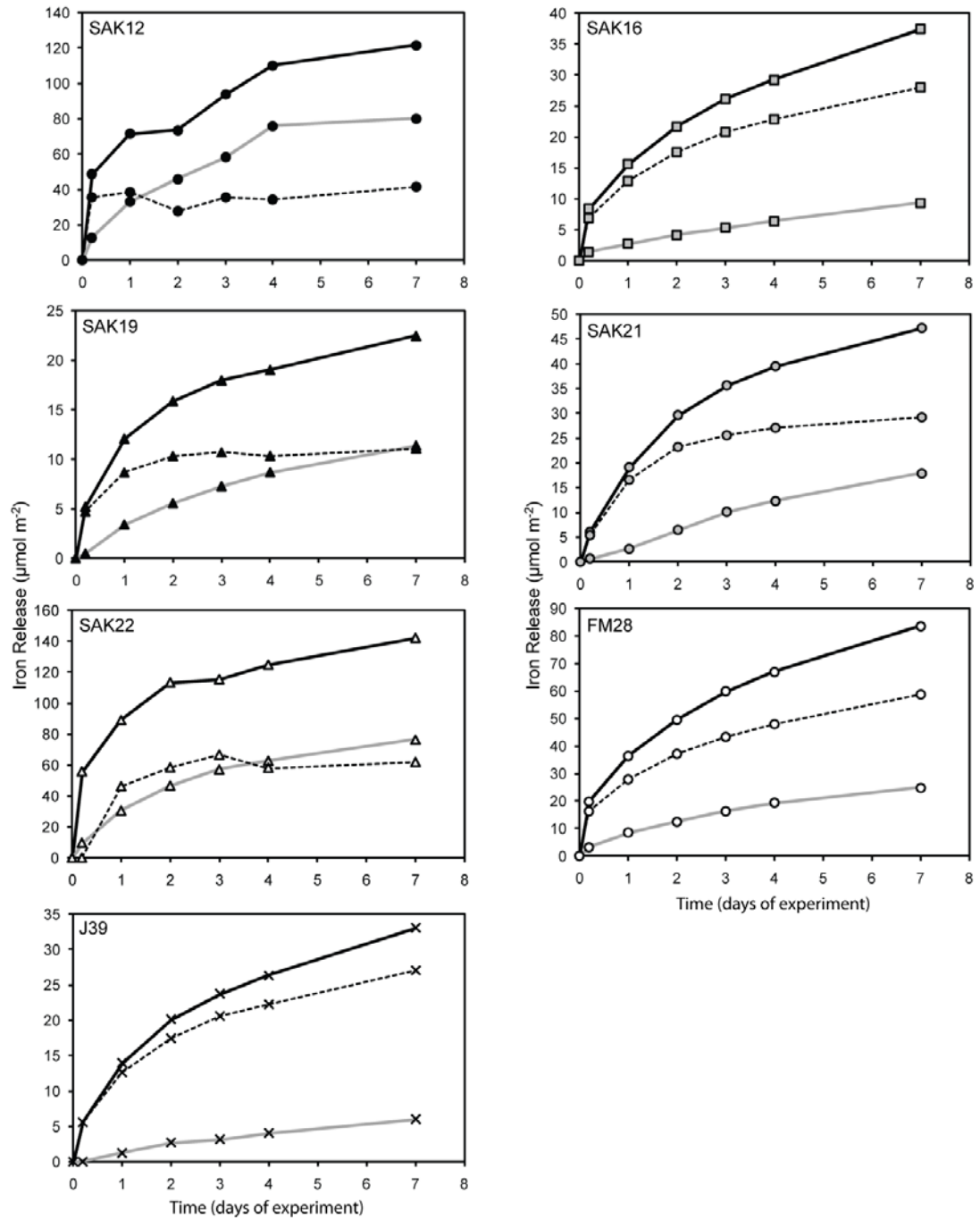
Figure 4.18: Separate graphs showing the amount of iron released over the period of the experiment for each sample. The black solid line represents total Fe released, the dotted line shows the amount of Fe^{3+} released and the grey solid line indicates the amount of Fe^{2+} released.

4.5.4   Relationship between hydroxyl radical and iron release

Figures 4.19a – c show the relationship between the number of hydroxyls released at 60 minutes and the iron released at 7 days for total Fe, Fe^{2+} and Fe^{3+}. The iron release measured at 7 days was chosen to eliminate any kinetic differences between the samples. The hydroxyl radical release for most samples was similar over the course of the experiment, apart from the increases at 30 minutes for samples SAK12 and SAK16. However the differences were so small that they did not affect the interpretations made here. The hydroxyl radical release at 60 minutes was chosen as the results for sample J39 showed a steady increase over the course of the experiment.
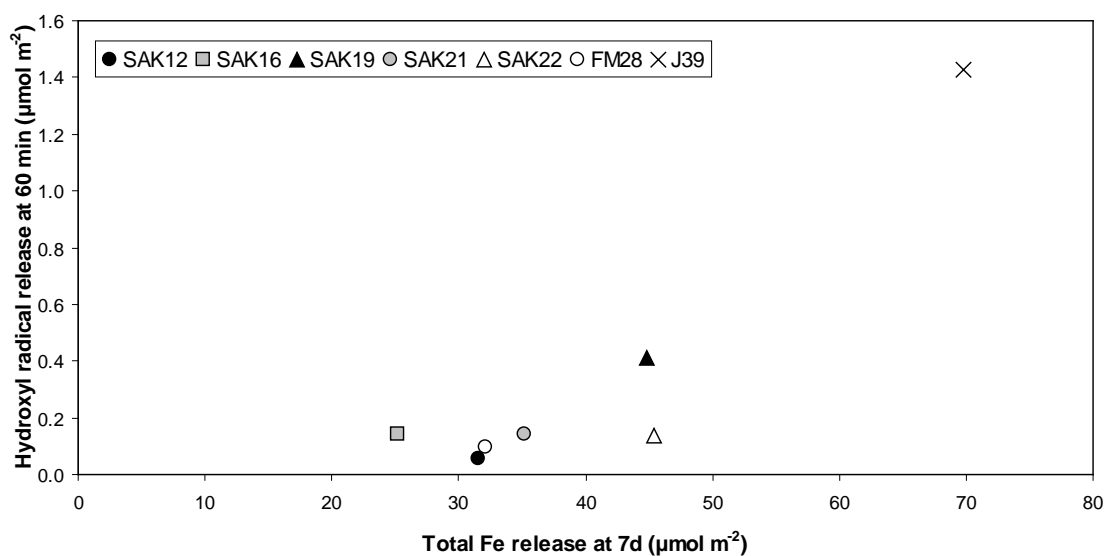
Figure 4.19a: The number of hydroxyl radicals released at 60 minutes after the start of the experiment compared to the total iron released after 7 days.
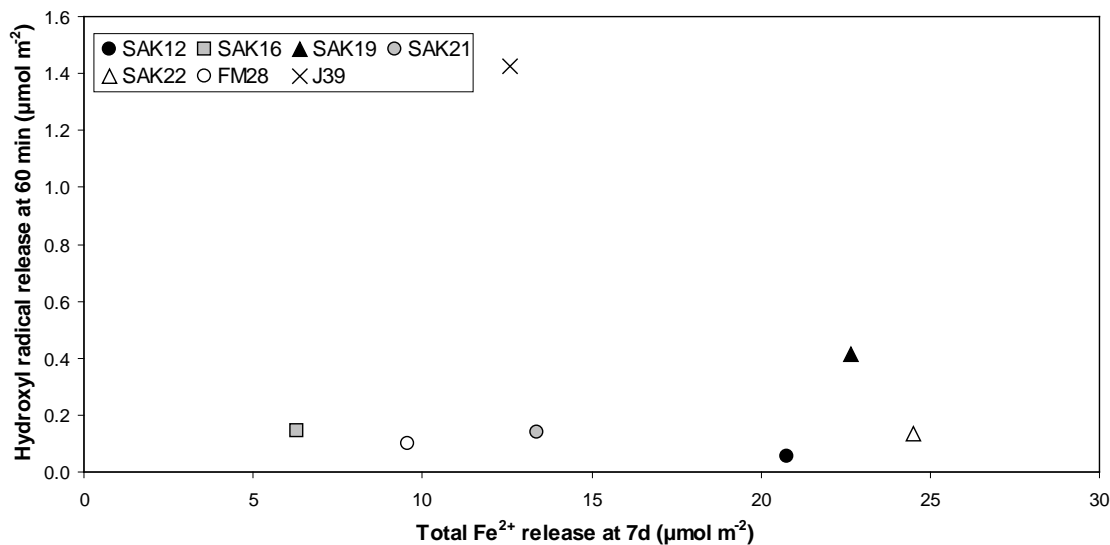
Figure 4.19b: The number of hydroxyl radicals released at 60 minutes after the start of the experiment compared to the amount of Fe^{2+} released after 7 days.
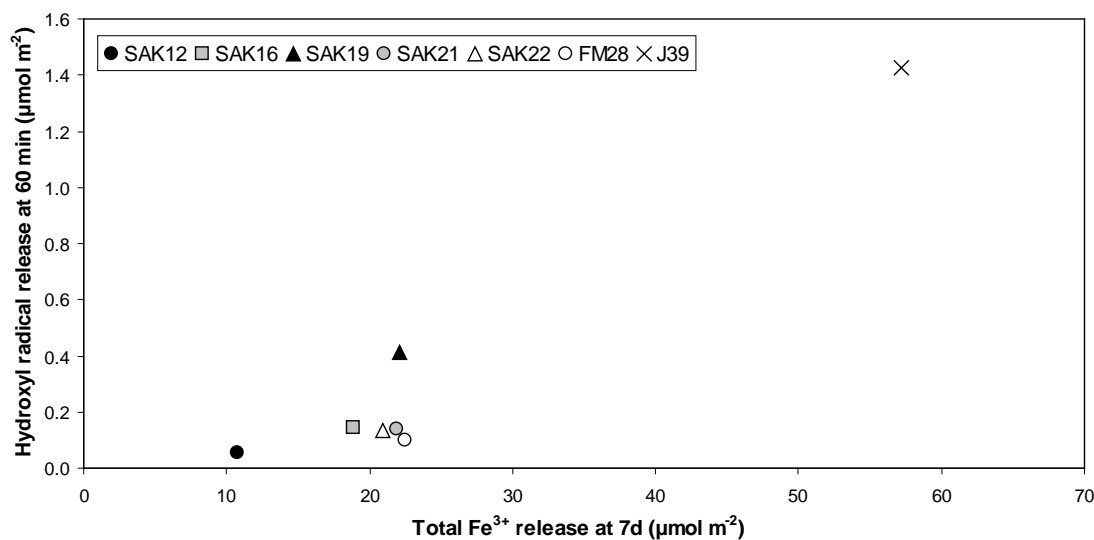
Figure 4.19c: The number of hydroxyl radicals released at 60 minutes after the start of the experiment compared to the amount of Fe^{3+} released after 7 days.

The graphs show that the amount of total iron appears to influence the number of hydroxyl radicals released, with a general increasing trend. No apparent trends between hydroxyl radical and Fe^{2+} released are evident. The only sample with significantly higher quantities of hydroxyl radicals release is sample J39. The results for this sample could have a large impact on the assessments made. Therefore the lack or presence of general trends are insignificant when making comparisons between these samples.

Chapter 5

Discussion

5.1 Introduction

A number of aspects regarding potential respiratory toxicity of the ash samples were considered in this study, including physical characteristics, mineralogy and geochemistry. Therefore several very different data sets have been obtained and each area needs to be discussed individually. Hence this chapter will interpret the data set for each area separately to maintain clarity, before all the strands of evidence are discussed together in the second part of the chapter (Sections 5.5 - 5.6). In each section, the implications of the results will be considered in accordance with the research aims. After a brief summary of the potential hazard inferred from each analysis, attempts will be made to reconcile these results with previous literature on Sakurajima to try to address the disparities between various studies. I will then consider the results within a more global context, using comparisons to other eruptive styles, and examining other volcanoes where potential risks have been better constrained, to justify my assumptions of the potential hazard posed by Sakurajima volcano. I will present possible explanations for the results seen, building on knowledge of other volcanoes and the eruption mechanics at Sakurajima volcano. An assessment of the potential hazard posed by the Sakurajima ash overall can then be examined in Section 5.5. Limitations of the study will be discussed throughout the chapter and suggestions for the direction of future research in this area are presented in Section 5.6 in light of what has been learnt from this study.

5.2 Respirable Material

5.2.1 *How much respirable material is in Sakurajima ash? Addressing disparities in the literature.*

The key conclusion from examination of the grain-size distributions is the variability of ash produced at Sakurajima volcano. The volcano has the potential to produce large proportions of very fine ash that could pose a hazard to human health, but many samples are also very coarse-grained and do not contain

harmful amounts of respirable material. This is unsurprising considering the range in eruption types, eruption sizes and weather conditions at Sakurajima. However, it also makes assessing the health hazard based on grain size very difficult.

Previous observations of the grain size of Sakurajima ash led to conclusions that varied between the ash being extremely coarse, with hardly any respirable or thoracic material (e.g. Horwell, 2007; Koizumi et al., 1988; Yano, 1990) to the ash containing large proportions of thoracic material that could be potentially harmful (e.g. Shirakawa et al., 1984; Yano et al., 1986; Oba et al., 1984; Toyama et al., 1980). The range in results seen here easily accounts for the large disparities within the literature, which appear to be caused by the natural variability of ash produced by the volcano. Estimates of respirable material may also differ due to different analysis techniques used. Upon examining the ash under an SEM microscope, it was evident that many particles had formed aggregates or were adhered to the surfaces of larger particles. Hence, studies that examined respirable particulates by count, or using ultrasonic treatment, could differ substantially from analyses where aggregates have not been taken into account. Still, the heterogeneity observed between samples in the results of this study suggest that generalisations for the volcano as a whole could not be made from single sample analyses or small data sets as have been used in previous studies.

5.2.2 *Mechanisms of fine ash production*

Comparisons to other studies at different volcanoes using the same analysis techniques show that, although Sakurajima has produced substantial amounts of respirable material on occasion during the last eruptive phase, overall, the amount of respirable material is less than samples derived from larger, more explosive eruptions or dome-collapse (Table 5.1). Rose and Durant (2009), Horwell (2007) and Toprak (2007) have examined in detail the proportion of fine ash in samples from many different types of eruption. All concluded that the largest amounts of fine ash are likely to be produced by large, silicic eruptions and by fragmentation

processes in pyroclastic flows produced by dome collapse, causing fines-rich lofted ash clouds. These conclusions are supported by studies of individual volcanoes, as detailed in Table 5.1. Horwell et al. (2010) also showed that very large amounts of fine ash are generated when magma interacts with water during explosive phreatomagmatic eruptions, when examining samples from Vesuvius.

Table 5.1: The amount of respirable material in ash from volcanoes with various eruption styles and the suggested mechanisms of fine ash production.

Volcano	Magma type/eruptive style	Cumulative Vol. % < 4 um	Mechanism of fine ash production / trends examined.
Sakurajima, Japan	Andesite, stombolian-vulcanian	0.86 – 9.6[1,2]	Large range in amounts of fine material produced. Most samples contain <6 vol. % respirable material.
Sakurajima, Japan	Andesite-Dacite, plinian	1.5 – 18.8[1]	Plinian style eruptions. All collected very close to the crater.
Unzen, Japan	Dacite, Dome collapse	4.3 – 9.51[1]	Various dome-collapse ashfall samples collected from close to the volcano.
Soufriére Hills, Montserrat	Andesite, vulcanian-dome collapse	5.9 – 12.7[2,3]	Dome collapse ash-fall contained significantly more fine material than vulcanian ashfall. Finest ash is produced by fragmentation in pyroclastic flows and preferential elutriation of the fines. [4,5,6]
Colima, Mexico	Andesite, vulcanian-dome collapse	5.9 (vulcanian sample)[3]	Co-pyroclastic samples contained larger amounts of fine material than produced in vulcanian eruptions. Very fine ash was produced by milling in pyroclastic flows.[7]
Vesuvius, Italy	Phonolitic/ tephritic, strombolian-plinian	0.36-17.19[8]	Grain-size broadly related to eruption size, but with very large amounts of fine ash from phreatomagmatic eruptions.[8]
Chaiten, Chile	Rhyolitic, vulcanian, dome growth	8.8 – 17.7[9,10,]	Grain-size was a function of plume height, eruption intensity and distance from the crater. Detailed mechanism not outlined.[11]
Mt. St. Helens, USA	Dacitic, Plinian	3.2 – 14.5[2,3]	Particle aggregation strongly influenced trends in fine ash with distance from the volcano. Distal locations included higher proportions of fine ash, but increases did not occur in incremental steps. [12]
Etna, Italy	Basaltic, strombolian	0.2 – 1.83[2,13]	Ash is produced by various eruptive mechanisms, but is fines-depleted.[14]

N.B. Ranges quoted here only include cumulative volume % data obtained using laser diffraction techniques.
[1] data obtained from this study; [2] Horwell (2007); [3] Toprak (2007); [4] Baxter et al. (1999); [5] Horwell et al. (2003b); [6] Bonadonna et al. (2002); [7] Evans et al. (2009); [8] Horwell et al. (in press); [9] Horwell et al. (2010); [10] Reich et al. (2009); [11] Watt et al. (2009); [12] Durant et al. (2009); [13] Sargeant (2009); [14] Andronico et al. (2009).

General theories regarding the production of fine ash may help to explain the range of respirable material seen in the ash samples from the most recent eruptive phase. Certainly, the explosivity of the vulcanian eruptions at Sakurajima is likely to create some fine ash particles, similar to the andesitic vulcanian eruptions at Montserrat (Horwell et al., 2003b; Horwell, 2007). However, the proportion of respirable material in some samples is greater than expected considering the proximity of samples to the crater and the comparatively small size of eruptions. This could be because of a high degree of fragmentation from the explosive destruction of the lava plug/dome that seals the conduit before an eruption (see Section 2.4.2). Coarser samples are more likely to be produced by non-explosive ash venting and strombolian activity at Sakurajima, although ash deposited in the crater after a previous vulcanian eruption may still be erupted during these phases. Many of the deposit samples from plinian eruptions are quite coarse, as the deposits are located within 5 km of the volcano. However, the extremely fine-grained ash layers in the 1470s deposit demonstrate the potential of historical plinian eruptions to create large amounts of fine ash.

The results here cannot directly support theories regarding mechanisms of fine ash production as generally samples were collected over 24 hours so may include ash from several eruptions and eruptive styles. Still, the strong evidence for the influence of eruption mechanics on grain size from many other volcanoes (as seen in Table 5.1) provide good substantiation that strombolian eruptions will produce lower amounts of respirable material than the more explosive vulcanian eruptions at Sakurajima.

5.2.3   Estimating Exposure

Obtaining accurate ash dispersal and exposure data over large areas is difficult for any volcano but is likely to be particularly complex at Sakurajima due to the number of variables that need to be considered. Epidemiological studies have tried to examine exposure trends, using various parameters as a proxy for ashfall exposure. In Section 2.4.4 the epidemiological studies were summarised in detail,

highlighting the inconsistent conclusions between the different papers. Different assumptions about exposure of the populations, some using amount of ashfall, others using TSP or PM_{10} measurements, and others using proximity to the volcano in conjunction with ash dispersal models, may have been a major reason for the different conclusions regarding prevalence of respiratory disease in populations exposed to volcanic ash. Indeed, estimating exposure without taking into account the amount of thoracic or respirable material is likely to be particularly inaccurate.

This was highlighted by Nishii et al. (1986) who found that they could not correlate the amount of ashfall with PM_{10} measurement under the plume. They highlighted that the focus of many respiratory studies on populations close to the volcano may not be appropriate due to low amounts of thoracic material being observed in their measurements for these areas. However, all of the results obtained for this study were collected within 12 km of the volcano and included large ashfalls with high proportions of respirable material. In fact, the sample with the highest amount of respirable material for the current study was collected only 3 km from the crater.

Hence, even estimates using TSP or PM_{10} are likely to be over-simplistic for Sakurajima. Measurements will still include particulate from other sources (e.g. pollution). Furthermore, the studies only examined data collected during volcanic eruptions and did not allow for ash remobilisation, which could break up aggregates of small particles that would not have been apparent in initial PM_{10} measurements. None of the epidemiological studies took into account the influence of human behaviour on exposure. For example, during a second visit to Japan during August 2009, there were a series of small explosions, erupting small amounts of ash. I observed that, even during small ashfalls, most of the population in Kagoshima and on Sakurajima used some form of protection over their mouth and nose. This is likely to greatly reduce exposure to respirable ash. It could be that close to the volcano, where awareness of the ash is high, most residents use appropriate protection, whilst at more distal locations where the

amount of ashfall is less obvious, a lack of awareness means that residents are less likely to take precautions. This could have a large influence on exposure patterns. This is speculative, based on the few observations made here, but highlights an important issue that has not been addressed in epidemiological studies.

In this study, no general trends correlating eruption characteristics, location of the sample or weather conditions could be identified, and this is attributed to an inadequate data set. On the other hand, the variability seen may actually be the essence of the results, highlighting the localised nature of the eruptions, rather than a function of the problems in obtaining a comprehensive data set. Application of large-scale trends may be over-simplistic and give misleading conclusions considering the complex, rapidly changing and generally unpredictable conditions at Sakurajima. The results from this study, and lack of consistent trends between other studies, emphasize the need for more comprehensive exposure studies that examine ashfall over much longer timescales and include measurements of respirable material and examination of the influence on human behaviour; to prevent inaccurate assumptions being made about exposure in the future.

Currently, yearly reports are published that examine pollution levels in Kagoshima Prefecture from hourly TSP data that are collected at several points. Measurements of PM_{10} would be more informative for monitoring potential ash exposure. This study and those of Horwell (2007) and Horwell et al. (2010) found strong correlations between the amount of thoracic, respirable and ultra-fine material. This suggests that there may be potential to correlate airborne PM_{10} measurements with the amount of respirable and ultra-fine material found in bulk ash, although further study would be needed. Respirable ash could also be estimated by sieving deposited samples if laser diffractometers are unavailable. Horwell (2007) and Horwell et al. (2010) examined the relationship between the amount of material < 63 μm (the lowest sieve aperture) and the respirable content of deposited ash samples. They demonstrated that strong correlations

between the fractions existed when using a polynomial fit. A polynomial fit also gave the best correlation to describe the relationship between the fraction < 63 μm and that < 4 μm for the Sakurajima samples (Figure 5.1). It does not show the same pattern as the studies mentioned previously, and also has a lower R^2 value overall, 0.749. This, and considering that trends between the amount of ashfall deposited and the TSP values are poorly correlated, means that continuous monitoring of PM_{10} data may be more appropriate.

The equation shown on the chart:

$$y = -0.0195x^3 - 0.2528x^2 + 10.294x + 2.9442$$

The axes are labelled "Cumulative Vol. % < 63 μm" (y-axis) and "Cumulative Vol. % < 4 μm" (x-axis).
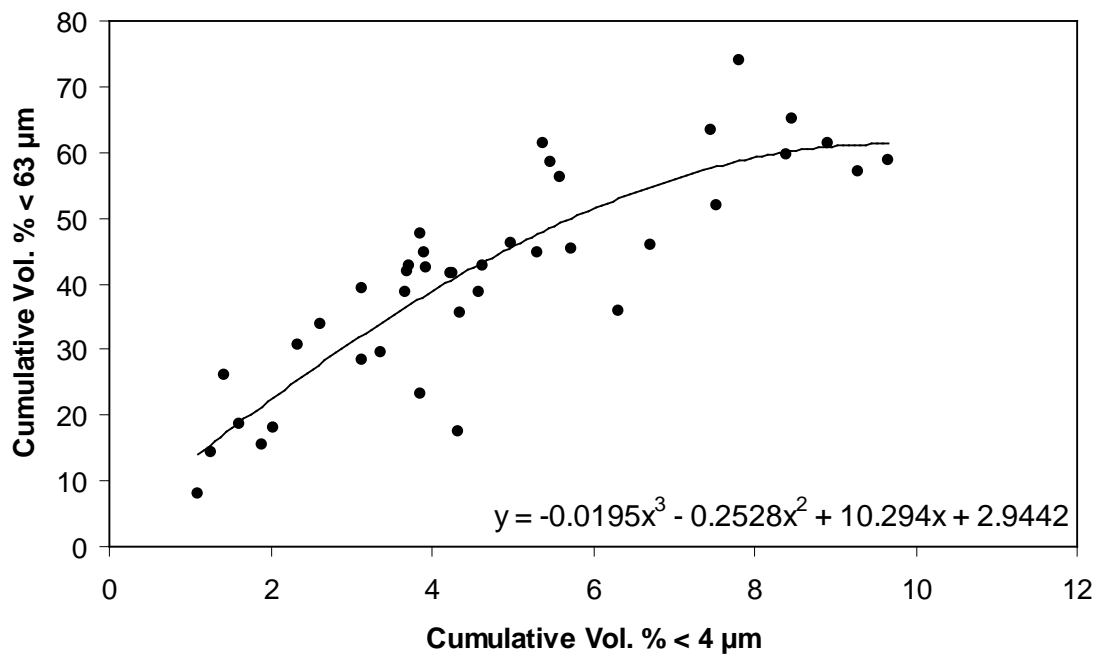
Figure 5.1: Polynomial relationship between the amount of respirable material and the proportion of ash in the lowest sieve size bin.

5.2.4   Examination of other health relevant fractions

It is well-established that respirable particles (< 4 μm) can reach the deep areas of the lung where chronic disease may be initiated (Donaldson et al., 2002). However large amount of thoracic material may provoke acute respiratory problems such as asthma and airway irritation. Many of the samples from Sakurajima contain moderate to large amounts of thoracic material, and acute respiratory complaints in local populations have been well-documented (e.g. Wakisaka et al., 1984). Such effects are easily reduced by decreasing or avoiding ash exposure. Recently, concerns have been expressed about the increased

toxicity of nano-particles, (particles with one dimension <0.1 μm, Kreyling et al., 2006) due to higher surface reactivity properties and also their ability to be redistributed around the body from the site of deposition (Donaldson et al., 2004). Very little information about nano-particles or ultra-fine material in volcanic ash has been examined. Laser Diffraction estimates of very fine particles have limited accuracy. However, an attempt to examine extremely fine particles close to the nanoscale has been made here to assess whether further work is necessary in this area. The samples from Unzen volcano analysed included 0.09 – 0.29 vol. % < 0.5 μm, whilst the Sakurajima samples only contained <0.001 – 0.11 vol. % < 0.5 μm. The relatively large estimated quantities of sub 0.5 micron material in some samples, particularly for Unzen volcano demonstrate that investigation into ultra-fine and nano-particles in volcanic ash may be an appropriate area of future research to better constrain the overall hazard from volcanic ash.

5.2.5   Limitations

The lack of data appropriate to estimate the exposure of populations to respirable ash from Sakurajima has been the major limitation of this study. As the volcano was not active during the trip, a single comprehensive data set, with well-described eruption characteristics could not be obtained. Samples from the archive sources had generally been collected from outside the institution or from Sakurajima itself, and therefore it was difficult to find samples from a range of locations around the volcano, particularly in Kagoshima city. No samples were found which had been collected from Tarumizu city, although it is also regularly exposed to ashfall. This is a significant gap in analyses when it comes to risk assessment. All samples were collected within 12 km of the volcano, so ash dispersion over larger distances could not be examined. Ideally, to better represent the characteristics of ash that people are exposed to, airborne samples would have also been collected. However, due to the inactivity of the volcano during the fieldtrip and the quantity of ash needed for detailed analyses, only settled samples could be used.

Limitations regarding the laser diffraction method to examine grain-size distributions for health-pertinent fractions should also be outlined here. Laser diffraction produces results expressed as "equivalent spherical diameter". This poses two problems for analysing the amount of respirable particulate. Firstly, many of the Sakurajima ash particles observed under SEM were elongate. Many studies have examined the effect of particle shape on laser diffraction results, some finding that elongate particles led to over-estimation of the fine fraction (e.g. Beuselinck et al., 1998), while others concluding that elongate particles were often assigned to coarser size bins (e.g. Eshel et al., 2004). The similarity between all studies is the conclusion that shape does have an effect on grain-size distributions (GSDs) measured by laser diffraction methods (e.g. Naito et al., 1998; Ma et al., 2000; Bowen, 2002). The exact effects that shape has on the GSD appears to depend on the type of particles being analysed. This has not been quantified for volcanic ash samples, but could affect the comparisons made between results for different volcanoes, where particle shapes may differ. Problems regarding reproducibility of results measured by instruments from different manufacturers and the choice of theory and experiment parameters used have also been identified (e.g. Etzler and Deanne, 1997; Black et al., 1996).

However most studies still recognise that the wide-spread use and ease of laser diffraction often outweighs the inherent inaccuracies, as long as the method is applied appropriately. Horwell (2007) discussed the various methods to estimate the amount of respirable material in volcanic samples. She highlighted the necessity of a method that is relatively quick and easy in order for results to be available as quickly as possible for hazard managers. Furthermore, Horwell (2007) set out appropriate methodologies for estimating respirable material in volcanic ash samples using laser diffraction which have been applied in this study.

In addition, equivalent spherical diameter is not the same as the aerodynamic diameter of particles. Numerous studies have examined the use of laser diffraction techniques, especially for estimating particle size for medical

nebulizers, against other methods that measure aerodynamic diameter. Most of these studies have found good correlation between the results obtained by laser diffraction and aerodynamic diameter measurements (e.g. Stevens et al., 2007; Zeng et al., 2006; Mitchell et al., 2006). Although these studies examined aerosols, the good correlations for their results demonstrate the applicability of using equivalent spherical diameters to assess the amount of respirable particulate, especially for estimate studies such as this one.

As can be seen, there are many difficulties when trying to examine the amount of respirable material that local populations are potentially exposed to. To date, no studies have quantitatively compared different techniques, using deposited ash samples or ash aerosols, nor examined which technique may best reflect actual ash exposure. Hence, there are many limitations of the results obtained here that can only be assumed and cannot be quantitatively analysed. However, mineralogical assessment of the ash with respect to respiratory health was developed to provide a quick and relatively easy indication of the potential hazard which could advise further study and actions. Despite the limitations, the use of deposited samples allows easy, rapid collection and laser diffraction provides the quickest, easiest, but also one of the most robust and accurate methods for estimating grain size distributions.

5.3   Crystalline silica in the ash

5.3.1   Observations of cristobalite in Sakurajima ash

The XRD results showed that the amount of cristobalite in the archive samples was between 4-8 wt. %. These samples included a range of eruption types and dates. The variability of the ash has been emphasised in previous sections (4.2-4.3 and 5.2), but the amount of cristobalite produced by Sakurajima appears to be relatively constant. However, only those samples with at least 4 vol. % < 4 μm were analysed, as very coarse samples are unlikely to be potentially hazardous to the respiratory system. It could be that if coarser samples were included a larger

range in cristobalite values may be seen. Although not directly comparable, due to differences in quantification techniques, previous reports of cristobalite in ash samples from the most recent eruptive phase have ranged between negligible to 5 wt. % (Yano et al., 1985; Yano et al., 1990). Oba et al. (1984) and Oba et al. (1980) also identified cristobalite in the XRD patterns of their Sakurajima volcanic ash samples, but did not quantify the amount.

For the quarry samples analysed, the dacitic samples from the 1470s ash layers contained very little cristobalite (2-3 wt. %), whilst the ash analysed from the 1914 eruption had a larger amount, similar to the quantities observed in the archive samples (~6 wt. %). Kawano and Tomita (2001)b observed 10 wt. % cristobalite in some 1914 volcanic ash. The results are in good agreement with Shiraki and Tomita (1993), who did not quantify, but gave a general indication of the amount of cristobalite in ash layers from a different sequence at Gongenyama, on Sakurajima. They examined ash and pumice falls from before 6,300 years B.P. to 1914. Their results showed no cristobalite in ash layers located above a 1470 pumice fall, but "distinctly noticeable" cristobalite peaks for the ash layers that overlay the 1914 pumice. The ash layers had comparable XRF results to those seen for the samples used in this study. As each large historical eruption has distinct silica concentrations, decreasing with time (Uto, 2005), the similarity between XRF results indicates that the ash layers from the two studies are likely to be derived from the same eruption periods. Shiraki and Tomita (1993), however, also identified small amounts of tridymite in the 1914 sample, which were not present in the sample used in this study. In the older ash layers, Shiraki and Tomita identified varying amounts of cristobalite, with particularly large amounts for ash erupted before 4,900 years B.P. Increased amounts of tridymite were also present in the older ash samples.

Again, these results were obtained by different XRD instruments and quantification techniques which, in particular, may not have taken into account the importance of the overlap of the plagioclase feldspar and cristobalite peaks (which the technique used in this study is the first to overcome). However their

results can help to provide additional general information where only a few deposited samples were available for this study. Their results are broadly consistent with the samples examined in this study, but also demonstrate that larger amounts of cristobalite appear to have been produced in the ash of even older eruptions. This is not only important for the health hazard implications should Sakurajima return to previous eruptive styles, but also because the historical ash deposits could be remobilised, especially in the quarry samples, and could therefore be a source of potential hazards in addition to the current eruptions.

5.3.2   The potential risk from cristobalite

Although little is known about cristobalite toxicity in volcanic ash, previous studies of other volcanoes, such as Soufrière Hills and Mount St. Helens, where the risk from cristobalite has been well-constrained demonstrate that, at Sakurajima, the cristobalite content is relatively low. Table 5.2 shows some recent analyses of cristobalite for other volcanoes using the IAS method.

Table 5.2: The amount of cristobalite in various ash samples and any risk interpreted. All cristobalite results are derived with the new IAS method. All values for respirable material use Malvern Mastersizer laser diffractometer and are for the corresponding samples analysed for cristobalite.

Volcano	Eruption Type	Wt. % cristobalite	Vol. % < 4 µm	Risk from cristobalite?
Vesuvius, Italy[1]	Plinian/sub-plinian eruptions (AD 79, AD 472, AD 512)	1 – 2	8 – 17	Risk specifically from cristobalite was low due to silica-undersaturated magma.
Rabaul, Papua New Guinea.[2]	Strombolian/ vulcanian (samples derived from several volcanoes)	1 – 5	2 – 6.5	Low – low respirable and cristobalite contents means minimal risk to local populations from cristobalite in the ash.
Mt. Unzen, Japan[3]	Vulcanian/dome collapse, (Samples are only from dome collapse ash)	8 – 10	9 – 10	Content lower than for other dome-collapse ash samples. Only a few samples analysed. No firm conclusions can be drawn.

Soufrière, Hills Montserrat[4]	Vulcanian/dome-collapse ash	8 – 15	6 – 11.5	Yes – similar toxicity to coal dust, ongoing eruptions could lead to high exposures, particularly from dome-collapse ash.
Mt. St. Helens, USA[5]	Plinian		–	No – exposure not high enough considering low cristobalite content and short-lived eruption.
Chaitén, Chile[4]	Vulcanian/dome collapse	2.2 – 19	8.7 – 17.65	Potential hazard observed, particularly from samples related to dome-growth/collapse. Exposure studies being carried out to assess the risk.
Sakurajima Japan[3]	Plinian/strombolian-vulcanian	2 – 8	3.9 – 15.12	Currently unknown.

[1] Horwell et al. (in press); [2] LeBlond et al. (in review); [3] results obtained from this study; [4] Horwell et al. (2010); [5] results used with permission of D.Damby, 2010.

In particular, samples from Chaitén and the Soufrière Hills volcanoes, where cristobalite values are as large as 19 wt. %, highlight the comparatively small amounts of cristobalite produced at Sakurajima. At Mt. St. Helens cristobalite values were low (although data is not available using the IAS method) and the conclusion after numerous well-constrained and multi-disciplinary studies for Mt. St. Helens was that, although care should be observed, exposure was not high enough to potentially lead to the development of chronic disease (Buist et al., 1986). A similar conclusion could then be made for Sakurajima, especially considering that the amount of ash and proportions of respirable material produced by Sakurajima overall are lower. Yet, Sakurajima differs due to the unprecedented long-term nature of the eruptions (Tsutsumi et al., 1995). The eruption of Mt. St. Helens was large, however exposures were relatively short-lived, a principal reason for concluding that exposure was not high enough to develop chronic diseases (Martin et al., 1983). Eruptions at Sakurajima have been ongoing since 1955. Although there have been periods of high and low activity, the time period for potential exposure has been much longer at Sakurajima.

The toxicological studies that have been carried out using Sakurajima ash, gave a range of conclusions depending on the dose and timescales used in the experiments, finding the ash to have no effect, to be easily phagocytosed but cause release of profilins related to carcinogenesis, or to cause serious negative symptoms (Samukawa et al., 2003; Yano et al., 1990; Yano et al., 1985; Shirakawa et al., 1984). The small, but nonetheless noteworthy, amounts of cristobalite in the Sakurajima samples could explain the reasons for any symptoms only being apparent in studies that used very high exposures and significant symptoms only developing over long timescales. This is consistent with the toxicological work carried out on ash from Mt. St. Helens (e.g. Martin et al., 1986; Grose et al., 1985; Green et al., 1982).

In occupational settings, mineral dust exposures are likely to be at greater doses than for volcanic ash, and may help to estimate potential threats from Sakurajima ash. Chronic problems generally only occur after years of exposure on an almost daily basis and with high concentrations of respirable crystalline silica (AIOH, 2009). Some recent studies have highlighted that risk from crystalline silica may have been underestimated, with reported cases of silicosis in people working within legal exposure limits (Park, 2002) and with cumulative models being criticised, as short-term, very high exposures are likely to be more hazardous than equivalent exposures at lower levels over longer timescales (Buchanan et al., 2003). Despite this, the low amounts of cristobalite in the Sakurajima ash samples and the generally lower toxicity of ash samples in toxicological tests compared to pure standards (e.g. Yano et al., 1985; Koizumi et al., 1988) means that any potential hazard will only occur if exposure to the cristobalite in ash is high and persistent.

5.3.3   The form of cristobalite

From the XRD patterns, it seems likely that the cristobalite being formed at Sakurajima is beta cristobalite. Reich et al. (2009) also identified beta cristobalite in the ash samples from Chaitén volcano. The presence of beta cristobalite (the

high-temperature form of cristobalite) is of interest because it should not be possible for the high temperature form of a mineral to be present at room temperatures. The cristobalite should go through a transition to alpha cristobalite at around 240 °C. Horwell (pers. comm., 2009) has noted this in the Soufrière Hills ash too and the mechanism by which the beta form may be preserved is currently a topic of research at Durham.

Reich et al. (2009) also observed cristobalite in the form of nano-fibres. Very small fibre-like particles were observed by SEM in some of the Sakurajima samples. Similar particles have been examined in other studies of Sakurajima ash that were suggested to be gypsum (Shiraki and Tomita 1992). Elemental analysis could not be carried out in this study, therefore this cannot be confirmed for the samples examined here although they are more likely to be gypsum than cristobalite, as the particles appear to be more like condensates than individual particles adhered to larger ones.

5.3.4   *Mechanism for cristobalite formation*

The conditions for cristobalite formation in volcanoes remain unclear. In other studies, the largest proportions of cristobalite have come from dome-collapse ash elutriated from pyroclastic flows such as at Chaitén and the Soufrière Hills volcano (Horwell et al., 2003b; Horwell et al., 2010). The results obtained here for the samples from dome-collapse eruptions at Unzen Volcano are slightly lower than other dome forming volcanoes (8-10 wt. %), although only two samples have been analysed. Horwell et al. (2003b) suggested that dome-collapse ash is enriched in cristobalite because the crystals, formed mainly by vapour-phase deposition in the lava dome, are preferentially lofted from pyroclastic flows as the dome rock is fragmented.

The cristobalite contents of the archive Sakurajima samples are lower than those of erupted ash at the larger dome-forming volcanoes, but are higher than those analysed for vulcanian-style eruptions where no dome has been present (e.g. at

Rabaul; Le Blond et al., in review). This is important as cristobalite can also be formed by hydrothermal alteration, as suggested by Oba et al. (1984) for Sakurajima. The higher cristobalite quantities and the presence of the small dome at Sakurajima suggests that formation is more likely to be due to vapour-phase deposition of cristobalite in vugs in the dome or devitrification of volcanic glass, as described for other dome-forming volcanoes. Studies at Chaitén volcano have demonstrated that cristobalite can be formed rapidly, with large amounts of cristobalite being formed within 3 months by vapour-phase crystallisation (Horwell et al., 2010). Therefore small amounts of cristobalite could be formed at Sakurajima, even within several days or weeks. Variations in older deposited samples from previous eruptive styles cannot be explained as there is insufficient information regarding eruption mechanics.

5.3.5   Limitations

Results produced by the IAS method carry quite a large, 1-3 wt. % error margin. Therefore the results described here are best estimates of the quantities of cristobalite in the Sakurajima ash. However, once again the ease and speed of the technique outweighs the errors for this study. Although the method is designed to more easily quantify the cristobalite phases, problems were still encountered when distinguishing the cristobalite peak from the plagioclase pattern and trying to match appropriate standards. The XRD analyses were only carried out on the < 1 mm fraction, and therefore the exact proportion of the bulk ash which is respirable cristobalite is unknown. Further work would be useful to examine in detail the amount of cristobalite in the respirable fraction, as the consistency of cristobalite values through time, over various eruptive styles and between two source craters, means there is the potential to estimate exposure to respirable cristobalite using only the grain-size results.

5.4   Surface Reactivity

5.4.1   *Factors affecting hydroxyl radical release*

Examination of surface reactivity in the ash samples shows the production of hydroxyl radicals, under similar conditions to those in the lung, to be low in comparison to more iron-rich ash samples. This is consistent with Horwell et al. (2003a) and Horwell et al. (2007) who found that hydroxyl radical release correlated with surface iron and andesitic ash samples tended to have much lower surface reactivity than basaltic samples. However, Horwell et al. (2007) also highlighted that the ability of surface iron to produce radicals is influenced by the state of the iron at the surface. For example, Fe_2O_3 and Fe_3O_4 have been shown to be 'inactive' (Fubini et al. 1995) and excess surface iron may reduce reactivity. The iron release experiment was designed using chelators that extracted poorly co-ordinated surface iron ions that would be more likely to be available to react in the lungs (Horwell et al., 2007). The results for iron and hydroxyl radical release in this study did seem to indicate that higher amounts of iron available at the surface led to increased hydroxyl radical release, although comparatively high errors made the differences between most samples insignificant.

5.4.2   *Consideration of surface area*

Surface reactivity was estimated and standardized per unit area as a large range of surface areas were seen in the Sakurajima samples ($0.47 - 3.86$ m^2 g^{-1}), especially considering the small range of surface areas observed for volcanic ash samples overall ($0.1 - 6$ m^2 g^{-1}; Le Blond et al., in review). Standardization was particularly important as bulk ash samples were analysed. Only respirable particles will be available to react in the lungs, which are likely to have more similar surface areas between samples than the bulk ash. This is supported by the strong correlation (0.899) seen between the amount of respirable material and the surface area (Figure 5.2).
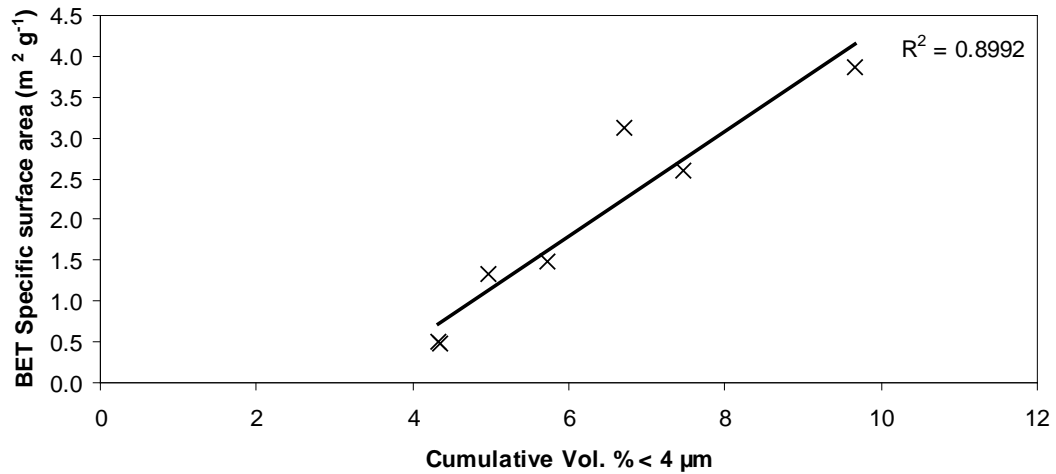
Figure 5.2: Relationship between the amount of respirable material and the specific surface area.

The SEM observations showed ash morphology to be similar through all of the samples analysed in these experiments. Therefore, additional factors that could affect the surface area apart from grain-size distributions, such as porosity (Delmelle et al., 2005), are unlikely to cause significant effects in these samples. However the amount of fine ash in the samples will still affect the potential for hydroxyl radical release in the lungs. Care should be taken not to assume that greater surface reactivity in bulk samples directly affects the potential toxicity of the ash. This is particularly emphasised when comparing the surface reactivity of Sakurajima ash samples to samples erupted from Mount Etna that were analysed at the same time (Figure 5.3).
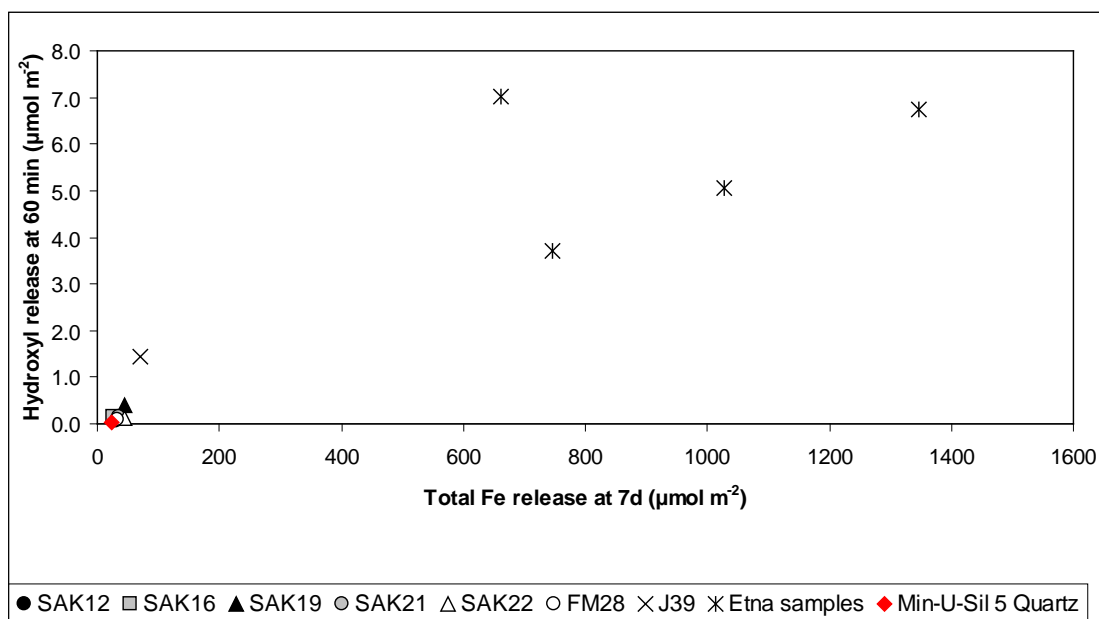
Figure 5.3: The number of hydroxyl radicals released at 60 minutes after the start of the experiment compared to the amount of total Fe released after 7 days. Samples IN1, 4, 5, 8 erupted from Mt. Etna, data courtesy of Paul Sargeant, (2009)

Figure 5.3 shows that the amount of iron and also the number of radicals produced by the basaltic Etna samples per unit area are very much higher than the samples for Sakurajima. The Etna samples have very low surface areas, and when comparing the absolute amounts of radicals produced, the results are more similar, as shown in Table 5.3. These results show that although Etna samples have an extremely high surface reactivity, the low amounts of respirable material ($0.2 - 1.83$ vol. % < 4 μm), means that toxic potential of the samples is unlikely to be much greater than for Sakurajima volcano.

Table 5.3: Surface reactivity compared with absolute hydroxyl radical release for Sakurajima and Etna samples at 60 minutes.

Sample I.D	Hydroxyl release (μmol m^{-2})	Absolute hydroxyl release (μmol)
Sakurajima samples	0.06 – 1.43	0.028 – 0.101
ETNA samples	3.71 – 7.02	0.072 - 0.147

127

5.4.3   Assessment of toxicity

In Figure 5.3, a quartz standard (Min-U-Sil 5 quartz) has also been plotted. All of the samples produced more radicals than the standard, although it was measured at a different time which has been observed to affect the comparability between the results (Horwell, pers. com.). Min-U-Sil 5 quartz is used as a toxic standard for radical release experiments for mineral dusts. To date, all volcanic ash particles analysed have produced larger amounts of radicals than the standard (e.g. Horwell et al., 2007; Horwell et al., in press; Le Blond et al., in review). However, samples producing large numbers of radicals have still been shown to have low biological reactivity in toxicological tests (Le Blond et al., in review). Results between bulk volcanic ash samples and powdered, respirable standards may not be directly comparable. Furthermore, surface reactivity may be different when using only the PM_{10} fraction of the ash (e.g. Horwell et al., 2003a). Separation of the respirable fraction is challenging and may not be appropriate for this and similar types of study where the emphasis is to give a general indication of potential hazards that can be made available quickly.

Further work examining the toxicity of respirable-size ash particles in conjunction with toxicological work to try to examine the effects of hydroxyl radical release from volcanic ash on lung cells is needed before justified assumptions about the extent of the hazard posed by radical release from ash samples can be made using bulk experiments as in this study. However, the results do emphasize the need to examine potential sources of toxicity other than the crystalline silica content of the ash. The release of hydroxyl radicals seen in this experiment should be taken into account, but the potential of the samples to cause long-term respiratory problems via this mechanism is likely to be low.

5.5   What potential hazard can be inferred?

This study has shown that the overall potential health hazard from Sakurajima volcanic ash is not likely to be great but is certainly not non-existent. Potential

risks to people with a high occupational exposure to ash, e.g. those involved with ash clean-up activities are likely to be higher due to higher exposures. Of particular concern are quarry workers excavating ash deposits on Sakurajima volcano. Both this and a previous study have identified cristobalite in the deposited ash on Sakurajima, where respirable material is likely to be abundant, not only from very fine ash layers but through fragmentation and remobilisation during the quarrying process. Quarry workers may be at particular risk and further study is warranted in this area.

Although this study did not examine potential exposures, it should be noted that awareness of at least the acute and irritant effects of ash is high in the local population, most inhabitants wear dusk masks during ashfall, and workers wear masks during ash clean-up activities. Such simple precautions greatly reduce exposure to respirable ash and hence the risk of chronic disease. The rapid clearance of ash deposits will also help to reduce the potential risk.

Although the small quantities of crystalline silica, varying amounts of respirable material and low radical release point towards a low potential risk, care still needs to be observed. The very long-term nature of the eruption means that even a small risk cannot be neglected. Furthermore, large uncertainties still exist regarding ash toxicity, and particularly beta-cristobalite which was apparent in the XRD patterns. Preventative measures against ash exposure (e.g. masks) are easy to implement, so assumptions can be made using the precautionary principle approach to advise populations about the ash risk. As the current activity of Sakurajima volcano is high, and is predicted to increase (Ishihara, 2006); ash characteristics should be frequently monitored and the importance of taking precautions to protect against ash exposure should be highlighted. Current levels of gases and the amount of total ashfall and TSP are measured in the local area, however PM_{10} values will be much more informative about the ash risk.

The results discussed here have highlighted some issues and uncertainties regarding the volcanic ash from Sakurajima volcano. The low cristobalite content may only pose a potential hazard at very high exposures. This study has highlighted the need for more detailed examination of exposure to volcanic ash. Finding direct causal links between ash exposure and development of chronic respiratory diseases is likely to be almost impossible to achieve. However, further work examining ash exposure, particularly in more distal locations may be particularly helpful in constraining the ash hazard from Sakurajima. Little gain will be made from further toxicological or even epidemiological studies until the large uncertainties regarding exposures have been resolved, so that meaningful, and accurate, analysis of the trends seen in epidemiological work and results obtained for toxicological work can be made. In particular the exposure of those with higher occupational exposures to ash, and more distal populations, which have often been ignored in previous studies, seem to be important areas to address in the light of this research, especially as, at the current level of activity, the threats to human health are likely to come from secondary and long-term effects of volcanic emissions.

However, trying to meaningfully examine a single cause and effect in this manner is close to impossible. Risk assessment is now beginning to embrace a more holistic approach that examines whole system interactions (de Guzman, 2003). Examination of exposures to volcanic ash from Sakurajima only may be useful to an extent. It is well-documented that fine ash particles can travel great distances in the atmosphere, but may also fall out close to the source. In Japan, there are hundreds of active volcanoes and populations are likely to be exposed to ash from more than one source. Furthermore, the significant amounts of damaging SO_2 released locally at Sakurajima should not be ignored (Kinoshita et al., 2000). It has often been suggested that the effects of SO_2 are worse when exposure to SO_2 is combined with exposure to large amounts of PM_{10}. Indeed, Samukawa et al. (2003) identified profilin release associated with carcinogenic responses only in

rats that were exposed to both ash and SO₂. Levels of urban pollution are also likely to affect the respiratory health of inhabitants and also their susceptibility to any effects that volcanic ash may cause. A recent focus in the field of inhalation toxicology has been on the effect of nano-particles, especially from Asian dusts and those produced by urban pollution (Kinoshita, 2005). These are factors that should be considered in Japan, along with the other sources of respiratory particulate.

It is evident that there are still large unknowns regarding the toxicity of cristobalite and other characteristics of volcanic ash in general, and these urgently need to be resolved in order to identify areas of risk. However, at Sakurajima, the exposures are unlikely to be so high that volcanic ash will have a dominant and overriding effect on the respiratory health of populations as is perhaps the case for larger eruptions. Exposure to high levels of urban pollution, volcanic gases, ash from other volcanoes and Asian dusts are all also very likely. The results shown in this study seem to suggest that, although the ash from Sakurajima is unlikely to cause chronic disease on its own, it could be an important contributor to combined adverse affects from many sources, each of which may have a low individual perception of risk but may add up to have adverse effects on respiratory health. Rather than trying to examine single cause and effect patterns for each individual factor, in this case, a more holistic approach is likely to give a more realistic picture of the risk of developing chronic respiratory health problems.

The holistic approach suggested will be extremely complex, and is likely to be hindered by many uncertainties, especially considering the limited scientific knowledge surrounding toxic responses in the lungs to particles for many of the potential hazards highlighted. However, whole-system approaches from risk assessment and management have been successfully applied to other complex systems, and, although an ambitious aim, producing meaningful results that can be used to give well-constrained advice about risk to the local populations is a possibility. To achieve this, close monitoring of the ash, especially if the volcano

should return to its previous, larger eruptive style, or if volcanic activity continues to intensify and remain at high levels as has been predicted, is essential. Although it is unlikely that ash alone is a dominant influence on the overall potential respiratory hazard currently, this does not mean that it will not become so in the future.

Chapter 6

Conclusion

The potential respiratory hazard from Sakurajima ash was examined from a mineralogical and geochemical perspective. The grain-size and bulk chemistry were variable due to a combination of different eruption styles, explosivity and weather conditions. A large range in respirable material was observed, with some samples containing substantial amounts of respirable particulate. Detailed examination of the trends regarding the production of, and exposure to, respirable material could not be identified with these data. However, the grain size results helped to fulfil the research aims of this study, identifying some of the reasons for disparities in the previously-published grain-size data, and providing the most comprehensive data set on grain-size and respirable material for the volcano found to date.

The data resolve the main issue, that Sakurajima does have the potential to produce considerable amounts of respirable material on occasion; enough to merit further investigation of the ash. Links between eruption type and the production of fine ash at Sakurajima have been considered. Some samples with higher amounts of fine material than expected considering the generally low explosivity were attributed to increased fragmentation as the lava plug was destroyed. The results for the thoracic, respirable and ultra-fine material correlated well. A function was given that could be used to estimate the amount of respirable material from sieved samples, which could aid rapid health-hazard assessment in the future. Detailed examination of exposure patterns is recommended, although care should be taken that the complexity at Sakurajima is not over-simplified.

Cristobalite was identified in all samples, but was the only crystalline silica polymorph observed. It probably formed by vapour phase interactions between the lava plug and accumulated gases at the top of the conduit. From the most recent eruptive phase low amounts of cristobalite (6-8 wt. %) suggested that high and long-lasting exposure would be needed to develop respiratory problems. The fact that many samples did not contain large amounts of respirable material in conjunction with the seasonal wind direction and often narrow ash dispersal

areas (see Section 2.4.3), suggests that exposures are only likely to reach sufficiently elevated levels for prolonged periods in occupational settings that incur high levels of exposure to remobilised ash. In particular, the presence of cristobalite in the deposited ash samples, which included some extremely fine-grained samples and the suggestion that there may be other deposits with significantly higher levels (Shiraki and Tomita, 1993) is worrying for quarry or construction workers, where deposits from previous eruptions are more likely to be exposed and remobilised. Further work examining deposited samples and exposure in quarry workers should be undertaken.

Hydroxyl radical release from the samples was very low compared to other volcanic samples that have been analysed. It seemed that the surface reactivity was generally influenced by the amount of surface iron available, although trends were difficult to analyse as only a few samples were examined. Further work is needed to examine the toxicity of radicals released from volcanic ash on lung cells but it is thought that the likelihood of severe respiratory problems being developed due to hydroxyl radical release from these samples is low.

Although the risk appears to be small, the ash is still probably a potential hazard. Further work examining ash toxicity in general is needed but, assuming similar toxicity to cristobalite in mineral dusts, precautions should be taken to reduce ash exposure, especially in occupational settings that may cause higher ash exposure or exposure to ash deposited during previous eruptions (e.g. road cleaning, quarry workers). Currently, it cannot be proven that the volcanic ash from Sakurajima has a direct effect on the respiratory health of exposed populations. This is probably because the low amounts of cristobalite and radical release, in conjunction with very variable and generally sporadic exposure to respirable ash means that exposure is not sufficiently high or prolonged to directly cause adverse respiratory effects. However, from this study it seems that volcanic ash could be a contributing factor, and the need for a more holistic approach to the study of causes for chronic respiratory disease is needed.

Further study examining in detail exposure patterns would be invaluable in better constraining the ash hazard. The characteristics of the volcanic ash should continue to be monitored to help give current and relevant advice to the exposed populations. More generally, mechanisms of ash toxicity and formation of crystalline silica in volcanoes still needs to be addressed. However, as the potentially toxic properties of the volcanic ash from Sakurajima are small, the results and samples from the volcano are of little use in this respect.

The limitations of this study have been highlighted, particularly regarding using samples that realistically represent the exposure of inhabitants. However, the use of mineralogical examination of the ash to make a rapid assessment of any potential hazards that could be posed by the volcanic ash has been successful. The research aims were addressed adequately in most cases and areas of further research needs, and advice about realistic precautions to be taken have been suggested. As advancements in the understanding of ash toxicity continue, so the protocol used in this study can be adjusted and results interpreted with more conviction.

References

Australian Institute of Occupational Hygienists Inc. (AIOH). (2009). *AIOH Position Paper on Respirable Crystalline Silica and Occupational Health Issues.* AIOSH Exposure Standards Committee: Australia.

AIST, GSJ: National Institute of Advanced Industrial Science and Technology: Geological Survey Japan. (2006). *Geological Map of Sakurajima.* Online at: http://riodb02.ibase.aist.go.jp/db099/volcmap/01/index-e.html [Accessed 02.12.2009].

Akbar-Khanzadeh, F., and Brillhart, R.L. (2002). Respirable crystalline silica dust exposure during concrete finishing (grinding) using hand-held grinders in the construction industry. *The Annals of Occupational Hygiene.* Vol. 46 (3), pp. 341-346.

Allison, A.C., Harington, J.S., and Birbeck, M. (1966). An examination of the cytotoxic effects of silica on macrophages. *Journal of Experimental Medicine.* Vol. 124, pp. 141-154.

Andronico, D., Scollo, S., Cristaldi, A., Ferrari, F. (2009). Monitoring ash emission episodes at Mt. Etna: The 16 November 2006 case study. *Journal of Volcanology and Geothermal Research.* Vol. 180 (2-4), pp. 123-134.

Batchelder, M., and Cressey, G. (1998). Rapid, accurate phase quantification of clay-bearing samples using a position-sensitive X-ray detector. *Clay and Clay Minerals.* Vol. 46 (2), pp. 182-194.

Baxter, P.J. (2005). Human impacts of volcanoes. In: Martí, J., and Ernst, G.G.J. (Eds.) *Volcanoes and the Environment*, Cambridge University Press, Cambridge. Pp. 273–303.

Baxter, P.J., Bonadonna, C., Dupree, R., Hards, V.L., Kohn, S.C., Murphy, D., Nichols, A., Nicholson, R.A., Norton, G., Searl, A., Sparks, R.S.J., and Vickers, B.P. (1999). Cristobalite in volcanic ash of the Soufriere Hills Volcano, Montserrat, British West Indies. *Science.* Vol. 283, pp. 1142-1145.

Baxter, P.J., Ing, R., Falk, H., French, J., Stein, G.F., Bernstein, R.S., Merchant, J.A., and Allard, J. (1981). Mount St. Helens eruptions, May 18 to June 12 1980. *Journal of the American Medical Association.* Vol. 246, pp. 2585-2589.

Baxter, P.J., Ing, R., Falk, H., and Plikaytis, B. (1983). Mount St Helens eruptions: the acute respiratory effects of volcanic ash in a North American community. *Archives of Environmental Health.* Vol. 38 (3), pp. 138-143.

Beck, B.D., Brain, J.D., and Bohannon, D.E. (1981). The pulmonary toxicity of an ash sample from the Mt. St. Helens Volcano. *Experimental Lung Research.* Vol. 2 (4), pp. 289-301.

Bernstein, R.S., and Buist, S. (1984). Public health aspects of volcanic hazards: Evaluation and prevention of excessive morbidity and mortality due to natural disasters. *Disasters.* Vol. 8 (1), pp. 6-8.

Bernstein, R.S., McCawley, M.A., Attfield, M.D., Green, F.H.Y., and Olenchock, S.A. (1982). Epidemiological assessment of the risk for adverse pulmonary effects from persistent occupational exposures to Mount St. Helens volcanic ash (tephra). Pp. 207-213. In: Keller, S.A.C. (Ed.). *Mount St. Helens: one year later.* Eastern Waskington University Press: Cheney, WA.

Bernstein, R.S., Baxter, P.J., and Buist, A.S. (1986)a. Introduction to the epidemiological aspects of explosive volcanism. *American Journal of Public Health.* Vol. 76, Supplement, pp. 3-9.

Bernstein, R.S., Baxter, P.J., Falk, H., Ing, R., Foster, L., and Frost, F. (1986)b. Immediate public health concerns and actions in volcanic eruptions: lessons from the Mount St. Helens eruptions, May 18 – October 18, 1980. *American Journal of Public Health.* Vol. 76, Supplement, pp. 25-37.

Berube, K.A., Jones, T.P., Housley, D.G., and Richards, R.J. (2004). The respiratory toxicity of airborne volcanic ash from the Soufriere Hills volcano, Montserrat. *Mineralogical Magazine.* Vol. 68 (1), pp. 47-60.

Beuselinck, L., Gover, G., Poesen, J., Degraer, G., and Froyen, L. (1998). Grain-size analysis by laser diffractometry: comparison with the sieve-pipette method. *CATENA.* Vol. 32 (3-4), pp. 193-208.

Black, D.L., McQuay, M.Q., and Bonin, M.P. (1996). Laser-based techniques for particle-size measurement: A review of sizing methods and their industrial applications. *Progress in Energy and Combustion Science.* Vol. 22 (3), pp. 267-306.

Blong, R. (2000). Volcanic hazards and risk management. In: Sigurdsson, H. (Ed.) *Encyclopaedia of Volcanoes.* Academic Press: New York. Pp. 1215-1228

Bonadonna, C., Mayberr, G.C., Calder, E.S., Sparks, R.S.J., Choux, C., Jackson, P., Lejeune, A.M., Loughlin, S.C., Norton, G.E., Rose, W.I., Ryan, G., and Young, S.R. (2002). Tephra fallout in the eruption of Soufriere Hills Volcano, Montserrat. In: Druitt, T.H., and Kokelaar, B.P. (eds.) *The Eruption of Soufriere Hills Volcano, Montserrat, from 1995-1999: Geological Society of London Memoir 21.* pp. 483-516.

Bowen, P. (2002). Particle size distribution measurement from millimetres to nanometers and from rods to platelets. *Journal of Dispersion Science and Technology.* Vol. 23 (5), pp. 631-662.

Bradshaw, L., Fishwick, D., Kemp, T., Lewis, S., Rains, N., Slater, T., Pearce, N., and Carne, J. (1997). Under the volcano: fire, ash and asthma? *The New Zealand Medical Journal.* Vol. 110, pp. 90-91.

Buchanan, D., Miller, B.G., and Soutar, C.A. (2003). Quantitative relations between exposure to respirable quartz and risk of silicosis. *Occupational Environmental Medicine.* Vol. 60, pp. 159-164.

Buist, A.S. (1982). Are volcanoes hazardous to your health? What have we learned from Mount St Helens? - The Oregon Health Sciences University (Speciality Conference). *The Western Journal of Medicine.* Vol. 137, pp. 294-301.

Buist, A.S., Johnson, L.R., Vollmer, W.M., Sexton, G.J., and Kanarek, P.H. (1983). Acute effects of volcanic ash from Mount Saint Helens on lung function in children. *American Review of Respiratory Disease.* Vol. 127, pp. 714-719.

Buist, A.S., Martin, T.R., Shore, J.H., Butler, J., and Lybarger, J.A. (1986)a. The development of a multidisciplinary plan for evaluation of the long-term health effects of the Mount St. Helens eruptions. *American Journal of Public Health.* Vol. 76, Supplement, pp. 39-44.

Buist, A.S., Vollmer, W.M., Johnson, L.R., Bernstein, R.S., and McCamant, L.E. (1986)b. A four-year prospective study of the respiratory effects of volcanic ash from Mt. St. Helens. *The American Review of Respiratory Disease.* Vol. 133 (4), pp. 526-534.

Castranova, V., Bowman, L., Shreve, J.M., Jones, G.S., and Miles, P.R., (1982). Volcanic ash: toxicity to isolated lung cells. *Journal of Toxicological, Environmental Health.* Vol. 9 (2), pp. 317-325.

Checkoway, H., Pearce, N., and Kriebel, D. (2004). *Research Methods in Occupational Epidemiology. 2nd Edition.* Oxford University Press: New York.

Cowie, H.A., Graham, M.K., Searl, A., Miller, B.G., Hutchison, P.A., Swales, C., Dempsey, S., and Russel, M. (2002). *A Health Survey of Workers on the Island of Montserrat.* Institute of Occupational Medicine: Edinburgh. IOM TM/02/02.

Cressey, G., and Schofield, P.F. (1996). Rapid whole-pattern profile-stripping method for the quantification of multiphase samples. *Powder Diffraction.* Vol. 11 (1), pp. 35-39.

Cronin, S.J., and Sharp , D.S. (2002). Environmental impacts on health from continuous volcanic activity at Yasur (Tanna) and Ambrym, Vanuatu. *International Journal of Environmental Health Research.* Vol. 12 (2), pp. 109-123.

Cullen, R.T., Jones, A.D., Miller, B.G., Tran, C.L., Davis, J.M.G., Donaldson, K., Wilson, M., Stone, V., and Morgan, A. (2002). *Toxicity of Volcanic Ash from Montserrat.* Institute of Occupational Medicine: Edinburgh. IOM TM/02/01.

Dallas, C.E. (2000). Pulmonotoxicity: Toxic Effects in the Lung. In: Williams, P.L., James, R.C., and Roberts, S.M. (Eds). *Principles of Toxicology: environmental and industrial applications. Second Edition.* John Wiley & Sons: Canada. Pp. 169-186.

De Guzman, E. (2002). *Towards total disaster risk management approach.* Asian Disaster Reduction Center (ADRC) and the Office of Coordinator for Humanitarian Affairs (OCHA). Online at: http://unpan1.un.org/intradoc/groups/public/documents/APCITY/UNPAN009657.pdf [accessed 2.12.09]

Delmelle, P., Villieras, F., and Pelletier, M. (2005). Surface area, porosity and water adsorption properties of fine volcanic ash particles. *Bulletin of Volcanology.* Vol. 67, pp. 160-169.

Dollberg, D.D., Bolyard, M.L., and Smith, D.L. (1986). Evaluation of physical health effects due to volcanic hazards: Crystalline silica in Mount St. Helens volcanic ash. *American Journal of Public Health.* Vol. 76, supplement, pp. 53-58.

Donaldson, K., Brown, D., Clouter, A., Duffin, R., MacNee, W., Renwick, L., Tran, L., and Stone, V. (2002). The pulmonary toxicology of ultrafine particles. *Journal of Aerosol Medicine.* Vol. 15 (2), pp. 213-220.

Donaldson, K., Stone, V., Tran, C.L., Kreyling, W., and Borm, P.J.A. (2004). Nanotoxicology. *Journal of Occupational Environmental Medicine.* Vol. 61 (9), pp. 727-728.

Durand, M., Gordon, K., Johnston, D., Lorden, R., Poirot, T., Scott, J., Shephard, B. (2001). *Impacts of, and responses to ashfall in Kagoshima from Sakurajima Volcano – lessons for New Zealand.* Institute of Geological and Nuclear Science report 2001/30. Institute of Geological and Nuclear Sciences Limited: New Zealand.

Durant, A.J., Rose, W.I., Sarna-Wojcicki, A.M., Carey, S., and Volentik, A.C.M. (2009). Hydrometeor-enhanced tephra sedimentation: constraints from the 18 May 1980 eruption of Mount St. Helens. *Journal of Geophysical Research: Solid Earth.* Vol. 114, B03204.

Eshel, G., Levy, G.J., Mingelgrin, U., and Sinder, M.J. (2004). Critical evaluation of the use of laser diffraction for particle-size distribution analysis. *Soil Science Society of America Journal.* Vol. 68, pp. 736-743.

Eto, T. (2001). Estimation of the amount and dispersal of volcanic ash-fall deposits ejected by vulcanian type eruption. *Report of the Faculty of Science, Kagoshima University.* Vol. 34, pp. 35-46.

Etzler, F.M., and Deanne, R. (1997). Particle size analysis: A comparison of various methods ii. *Particle and Particle Systems.* Vol. 14 (6), pp. 278-282.

Evans, J.R., Huntoon, J.E., Rose, W.I., Varley, N.R., and Stevenson, J.A. (2009). Particle sizes of andesitic ash fallout from vertical eruptions and co-pyroclastic flow clouds, Volcan de Colima, Mexico. *Geology.* Vol. 37 (10), pp. 935-938.

Farwell, S.O., and Gage, D.R. (1981). Crystalline silica in Mount St. Helens ash. *Analytical Chemistry.* Vol. 53 (13), pp. 1529A-1532A.

Fedotov, I. (2003). The ILO/WHO Global Programme on Elimination of Silicosis. *The Global Occupational Health Network Newsletter.* Issue 5, pp. 3-5.

Forbes, L., Jarvis, D., Potts, J., and Baxter, P.J. (2003). Volcanic ash and respiratory symptoms in children on the island of Montserrat, British West Indies. *Occupational Environmental Medicine.* Vol. 60, pp. 207-211.

Fruchter, J.S., Robertson, D.E., Evans, J.C., Olsen, K.B., Lepel, E.A., Laul, J.C., Abel, K.H., Sanders, R.W., Jackson, P.O., Wogman, N.S., Perkins, R.W., Vant Tuyl, R.L., Beauchamp, R.H., Shade, J.W., Daniel, J.L., Erikson, R.L., Sehmel, G.A., Lee, R.N., Robinson, A.V., Moss, O.R., Briant, J.K., and Cannon, W.C. (1980). Mount St. Helens ash from the 18 May 1980 eruption: Chemical, physical, Mineralogical and Biological Properties. *Science.* Vol. 209 (4461), pp. 1116-1125.

Fubini, B., and Hubbard, A. (2003). Serial review: Role of reactive oxygen and nitrogen species (ROS/RNS) in lung injury and diseases. *Free Radical Biology and Medicine.* Vol. 34 (12), pp. 1507-1516.

Fubini, B., Mollo, L., and Giamello, E. (1995). Free radical generation at the solid/liquid interface in iron containing minerals. *Free Radical Research.* Vol. 23, pp. 593-614.

Fubini, B., and Otero Areán, C. (1999). Chemical aspects of the toxicity of inhaled mineral dusts. *Chemical Society Reviews.* Vol. 28, pp. 373-381.

*Fukuyama, H., and Ono, K. (1981). *Geological Map of Sakurajima Volcano. 1:25,000.* Geological Survey of Japan: Tokyo.

Gordian, M.E., Ozkaynak, H., Xue, J., Morris, S.S., Spengler, J.D. (1996). Particulate air pollution and respiratory disease in Anchorage, Alaska. *Environmental Health Perspectives.* Vol. 104, pp. 290-297.

Green, F.H.Y., Bowman, L., Castranova, V., Dollberg, D.D., Elliot, J.A., Fedan, J.S., Hahon, N., Judy, D.J., Major, P.C., Mentnech, M.S., Miles, P.R., Mull, J., Olenchock, S., Ong, T., Pailes, W.M., Resnick, H., Stettler, L.E., Tucker, J.G., Vallyathan, V., and Whong, W. (1982). Health implications of the Mount St. Helens' eruption: Laboratory investigations. *Annals of Occupational Hygiene.* Vol. 26 (8), pp. 921-933.

Grose, E.C., Grady, M.A., Illing, J.W., Daniels, M.J., Selgrade, M.K., and Hatch, G.E. (1985). Inhalation studies of Mt. St. Helens volcanic ash in animals: IIII. Host Defence Mechanisms. *Environmental Research.* Vol. 37, pp. 84-92.

Hamilton, R.F.Jr., Thakur, S.A., and Holian, A. (2008). Silica binding and toxicity in alveolar macrophages. *Free Radical Biological Medicine.* Vol. 44 (7), pp. 1246-1258.

Hansell, A.L., Horwell, C.J., and Oppenheimer, C. (2006). The health hazards of volcanoes and geothermal areas. *Occupational Environmental Medicine.* Vol. 63, pp. 149-156.

Hickling, J., Clements, M., Weinstein, P., and Woodwrad, A. (1999). Acute health effects of the Mount Ruapehu (New Zealand) volcanic eruption of June 1996. *International Journal of Environmental Health Research.* Vol. 9 (2), pp. 97-10.

Hincks, T.K., Aspinall, W.P., Baxter, P.J., Searl, A., Sparks, R.S.J., and Woo, G. (2006). Long term exposure to respirable volcanic ash on Montserrat: a time series simulation. *Bulletin of Volcanology.* Vol. 68 (3), pp. 266-284.

*Hirano, M., and Hikida, M. (1988). A study of the method for estimation of the amount of erupted and deposited volcanic ash. *Journal of the Japanese Society for Natural Disaster Science.* Vol. 7 (1), pp. 26-36.

Horwell, C.J. (2007). Grain-size analysis of volcanic ash for the rapid assessment of respiratory health hazard. *Journal of Environmental Monitoring.* Vol. 9, pp. 1107-1115.

Horwell, C.J., and Baxter, P.J. (2006). The respiratory health hazards of volcanic ash: a review for volcanic risk mitigation. *Bulletin of Volcanology.* Vol. 69, pp. 1-24.

Horwell, C.J., Fenoglio, I., and Fubini, B. (2007). Iron-induced hydroxyl radical generation from basaltic volcanic ash. *Earth and Planetary Science Letters.* Vol. 261, pp. 662-669.

Horwell, C.J., Fenoglio, I., Ragnarsdottir, K.V., Sparks, R.S.J., and Fubini, B. (2003)a. Surface reactivity of volcanic ash from the eruption of Soufriere Hills volcano, Montserrat, West Indies with implications from health hazards. *Environmental Research.* Vol. 93, pp. 202-215.

Horwell, C.J., Le Blond, J.S., Michnowicz, S.A.K., and Cressey, G. (2010). Cristobalite in a rhyolitic lava dome: Evolution of ash hazard. *Bulletin of Volcanology.* Vol. 72, pp. 249 – 253.

Horwell, C.J., Sparks, R.S.J., Brewer, T.S., Llewellin, E.W., and Williamson, B.J. (2003)b. Characterization of respirable volcanic ash from the Soufriere Hills volcano, Montserrat, with implications for human health hazards. *Bulletin of Volcanology.* Vol. 65, pp. 346-362.

Horwell C.J., Stannett G.W., Andronico D., Bertagnini A., Fenoglio I., Fubini B., Le Blond J.S., and Williamson B.J. (In press) A physio-chemical assessment of the health hazard of Mt. Vesuvius volcanic ash. *Journal of Volcanological and Geothermal Research.* DOI: 10.1016/j.jvolgeores.2010.01.014

Housley, D.G., Berube, K.A., Jones, T.P., Anderson, S., Pooley, F.D., and Richards, R.J. (2002). Pulmonary epithelial response in the rat lung to instilled Montserrat respirable dusts and their major mineral components. *Occupational Environmental Medicine.* Vol. 59, pp. 466-472.

Iguchi, M., Hiroshi, Y., Tameguri, T., Hendrasto, M., and Hirabayashi, J. (2008)a. Mechanism of explosive eruption revealed by geophysical observations at the Sakurajima, Suwanosejima, and Semeru volcanoes. *Journal of Volcanology and Geothermal Research.* Vol. 178, pp. 1-9.

Iguchi, M., Takayama, T., Yamazaki, T., Tada, M., Suzuki, A., Ueki, S., Ohta, Y., and Nakao, S. (2008)b. Movement of magma at Sakurajima volcano revealed by GPS observation. *Disaster Prevention Research Institute Annals B.* vol. 51 (B), pp. 241-246.

*Imayoshi, M., Maeda, S., Nagata, S., and Takeshita, T. (1982). Investigation of the volcanic ashes erupted from Mt. Sakurajima (I) from Apr. 1978 to Mar. 1981. *Journal of the Japanese Society of Air Pollution.* Vol. 17 (4), pp. 319-327.

International Agency for Research on Cancer. (1997). *Silica, some silicates, coal dust and para-aramid fibrils.* World Health Organization: Geneva.

Ishihara, K. (1985). Dynamic analysis of volcanic explosion. *Journal of Geodynamics.* Vol. 3, pp. 327-349.

Ishihara, K. (1990). Pressure sources and induced ground deformation associated with explosive eruptions at an andesitic volcano: Sakurajima volcano, Japan. In: Ryan, M. (ed.), *Magma Transport and Storage.* John Wileys and Sons: Chichester. Pp. 335-356

Ishihara, K. (1999). Activity at Sakurajima volcano. In: *Reports on Volcanic Activities and Volcanological Studies in Japan for the Period from 1995 to 1998.* Found at: http://hakone.eri.u-tokyo.ac.jp/vrc/nr98/ [accessed 20-05-09].

Ishihara, K. (2006). Evaluation of eruption potential. *Annals of the Disaster Prevention Research Institute, Kyoto University.* Vo. 49, C, pp. 61-68.

Johnson, K.A., Loftsgaarden, D.O., and Gideon, R.A. (1982). The effects of Mount St. Helens ash on the pulmonary function of 120 elementary school children. *American Review of Respiratory Disease.* Vol. 126, pp. 1066-1069.

Kariya, M. (1992). Is there any effect of volcanic eruptions of Mount Sakurajima on human lungs? – Histopathological investigation and measurement of intrapulmonary particulate deposits amounts. *Tohoku Journal of Experimental Medicine.* Vol. 166, pp. 331-343.

Kariya, M., Goto, M., Hasui, K., Yamamoto, N., Tahiro, Y., and Sato, E. (1992). Is there any effect of volcanic eruptions of Mount Sakurajima on canine lungs exposed naturally? – Morphometric analysis of intrapulmonary particulate deposit amount and histopathological investigations. *Tohoku Journal of Experimental Medicine.* Vol. 167, pp. 197-205.

Kawano, M., and Tomita, K. (2001)a. TEM-EDX study of weathered layers on the surface of volcanic glass, bytownite, and hypersthene in volcanic ash from Sakurajima volcano, Japan. *American Mineralogist.* Vol. 86, pp. 284-292.

Kawano, M., and Tomita, K. (2001)b. Microbial biomineralization in weathered volcanic ash deposit and formation of biogenic minerals by experimental incubation. *American Mineralogist.* Vol. 86, pp. 400-410.

Kinoshita, K. (1994). Video Monitoring of Ejection and Dispersion of Volcanic Ash Clouds from Mt. Sakurajima. *Proceedings of the 3rd Asian Symposium on Visualisation., Chiba, Japan.* Pp. 416-421.

Kinoshita, K. (1996). Observation of flow and dispersion of volcanic clouds from Mt. Sakurajima. *Atmospheric Environment.* Vol. 30 (16), pp. 2831-2837.

Kinoshita, K. (2005). Long-term observation of Asian dust in Changchun and Kagoshima. *Water, Air and Soil Pollution: Focus.* Vol. 5 (3-6), pp. 89-100.

Kinoshita, K., Koyamada, M., and Kanagaki, C. (2000). High concentration events of SO_2 and SPM around Sakurajima and atmospheric dispersion of volcanic clouds. *Abstracts of the 7th International Conference on Atmospheric Sciences and Application to Air Quality, Taipei, 31 Oct-2 Nov.*

Kinoshita, K., and Togoshi, H. (2000). Rise and flow of volcanic clouds observed from the ground and from satellites. *Journal of Visualization.* Vol. 3 (1), pp. 71-78.

Kinoshita, K., Saitoh, S., and Goto, A. (1993). Atmospheric Dispersion of Volcanic clouds. Section 7.5 pp. 223-230 in Chapter 7. Radiative Processes in:

Jones, I., Sugimori, and Stewart. (eds). *Satellite Remote Sensing of the Oceanic Environment.* Seibutsu Kenkyusha: Tokyo.

Kiyotaka, D. (1990). Development of a ventilation system against volcanic ash fall in Kagoshima. *Energy and Buildings.* Vol. 15-16, pp. 663-671.

*Kobayashi, T. (1982). Geology of Sakurajima Volcano: A review. *Bulletin of the Volcanological Society of Japan. Second series.* Vol. 27 (4), pp. 277-292.

Kobayashi, T., Iguchi, M., and Kawanabe, Y. (2007). *C2: Sakurajima and Kaimondake Volcanoes, southern Kyushu.* COV5, C2 Field Excursion Guidebook.

*Kobayashi, T., and Tameike, T. (2002). History of eruptions and volcanic damage from Sakurajima Volcano, Southern Kyushu, Japan. *Quaternary Research (Japanese).* Vol. 41 (4), pp. 268-278.

Koizumi, A., Yano, E., Higashi, H., and Nishii, S. (1988). Health effects of volcanic eruptions. *Proceedings of the Kagoshima International Conference on Volcanoes 1988.* pp. 705-708.

Kraemer, M.J., and McCarthy, M.M. (1985). Childhood asthma hospitalization rates in Spokane County, Washington. *Journal of Asthma.* Vol. 22, pp. 37-43.

Kreyling, W.G., Semmler-Behnke, M., and Moller, W. (2006). Health implications of nanoparticles. *Journal of Nanoparticle Research.* Vol. 8 (5), pp. 543-562.

Le Blond, J.S., Horwell, C.J., Baxter, P.J., Michnowicz, S.A.K., Tomatis, M., Fubini, B., Delmelle, P., Dunster, C., and Patia, H. (in review). Mineralogical analyses and *in vitro* screening tests for the rapid evaluation of the health hazard of volcanic ash at Rabaul volcano, Papua New Guinea. *Bulletin of Volcanology.*

Le Blond, J.S., Cressey, G., Horwell, C.J., and Williamson, B.J. (2009). A rapid method for quantifying single mineral phases in heterogeneous natural dusts using X-ray diffraction. *Powder Diffraction.* Vol. 24 (1), pp. 17-23.

Lee, S.H., and Richards, R.J. (2004). Montserrat volcanic ash induces lymph node granuloma and delayed lung inflammation. *Toxicology.* Vol. 195 (2-3), pp. 155-165.

Lippmann, M., (1998). Structure and Function, 10.2-10.6. In: David, A., and Wagner, G.R. (Eds.) Chapter 10: Respiratory System. In: Stellman, J.M. *Encyclopaedia of Occupational Health and Safety. Fourth edition, volume 1.* International Labour Organisation: Switzerland.

Ma, Z.H., Merkus, H.G., de Smet, J.G.A.E., Heffels, C., and Scarlett, B. (2000). New developments in particle characterization by laser diffraction: size and shape. *Powder Technology.* Vol. 111 (1-2), pp. 66-78.

Malilay, J., Real, M.G., Ramirez Vanegas, A., Noji, E., and Sinks, T. (1996). Public health surveillance after a volcanic eruption: lessons from Cerro Negro, Nicaragua, 1992. *Bulletin of the Pan American Health Organization (PAHO)*. Vol. 30 (3), pp. 218-226.

Martin, T.R., Ayars, G., Butler, J., and Altmn, L.C. (1984). The comparative toxicity of volcanic ash and quartz. Effects on cells derived from the human lung. *American Review of Respiratory Disease*. Vol. 130 (5), pp. 778-782.

Martin, T.R., Chi, E.Y., Covert, D.S., Hodson, W.A., Kessler, D.E., Moore, W.E., Altman, L.C., and Butler, J. (1983). Comparative effects of inhaled volcanic ash and quartz in rats. *American Review of Respiratory Disease*. Vol. 128 (1), pp. 144-152.

Martin, T.R., Wehner, A.P., and Butler, J. (1986). Evaluation of physical health effects due to volcanic hazards: the use of experimental systems to estimate the pulmonary toxicity of volcanic ash. *American Journal of Public Health*. Vol. 86 (supplement), pp. 59-65.

Matsushima, T., and Takagi, A. (2000). GPS and EDM monitoring of Unzen volcano ground deformation. *Earth, Planets and Space*. Vol. 52, pp. 1015-1018.

Meldrum, M., and Howden, P. (2002). Crystalline silica: Variability in fibrogenic potency. *Annals of Occupational Hygiene*. Vol. 45, supplement 1, pp. 27-30.

Merchant, J.A., Baxter, P.J., Bernstein, R.S., McCawley, M., Falk, H., Stein, G., Ing, R., and Attfield, M. (1982). Health implications of the Mount St. Helens eruption: epidemiological considerations. *Annals of Occupational Hygiene*. Vol. 26, pp. 991-919.

Miller, B.G., Hagen, S., Love, R.G., Soutar, C.A., Cowie, H.A., Kidd, M.W., and Robertson, A. (1998). Risks of silicosis in coal workers exposed to unusual concentrations of respirable quartz. *Occupational Environmental Medicine*. Vol. 55, pp. 52-58.

Mitchell, J.P., Nagel, M.W., Nichols, S., Nerbrink, O. (2006). Laser diffractometry as a technique for rapid assessment of aerosol particle size from inhalers. *Journal of Aerosol Medicine*. Vol. 19 (4), pp. 409-433.

Naito, M., Hayakawa, O., Nakahira, K., Mori, H., and Tsubaki, J. (1998). Effect of particle shape on the particle size distribution measured with commercial equipment. *Powder Diffraction*. Vol. 100 (1), pp. 52-60.

Nakamura, K. (2006). Textures of plagioclase microlite and vesicles within volcanic products of the 1914-1915 eruption of Sakurajima Volcano, Kyushu, Japan. *Journal of Mineralogical and Petrological Sciences*. Vol. 101, pp. 178-198.

Nania, J., and Bruya, T.E. (1982). In the wake of Mount St. Helens. *Annals of Emergency Medicine.* Vol. 11, pp. 184-191.

Nania, J.M., Garcia, M.R., Fruchter, J.S., Olsen, K.B., Hooper, K.B., and Snyder, D.C. (1994). In the shadow of El Chichon: an overview of the medical impact of the 28 March to 4 April 1982 eruptions of the Mexican volcano. *Prehospital and Disaster Medicine.* Vol. 9 (1), pp. 58-66.

National Institute for Occupational Safety and Health (NOISH) (2002). *NIOSH Hazard Review: Health Effects of Occupational Exposure to Respirable Crystalline Silica.* DHHS (NIOSH) Publication No. 2002-129.

Naumova, E.N., Yepes, H., Griffiths, J.K., Sempertegui, F., Khurana, G., Jagai, J.S., Jativa, E., and Estrella, B. (2007). Emergency room visits for respiratory conditions in children increased after Guagua Pichincha volcanic eruptions in April 2000 in Quito, Ecuador observational study: Time series analysis. *Environmental Health: a global access science source.* Vol. 6:21.

Nishii, S., Koizumi, A., Yano, E., Yokoyama, Y., and Higashi, H. (1986). Behaviour of respirable particulates in the volcanic ash of Mt. Sakurajima. *Japanese Journal of Public Health.* Vol. 33, pp. 398-402.

Oba, N., Tomita, K., Yamamoto, M., Inoue, K., Nakamura, T., Ishii, T., and Kiyosake, S. (1984). Mechanism of the formation of volcanic ashes from Sakurajima volcano, Japan, and its influences to the environments. *Report of the Faculty of Science, Kagoshima University (Earth Sciences and Biology).* Vol. 17, pp. 1-22.

*Oba, N., Tomita, K., Yamamoto, M., Ohsako, N., and Inoue, K. (1980). Nature and origin of black ash, red ash and white ash from Sakurajima volcano, Kyushu, Japan. *Bulletin of Kagoshima University (Earth Science, Biology).* Vol. 13, pp. 11-27.

Okubo, A., Kanda, W., Tanaka, Y., Ishihara, K., Miki, D., Utsugi, M., Takayama, T., and Fukushima, M. (2009). Apparent magnetization intensity map on Sakurajima Volcano, Kyushu, Japan, inferred from low-altitude, high-density helicopter-borne aeromagnetic surveys. *Tectonophysics.* Vol. 478 (1-2), pp. 34-42.

Olenchock, S.A., Mull, J.C., Mentnech, M.S., Lewis, D.M., and Bernstein, R.S. (1983). Changes in hummoral immunologic parameters after exposure to volcanic ash. *Journal of Toxicological Environmental Health.* Vol. 11 (3), pp. 395-404.

Olsen, K.B., and Fruchter, J.S. (1986). Identification of the physical and chemical characteristics of volcanic hazards. *American Journal of Public Health.* Vol. 86, supplement, pp. 45-52.

Park, R., Rice, F., Stayner, L., Smith, R., Gilbert, S., and Checkoway, H. (2002). Exposure to crystalline silica, silicosis, and lung disease other than cancer in

diatomaceous earth industry workers: quantitative risk assessment. *Occupational Environmental Medicine.* Vol. 59(1), pp. 36-43.

Pyle, D.M. (1995). Reduction of urban hazards. *Nature.* Vol. 387, pp. 134-135.

Quality of Urban Air Group. (1996). *Airborne Particulate Matter in the United Kingdom.* Department of the Environment: London, UK.

Raub, J.A., Hatch, G.E., Mercer, R.R., Grady, M., and Hu, P-C. (1985). Inhalation studies of Mt. St. Helens volcanic ash in animals: II. Lung function, biochemistry and histology. *Environmental Research.* Vol. 37, pp. 72-83.

Reich, M., Zuniga, A., Amigo, A., Vargas, G., Morata, D., Palacios, C., Parada, M.A., and Garreaud, R.D. (2009). Formation of cristobalite nanofibers during explosive volcanic eruptions. *Geological Society of America.* Vol. 37 (5), pp. 435-438.

Rojas-Ramos, M., Catalan-Vazquez, M., Martin-Del Pozzo, A.L., Garcia-Ojeda, E., Vilalba-Caloca, J., and Perez-Neria, J. (2001). *Environmental Geochemistry and Health.* Vol. 23, pp. 383-396.

Rose, W.I., and Durant, A.J. (2009). Fine ash content of explosive eruptions. *Journal of Volcanology and Geothermal Research.* Vol. 186 (1-2), pp. 32-39.

*Ryusuke, I. (1998). Reconstruction of the sequence of the An-ei eruption of Sakurajima volcano (A.D. 1779-1782) using the historical records. *Bulletin of the Volcanological Society of Japan.* Vol. 43 (5), pp. 373-383.

SABO. (2009). *Volcanic SABO of Sakurajima: Volcanic Eruption and Soil Movement.* Online at: http://www.qsr.mlit.go.jp/osumi/sivsc/home/english/s01.html [accessed 02.12.2009].

Samukawa, T., Arasidani, K., Hori, H., Hirano, H., and Arima, T. (2003). C-jun mRNA expression and profiling mRNA amplification in rat alveolar macrophages exposed to volcanic ash and sulphur dioxide. *Industrial Health.* Vol. 41, pp. 313-319.

Sargeant, P. (2009). *The Mineralogical Health Assessment of Mount Etna Volcanic Ash..* MSi Thesis, University of Durham.

Schlesinger, R.B. (1995). Deposition and clearance of inhaled particles. In: McClellan, R.O., and Henderson, R.F. (eds). *Concepts in Inhalation Toxicology, 2nd Edition.* Taylor and Francis: USA. Pp. 191-217.

Searl, A., Nicoll, A., and Baxter, P.J. (2002). Assessment of the exposure of islanders to ash from the Soufriere Hills volcano, Montserrat, British West Indies. *Occupational Environmental Medicine.* Vol. 59, pp. 523-531.

Shimizu, H., Matsushima, T., Nakada, S., Fujii, T., Hoshizumi, H., Takarada, S., Miyabuchi, Y., Ui, T., Miyake, Y., Sugimoto, T., Nagai, D., Hata, K., Sugimoto, S., Matsushita, E., and Yoshida, D. (2007). *Cities on Volcanoes 5 Conference. Intra-Meeting Excursion B1, Nov. 21, 2007. Unzen Eruption: Disaster and Recovery. Field Guide.* COV5 Organising Committee: Japan.

Shirakawa, M., Fukushuma, R., and Kyushima, K. (1984). Experimental studies on the effects of Mt. Sakurajima volcanic ashes on the respiratory organs. *Japanese Journal of Industrial Health.* Vol. 26 (2), pp. 130-146**.**

*Shiraki, K., and Tomita, K. (1993). Weathering products of tephra from Sakurajima volcano. *Bulletin of Kagoshima University (Earth Science, Biology).* Vol. 26, pp. 35-52.

Small, C., and Naumann, T. (2001). The global distribution of human population and recent volcanism. *Environmental Hazards.* Vol. 3, pp. 93-109.

Smithsonian Institute, Global Volcanism Program. (2009). *Sakurajima Weekly Reports.* Online at: http://www.volcano.si.edu/world/volcano.cfm?vnum=0802-08=&volpage=weekly [accessed 02.02.2010].

Soutar, C.A., Robertson, A., Miller, B.G., Searl, A., and Bignon, J. (2000). Epidemiological evidence on the carcinogenicity of silica: factors in scientific judgement. *Annals of Occupational Hygiene.* Vol. 44(1), pp. 3-14.

Sparks, R.S.J.., Young, S.R., Barclay, J., Calder, E.S., Cole, P., Darroux, B., Davies, M.A., Druitt, T.H., Harford, C., Herd, R., James, M., Lejeune, A.M., Loughlin, S., Norton, G., Skerrit, G., Stasiuk, M.V., Stevens, N.S., Toothill, J., Wadge, G., and Watts, R. (1998). Magma production and growth of the lava dome of the Soufriere Hills Volcano, Montserrat, West Indies: November 1995 to December 1997. *Geophysical Research Letters.* Vol. 25 (18), pp. 3421-3424.

Stevens, N., Shrimpton, J., Palmer, M., Prime, D., and Johal, B. (2007). Accuracy assessments for laser diffraction measurements of pharmaceutical lactose. *Measurement Science and Technology.* Vol. 18, pp. 3697-3706.

Stuart, B.O. (1984). Deposition and clearance of inhaled particles. *Environmental Health Perspectives.* Vol. 55, pp. 369-390.

Takahashi, K., the Unzen-Fugendake Eruption Disaster Study Group, Department of Civil Engineering, and Nagasaki University. (2007). *Unzen-Fugendake Eruption Executive Summary. 1990 – 1995.* Unzen Restoration Project Office, Kyushu Regional Construction Bureau, Ministry of Land, Infrastructure and Transport: Nagasaki.

Talvitie, N.A. (1951). Determination of quartz in presence of silicates using phosphoric acid. *Annals of Chemistry.* Vol. 23 (4), pp. 623-626.

Tanguy, J.-C., Ribière, Ch., Scarth, A., and Tjetjep, W.S. (1998). Victims from volcanic eruptions: a revised database. *Bulletin of Volcanology*. Vol. 60, pp. 137-144.

Tilling, R.I. (2005). Volcano Hazards. In: Marti, J., and Ernst, G. (eds). *Volcanoes and the Environment, 1st Edition*. Cambridge University Press: Cambridge. Pp. 55-89.

Tilling, R.I., and Lipman, P.W. (1993). Lessons in reducing volcano risk. *Nature*. Vol. 364, pp. 277-280.

Tobin, G.A., and Whiteford, L.M. (2001). Children's health characteristics under different evacuation strategies: the eruption of Mount Tungurahua, Ecuador. *Applied Geography Conference*. Vol. 24, pp. 183-191.

Tobin, G.A., and Whiteford, L.M. (2004). Chronic Hazards: Health impacts associated with on-going ash-falls around Mt. Tungurahua in Ecuador. *Papers of the Applied Geography Conferences*. Vol. 27, pp. 84-93.

Tokyo Volcanic Ash Advisory Centre, Japanese Meteorological Society. (2009). *Archive Volcanic Ash Advisories for 2009*. Online at: http://ds.data.jma.go.jp/svd/vaac/data/Archives/2009_vaac_list.html [accessed 02.01.2010]

Tokyo Volcanic Ash Advisory Centre, Japanese Meteorological Society. (2010). *Recent Volcanic Ash Advisories*. Online at: http://ds.data.jma.go.jp/svd/vaac/data/vaac_list.html [accessed 02.02.2010]

Toprak, F.O. (2007). *Constraining the Potential Respiratory Health Hazard from Large Volcanic Eruptions*. PhD thesis, University of Cincinnati

*Toyama, T., Nakaza, M., Wakisaka, I., Adachi, S. (1980). Flyash-like particles in the eruption cloud from Sakurajima Volcano. *Find journal name*. Vol. 15 (4), pp. 173-175.

Tsutsumi, K., Masumizu, T., Kinoshita, K., Ishiguro, E., Tanaka, S., and Sugimura, T. (1995). Investigation of the dispersion of volcanic ash from Mount Sakurajima and detection of the ash deposit area. *Final Report of JERS-1/ERS-1 System Verification Program, MITI-NASDA, Japan, Vol. II*. Pp. 385-392

Uda, H., Akiba, S., Hatano, H., and Shinkura, R. (1999). Asthma-like disease in the children living in the neighbourhood of Mt. Sakurajima. *Journal of Epidemiology*. Vol. 9 (1), pp. 27-31.

Uhira, K., and Takeo, M. (1994). The source of explosive eruptions of Sakurajima volcano, Japan. *Journal of Geophysical Research – Solid Earth*. Vol. 99 (B9), pp. 17,775-17,789.

*Uto, k., Miki, D., Nguyen, H., Sudo, M., Fukushima, D., and Ishihara, K. (2005). Temporal evolution of magma composition in Sakurajima volcano, southwest Japan. *Disaster Prevention Research Institute Annals, Kyoto University.* Vol. 48 B, pp. 341-347.

Vallyathan, V., Mentnech, M.S., Tucker, J.H., and Green, F.H. (1983). Pulmonary response to Mount St. Helens' volcanic ash. *Environmental Research.* Vol. 30, pp. 361-371.

Vallyathan, V., Robinson, V., Reasor, M., Stettler, L., and Bernstein, R. (1984). Comparative in vitro cytotoxicity of volcanic ashes from Mount St Helens, El Chichon, and Galunggung. *Journal of Toxicological, Environmental, Health.* Vol. 14 (5-6), pp. 641-654.

Wakefield, J. (2000). An Eruption of Silicosis. *Environmental Health Perspectives.* Vol. 108 (7), pp. A302.

*Wakisaka, I., Takano, A., Watanabe, N. (1978). Health effects of volcanic ashes of Mt. Sakurajima. *Japanese Journal of Public Health.* Vol. 25 (9), pp. 455-461.

*Wakisaka, I., Yanagihashi, T. (1986). Week-to-week variations in mortality in areas exposed to volcanic air pollution. *Journal of the Japanese Society of Air Pollution.* Vol. 21 (4), pp. 322-329.

*Wakisaka, I., Yangihashi, T., Ono, M., Hirano, S. (1985). Health Effects of volcanic activities of Mt, Sakurajima in the mortality statistics. *Journal of the Japanese Society of Air Pollution* Vol. 20 (2), pp. 120-127.

*Wakisaka, I., Yanagihashi, T., Sato, M., and Tomari, T. (1989). Health effects of volcanic air pollution – an analysis of the national health insurance. *Nippon Eiseigaku Zasshi.* Vol. 44 (5), pp. 977-986.

*Wakisaka, I., Yangihashi, T., Tomari, T. (1984). Effects of the volcanic activities of Mt. Sakurajima on mortality figures. *Japanese Journal of Public Health.* Vol. 31 (10), pp. 548-556.

*Wakisaka, I., Yanagihashi, T., Tomari, T., Ando, T. (1983)a. Effect of volcanic activities of Mt. Sakurajima on mortality due to respiratory diseases. *Japanese Journal of Public Health.* Vol. 30 (3), pp. 109-116.

*Wakisaka, I., Yanagihashi, T., Tomari, T., Ando, T. (1983)b. Health effects of volcanic activities of Mt. Sakurajima on school children. *Japanese Journal of Public Health.* Vol. 30 (3), pp. 101-108.

Watt, S.F.L., Pyle, D.M., Mather, T.A., Martin, R.S., and Matthews, N.E. (2009). Fallout and distribution of volcanic ash over Argentina following the May 2008

explosive eruption of Chaiten, Chile. *Journal of Geophysical Research*. Vol. 114 B04207, doi:10.1029/2008JB006219.

Weinstein, P., and Patelxy, A. (1997). The Mount Ruapehu eruption 1996: a review of potential health effects. *Australian and New Zealand Journal of Public Health*. Vol. 21 (7), pp. 773-778.

Wiester, M.J., Setzer, C.J., Barry, B.E., Mercer, R.R., and Grady, M.A. (1985). Inhalation studies of Mt. St. Helens volcanic ash in animals: Respiratory mechanics, airway reactivity and deposition. *Environmental Research*. Vol. 36, pp. 230-240.

Wilson, M.R., Stone, V., Cullen, R.T., Searl, A., Maynard, R.L., Donaldson, K. (2000). In vitro toxicology of respirable Montserrat volcanic ash. *Occupational Environmental Medicine*. Vol. 57, pp. 727-733.

Wyart-Remy, M. (2003). Effects of silica dust. *ISSA/Chamber of Mines Conference 2003 – Mines and Quarries: Prevention of Occupational Injury and Disease*. Pp. 77-82.

Yamanoi, Y., Takeuchi, S., Okumura, S., Nakashima, S., and Yokoyama, T. (2008). Colour measurements of volcanic ash deposits from three different styles of summit activity at Sakurajima volcano, Japan: Conduit processes recorded in color of volcanic ash. *Journal of Volcanology and Geothermal Research*. Vol. 178, pp. 81-93.

Yanagi, T., Ichimaru, Y., and Hirahara, S. (1991). Petrochemical evidence for coupled magma chambers beneath the Sakurajima volcano, Kyushu, Japan. *Geochemical Journal*. Vol. 25, pp. 17-30.

Yano, E. (1986). The biological effects of volcanic ash of Mount Sakurajima – environmental experimental and epidemiological study. *Clean Air Congress 1986*. vol. 3, pp. 95-102.

*Yano, E., Higashi, H., Nishii, S., Koizumi, A., Yokoyama, Y. (1987). Pulmonary function of loggers exposed to the volcanic ash from Mt. Sakurajima. *Japanese Journal of Public Health*. Vol. 34, pp. 251-254.

Yano, E., Nishii, S., and Yokoyama, Y. (1986). Chronic pulmonary effects of volcanic ash: An epidemiologic study. *Archives of Environmental Health*. Vol. 41 (2), pp. 94-99.

Yano, E., Takeuchi, A., Nishii, S., Koizumi, A., Poole A., Brown, R.C., Johnson, N.F., Evans, P.H., and Yukiyama, Y. (1985). In vitro biological effects of volcanic ash from Mount Sakurajima. *Journal of Toxicological and Environmental Health*. Vol. 16, pp. 127-135.

Yano, E., Yokoyama, Y., Higashi, H., Nishii, S., Maeda, K., and Koizumi, A. (1990). The health effects of volcanic ash: A repeat study. *Archives of Environmental Health.* Vol. 45 (6), pp. 367-398.

Yokoo, A., and Ishihara, K. (2007). Volcanic activity around Showa Crater of Sakurajima Volcano monitored with infrared and video cameras. *Annals of Disaster Prevention Research Institute, Kyoto University.* Vol. 50 C, pp. 149-156.

Yokoo, A., Tameguri, T., and Iguchi, M. (2009). Swelling of a lava plug associated with a Vulcanian eruption at Sakurajima Volcano, Japan, as revealed by infrasound record: case study of the eruption on January 2, 2007. *Bulletin of Volcanology.* Vol. 71, pp. 619-630.

Zeng, X-M., MacRitchie, H.B., Marriott, C., and Martin, G.P. (2006). Correlation between inertial impaction and laser diffraction sizing data for aerosolised carrier-based dry powder formulations. *Pharmaceutical Research.* Vol. 23 (9), pp. 2200-2209.

* - Article in Japanese, information obtained from abstract and diagrams only.

Appendix A

IVHHN Ash Collection Protocol

IVHHN ASH SAMPLE COLLECTION PROCEDURES

Introduction

The methods recommended for ash collection depend on the purpose intended for the ash. For evaluation of health hazard, the grain-size distribution and composition of the ash may be assessed and the leachates may be analysed. If chemical analyses are carried out, ash should be dried at < 40 $_o$C, but for compositional or grain-size analysis, the temperature is not crucial. If research is to be carried out on the leachates and surface reactivity of samples (e.g. for toxicological analysis) it will be important to know the exact post-eruptive history of the ash in terms of rainfall and exposure. The quantity of ash needed should be assessed before collection. For example, grain-size analysis or compositional analysis may need small quantities (< 10 g) of ash whereas several kg may be required for toxicological analysis, particularly if a sample is to be shared between different laboratories. The following procedures should be adapted for the particular hazard assessment or research to be carried out but ensure that the ash samples can be used for grain-size analysis, characterization of composition and leachates, and assessment of volume of erupted material / total accumulated tephra (formation of isopach maps) etc.

Implements for ash collection

- The most cost-effective technique for ash collection is using plastic trays (or buckets) which are cheap and easily cleaned. Trays should have a high rim (> 5 cm) in order to avoid contamination and rain-water overflow. The tray should be large enough to collect a significant quantity of ash (ideally > 0.1 m$_2$). Netting may be secured across the opening to avoid contamination by birds, insects or plants. Metallic trays should be avoided due to possible contamination in contact with rain water.
- Commercial collection devices are available, such as the 'frisbee gauge' which consists of an open-bottomed dish fitted with a dry-foam trap to reduce sample contamination from organic matter. The sample is collected in a collection bottle at the base of the unit. The gauge is fitted with a bird guard and a tripod (lighter for 'new style' gauges) which can be spiked to the ground for increased stability. The frisbee gauge relies on precipitation to wash particles through the dish into the collection bottle. The ISO gauge, by the same manufacturer, conforms to ISO standard ISO/DIS 4222 for consistent performance but does not have the foam trap. Information on these products is available on the internet (see References section).

Routine ash monitoring

- A network of clean trays should be set up around a volcano to form a grid that covers the area of possible ash dispersal.
- Particular attention should be given to the direction of prevailing wind. In the case of a very large area of possible ash dispersal, trays should be distributed at least along the most-likely dispersal axis at increasing distances from the vent.
- Trays should be emptied daily to avoid contamination from organic or minor-eruptive material, ash re-suspension by wind and rain-water overflow.
- If water is present in the trays following eruption, both ash and water should be collected in a bag and then dried in the oven. Trying to remove water from the tray may result in loss of fines, which are crucial in the context of assessing health hazard.

Ash collection following an eruption

- Following an ash fall, samples should be collected as soon as possible to avoid re-suspension of fines by wind, water or human activity.
- If a tray network is not in place, ash should be collected on flat surfaces that were known to be clean before the eruption. Ash collection on grass and ground should be avoided.
- In the case where grass or ground areas are the only surfaces available, ash should be removed carefully, leaving a few mm at the ash-surface interface to avoid contamination.
- Ash can be sprayed or wetted with water to avoid loss of fines during collection (unless original un-contaminated particle surfaces are needed for analysis).
- In the case of heavy ash fall, a core can be taken using, for example, a 30 cm section of drainpipe, to retrieve a representative section of ash. This technique is most effective for compact deposits.
- Store ash in bags. One can use either 'Kraft' paper bags or plastic sealable bags. We recommend Kraft bags as fines may adhere more to the surface of plastic bags (see Kraft bag section).

Labelling of samples

In both routine monitoring and ash collection after an eruption, the following should be recorded:
- Time of eruption.
- Time of collection.
- Location of collection (including grid reference or GPS location).
- Note if the ash is just from one or from multiple events and how long since tray last emptied.
- Area of the tray used or of the surface sampled - ash accumulation is best recorded as mass per unit area.
- State of deposit – dry, wet, contains accretionary lapilli, lithics, pumice, organic matter etc.
- Information on the history of the sample between deposition and collection (e.g. rainfall).
- Distance from vent.
- Distance from main dispersal axis, if well defined.
- Assign a sample number.

After collection

- Dry ash in oven at < 40 ºC. If ash is collected in 'Kraft' bags, they can be put directly in the oven without the need for removal from bags. In hot climates, the ash can be dried naturally by leaving it in Kraft bags.
- Weigh the ash sample.
- For safety and transport, store the ash within several sealed bags. Recommended – 'zip lock' bags which are easily re-sealable.

Kraft Bags

Kraft bags can be any sort of tough brown paper bag. For ash collection we recommend bags designed specifically for geochemical soil sampling. For example, the bags manufactured and internationally distributed by Siliconpak (www.charapak.co.uk) are made of high wet-strength Kraft paper using waterproof adhesives and can withstand collection of wet samples and subsequent drying. The bags are available in the following sizes: 3x5, 4x8, 5x10 inches.

References

Frisbee Gauge and other similar instruments:
http://www.york.ac.uk/inst/sei/dust/mines1.html which also provides a downloadable protocol for use of the frisbee gauge.
http://www.hanby.co.uk/ - website of the manufacturer of the frisbee gauge and other similar dust collectors.
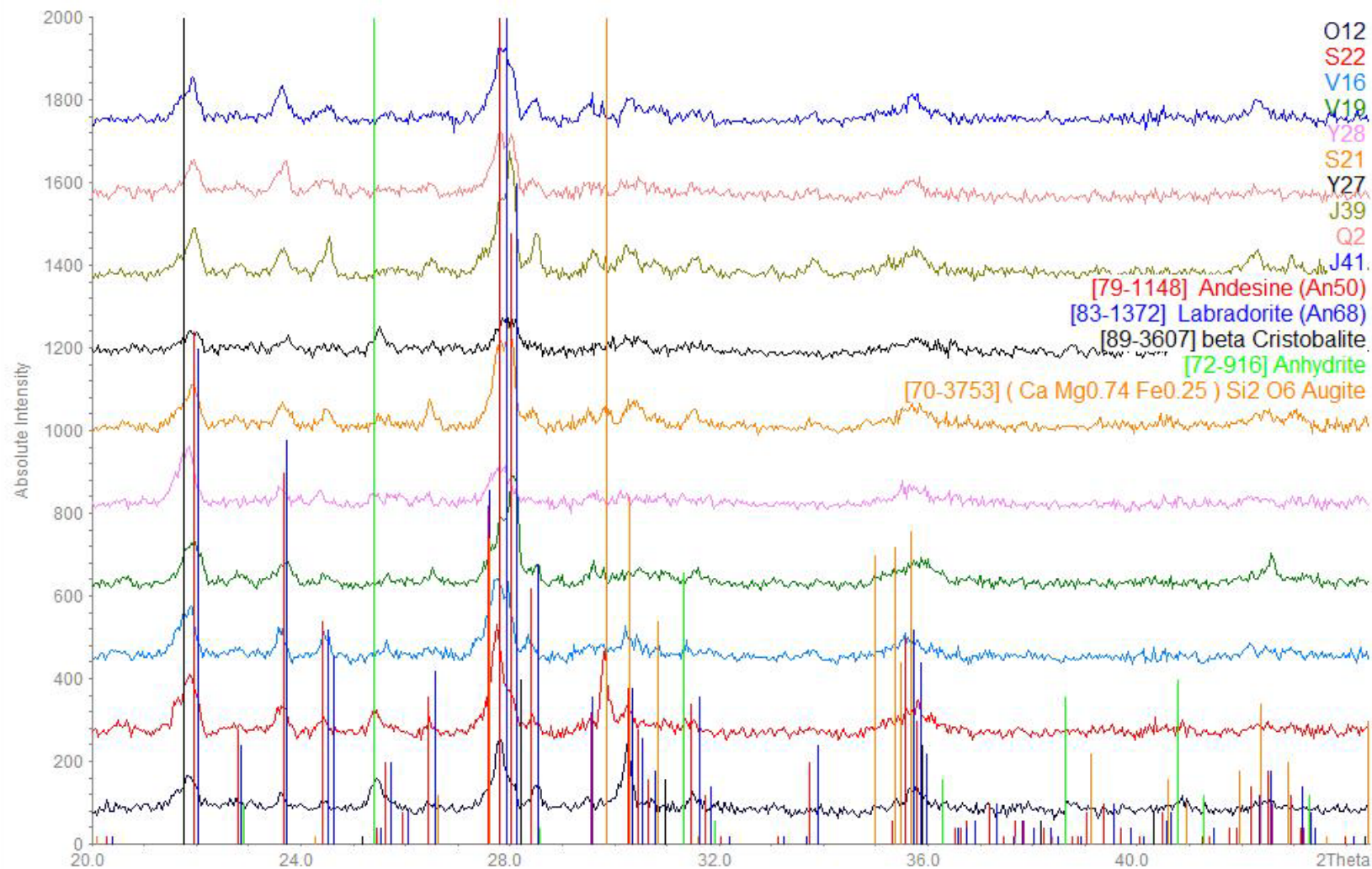Kraft Bags: Siliconpak Ltd, UK (www.charapak.co.uk)

Appendix B

CD of Raw Data and Analysis Calculations

Please see hard copy for data CD or contact sarah.hillman@live.com

Appendix C

'Stick fit' Diagrams for Mineral Identification

Appendix D

BET Isotherm and Surface Area Plots

The samples were analysed twice for BET surface area. Little can be distinguished between the repeat plots so only one isotherm and BET plot per sample are shown in this appendix. The correlation coefficient for the second run is given.

Sample SAK12

Isotherm Plot
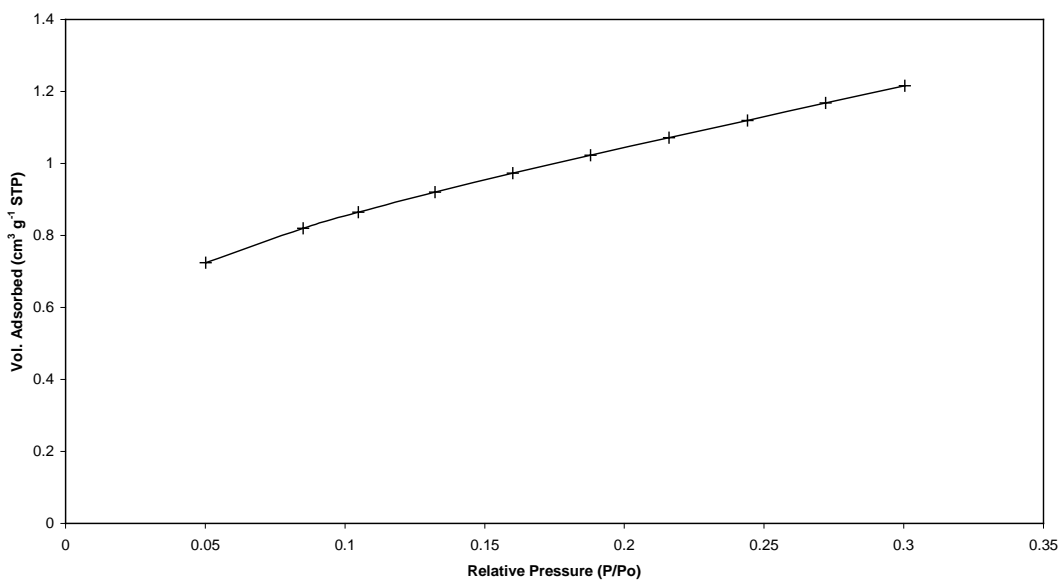
BET Surface Area plot
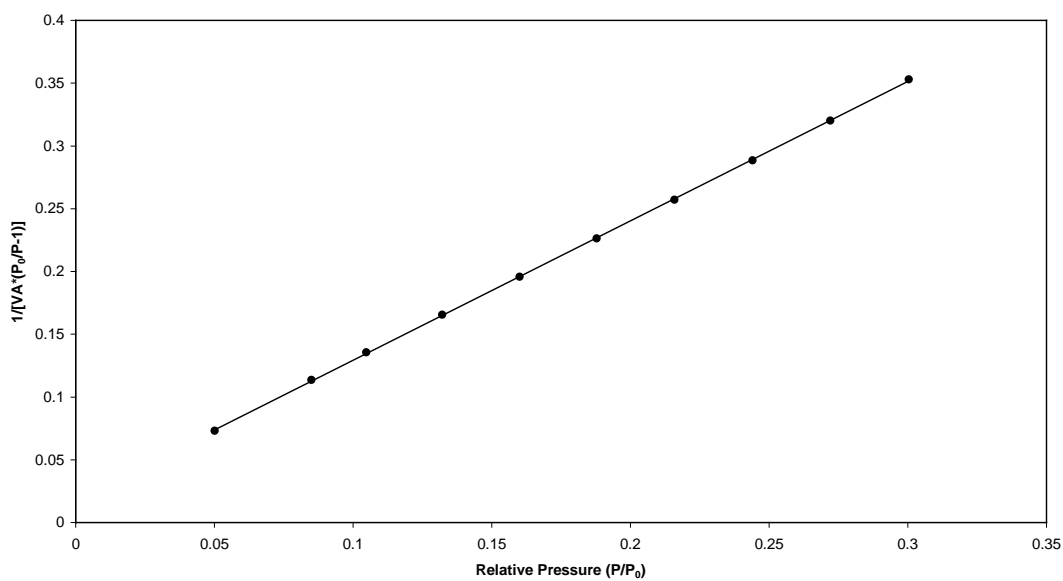
Gradient:	1.110
Intercept:	0.018
Correlation Coefficient:	0.999955
Correlation Coefficient (Run 2):	0.999963

Sample SAK16

Isotherm Plot
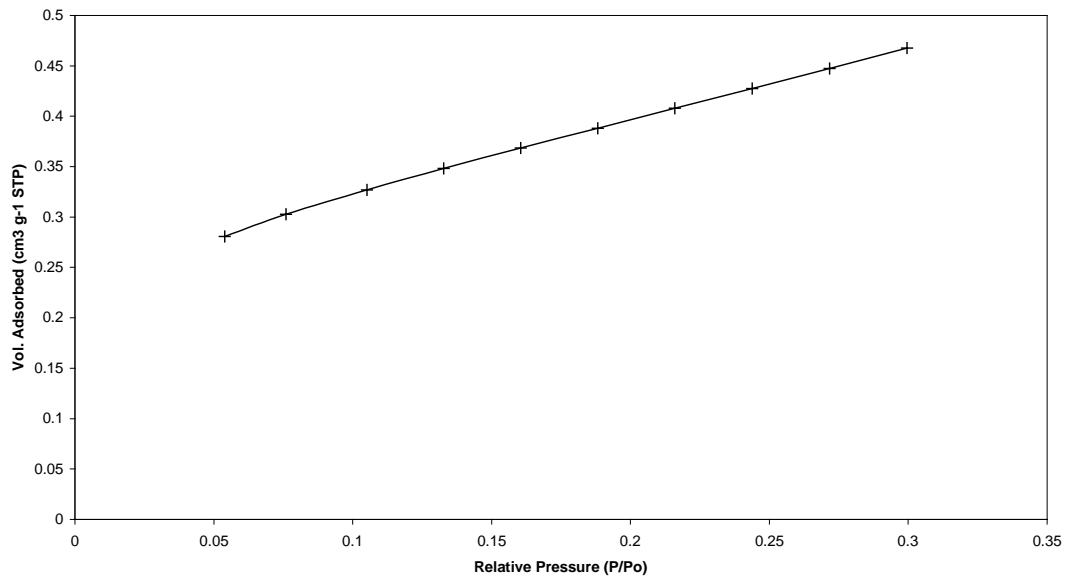
BET Surface Area Plot
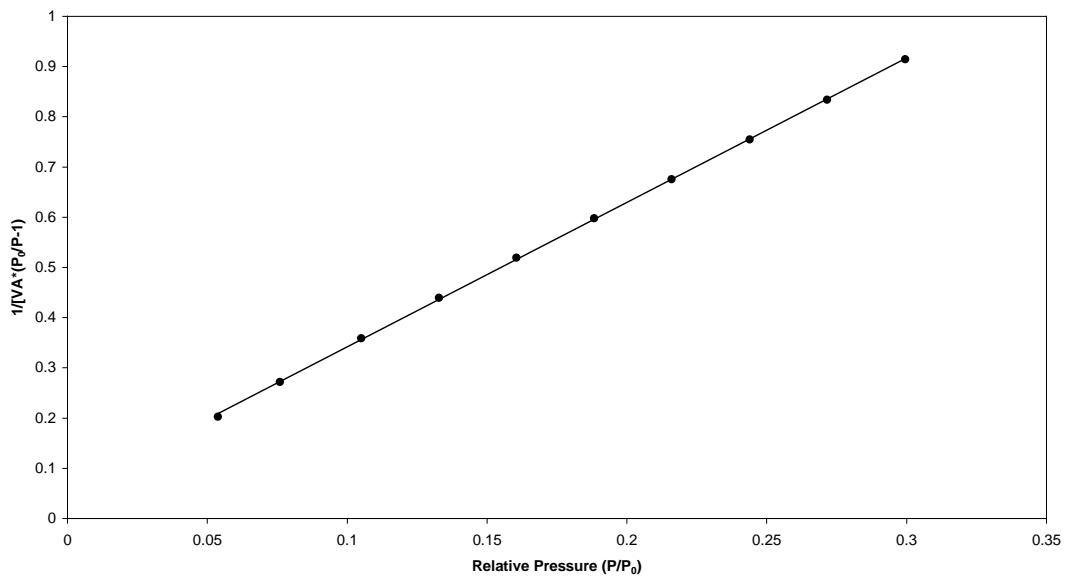
Gradient:	2.878
Intercept:	0.054
Correlation Coefficient:	0.9999238
Correlation Coefficient (Run 2):	0.999877

Sample SAK19

Isotherm Plot
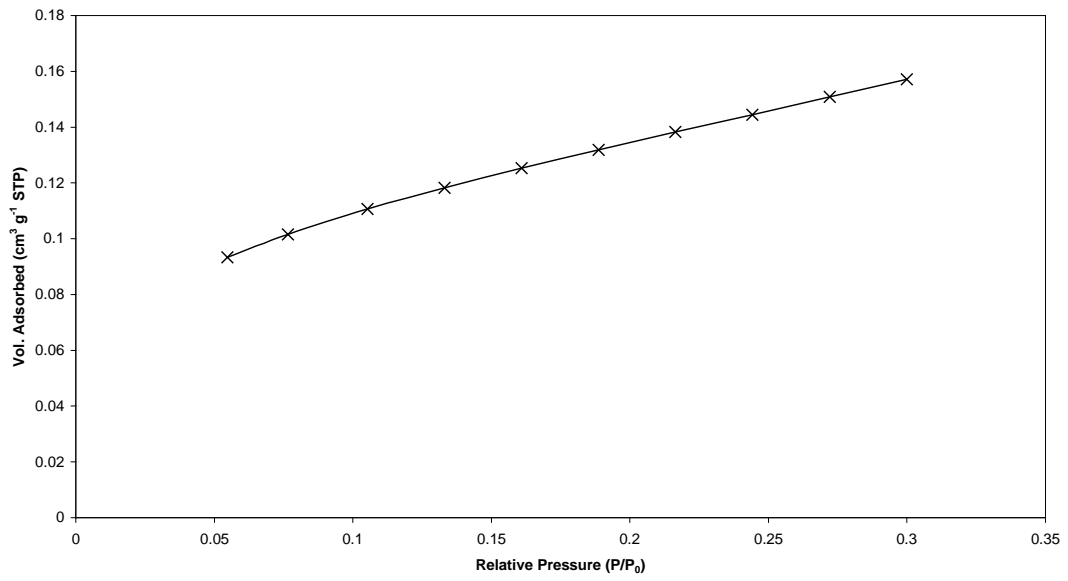
BET Surface Area Plot
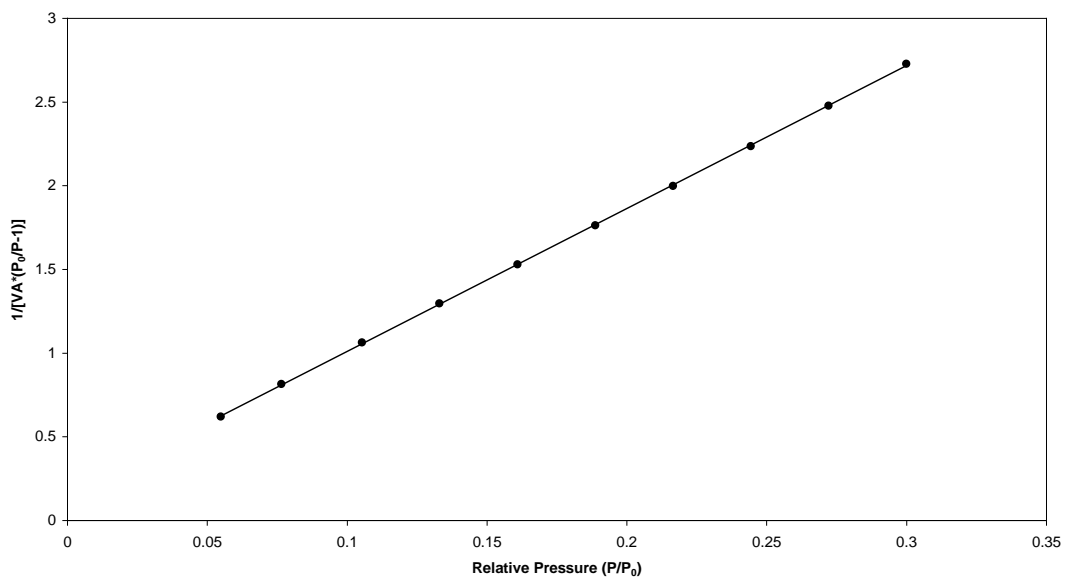
Gradient:	8.531
Intercept:	0.159
Correlation Coefficient:	0.9999635
Correlation Coefficient (Run 2):	0.9998986

Sample SAK21

Isotherm Plot
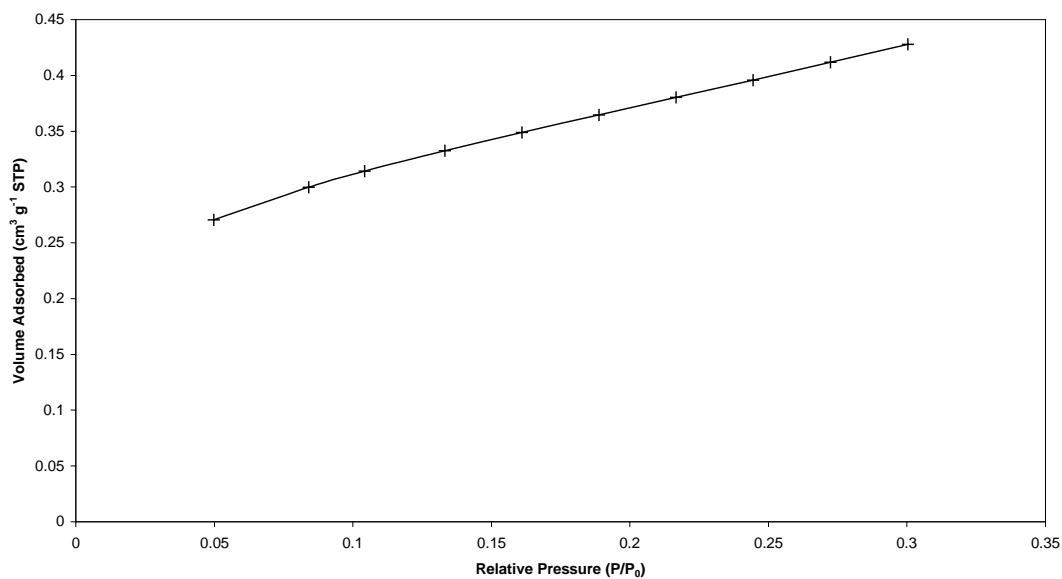
BET Surface Area Plot
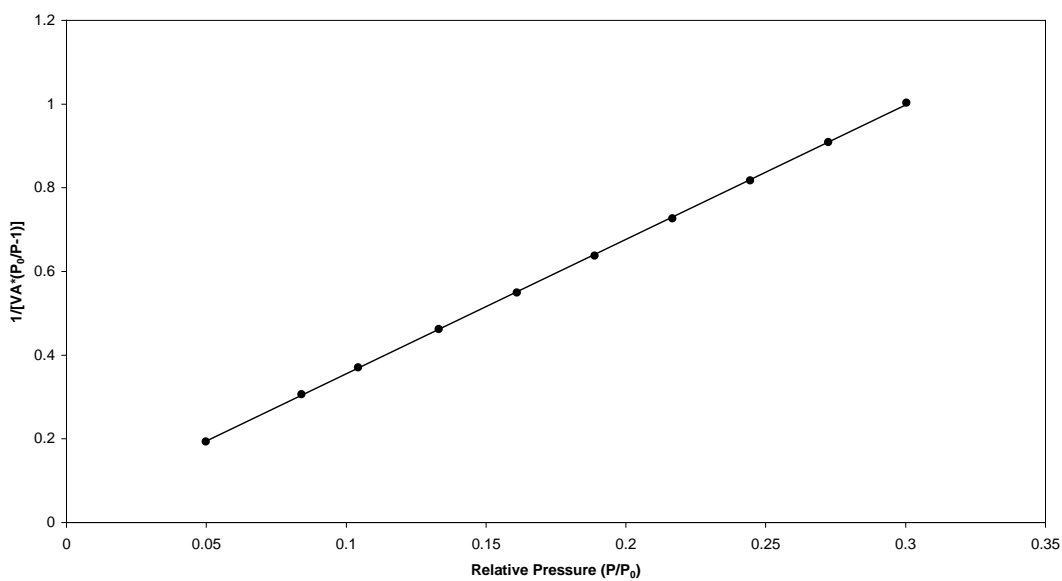
Gradient: 3.212

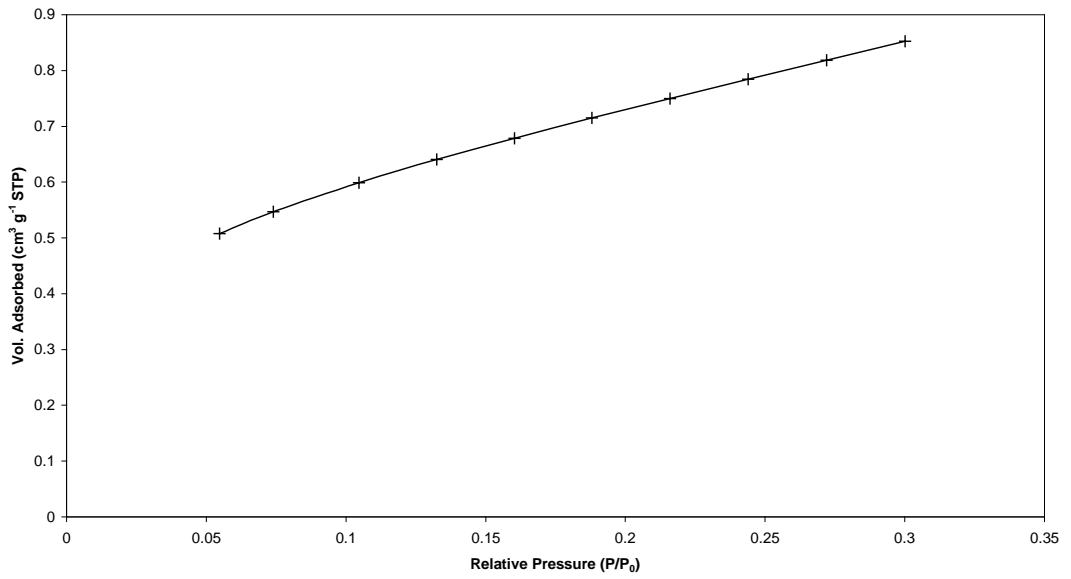| Intercept: | 0.034 |
| Correlation Coefficient: | 0.9998139 |
| Correlation Coefficient (Run 2): | 0.9999649 |

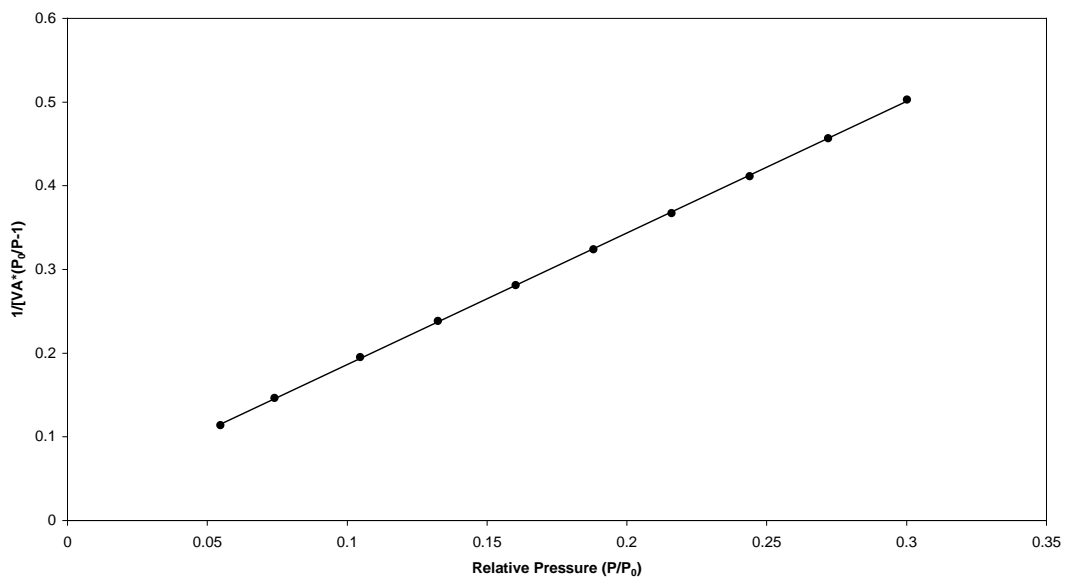## Sample SAK22

Isotherm Plot
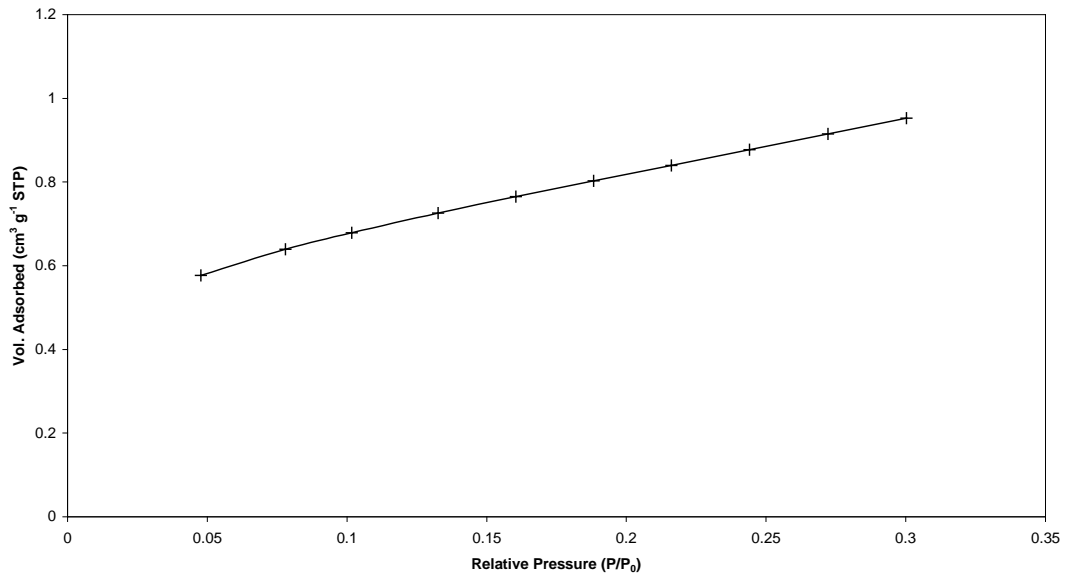
BET Surface Area Plot
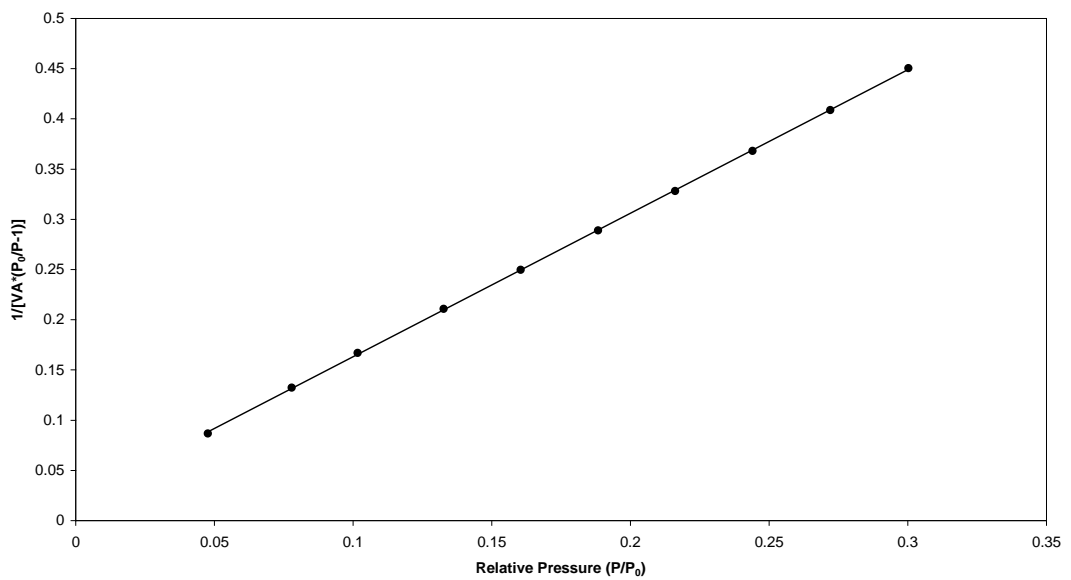
Gradient:	1.429
Intercept:	0.020
Correlation Coefficient:	0.9999677
Correlation Coefficient (Run 2):	0.9999583

Sample FM28

Isotherm Plot

BET Surface Area Plot

Gradient:	1.572
Intercept:	0.029
Correlation Coefficient:	0.9999572
Correlation Coefficient (Run2):	0.9999557

Sample J39

Isotherm Plot
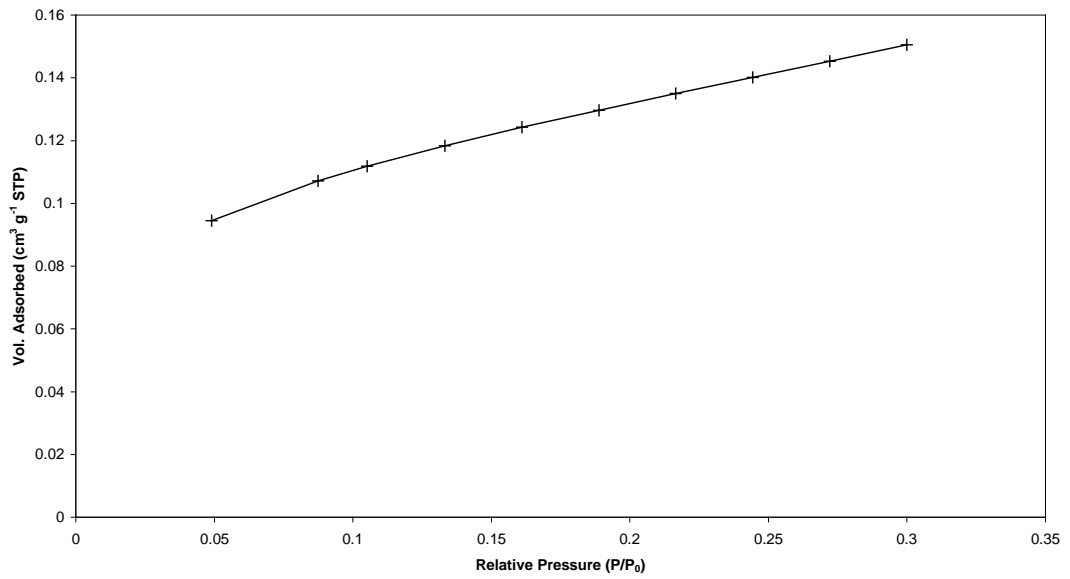
BET Surface Area Plot
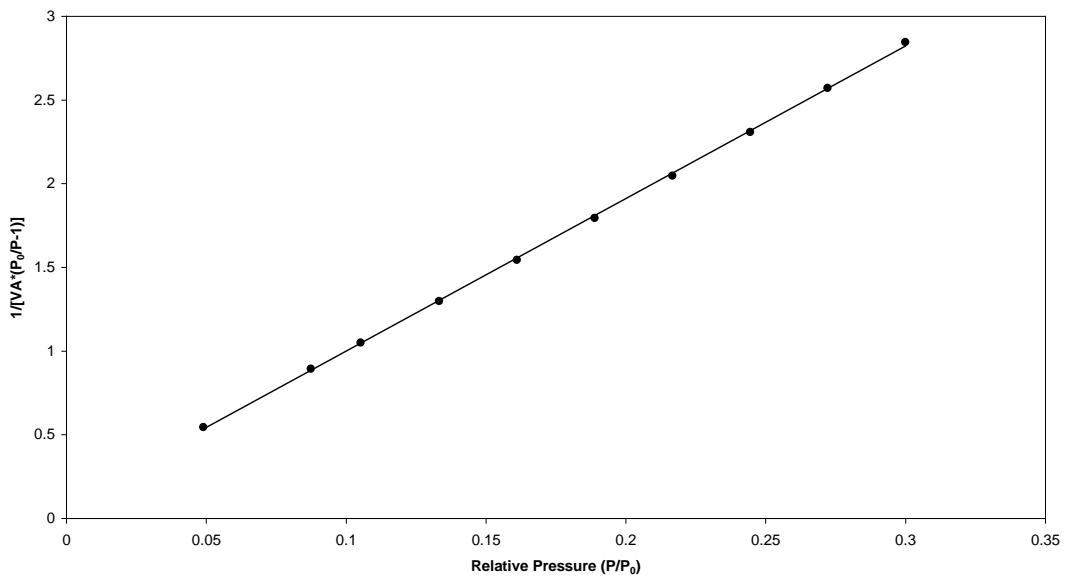
Gradient: 9.115

Intercept: 0.088

Correlation Coefficient: 0.9998593

Correlation Coefficient (Run2): 0.9998761